DOI: 10.14753/SE.2016.1869

INVOLVEMENT OF NESFATIN AND MELANIN-CONCENTRATING HORMONE IN THE REGULATION OF VIGILANCE; COMPARISON WITH THE EFFECT OF ESCITALOPRAM, THE SSRI ANTIDEPRESSANT

PhD thesis

Szilvia Vas, Kalmárné

Semmelweis University

János Szentágothai Doctoral School of Neurosciences

Supervisors:	Dr. György Bagdy, D.Sc. Dr. Zsuzsanna Tóth, PhD
Official reviewers:	Dr. Márk Molnár, D.Sc. Dr. Gergely Zachar, PhD
Head of the Final Examination Committee:	Dr. László Köles, PhD
Members of the Final Examination Committee:	Dr. Ildikó Miklya, PhD Dr. Lucia Wittner, PhD

Budapest

2015

DOI: 10.14753/SE.2016.1869

1. Table of Contents

DOI: 10.14753/SE.2016.1869

DOI: 10.14753/SE.2016.1869

DOI: 10.14753/SE.2016.1869

2. List of Abbreviations

ACTH	adrenocorticotropin
ANOVA	analysis of variance
ARAS	ascending reticular activating system
AW	active wake
BF	basal forebrain
CART	cocaine-amphetamine-regulated transcript
CNS	central nervous system
CRH	corticotrophin-releasing hormone
DAB	diaminobenzidine
DLH	dorsolateral hypothalamus
DRN	dorsal raphe nucleus
EEG	electroencephalography / electroencephalographic
EMG	electromyography / electromyographic
5-HT	5-hydroxytryptamine / serotonin
GABA	γ-aminobutyric acid
Hcrt	orexin/hypocretin
icv	intracerebroventricular/intracerebroventricularly
IHC	immunohistochemistry
ip	intraperitoneal/intraperitoneally
IR	immunoreactive
IS	intermediate stage of sleep
LC	locus coeruleus
LDT	laterodorsal tegmental nucleus
LH	lateral hypothalamic area
MCH	melanin-concentrating hormone
MCHR	MCH receptor
MnPO	median preoptic nucleus
MRN	median raphe nucleus
MS-DBB	medial septum-diagonal band of Broca
NA	noradrenaline

DOI: 10.14753/SE.2016.1869

nesfatin	nesfatin-1/NUCB2
NiDAB	nickel-enhanced diaminobenzidine
non-REM	non-rapid eye movement (sleep)
NUCB2	nucleobindin 2
PFA	perifornical area
PFH	perifornical hypothalamic area
PH	posterior hypothalamus
POA	preoptic area
POMC	proopiomelanocortin
PPT	pedunculopontine tegmental nucleus
PVN	hypothalamic paraventricular nucleus
PW	passive wake
qEEG	quantitative electroencephalography
REM	rapid eye movement (sleep)
SCN	suprachiasmatic nucleus
SON	supraoptic nucleus
SSRI	selective serotonin reuptake inhibitor
SWS	slow wave sleep
SWS1	light slow wave sleep
SWS2	deep slow wave sleep
TMN	tuberomamillary nucleus
TW	total wake
VLPO	ventrolateral preoptic area
VTA	ventral tegmental area
ZI	zona incerta / subzona incerta

DOI: 10.14753/SE.2016.1869

3. List of Figures

DOI: 10.14753/SE.2016.1869

DOI: 10.14753/SE.2016.1869

4. List of Tables

DOI: 10.14753/SE.2016.1869

5. Introduction

Sleep is one of the greatest mysteries: from birth, we spend nearly a third of our lives asleep. It is vital to our cognitive and physical performance, memory, health and well-being. Despite decades of research, we are still not sure why. The last decades saw a great progress in the understanding of sleep regulation. The relevance of this understanding is indicated by the fact that in our society sleep problems are often associated with a wide range of medical and psychiatric conditions, moreover, hypnotics are among the most frequently prescribed medications.

According to traditional concepts, sleep is a homeostatic function, that is, a prolonged wakefulness is followed by rebound sleep. It is a property of the whole organism: the animal is awake or asleep. However, in the past few years, a new theory of sleep was born, namely, sleep is a local process and use-dependent. This idea suggests that sleep is a fundamental property of neuronal networks; the homeostatic regulation of sleep can occur in any part of the brain as a result of former activity [1, 2].

5.1. The stages of sleep and wakefulness

Falling asleep takes only a few seconds or minutes, however, in the meanwhile, dramatic changes are processed in the central nervous system (CNS). During the transition, parallel alterations can also be observed in physiological variables, such as breathing, arousability, closure of the eyes and muscle tone. During switching between sleep and wake or between different sleep stages, changes in the global pattern of neuronal activity can be measured by electroencephalography (EEG) [3], while the alterations in muscle tone can be monitored by electromyography (EMG).

The observable extracellular field potential changes in the EEG stem from the synchronized electrical activity of large amount of cortical neurons. The summed synaptic currents of the apical dendrites of pyramidal neurons comprise the main contributors to EEG waves, although neuronal firing and intrinsic membrane properties are also involved [4].

DOI: 10.14753/SE.2016.1869

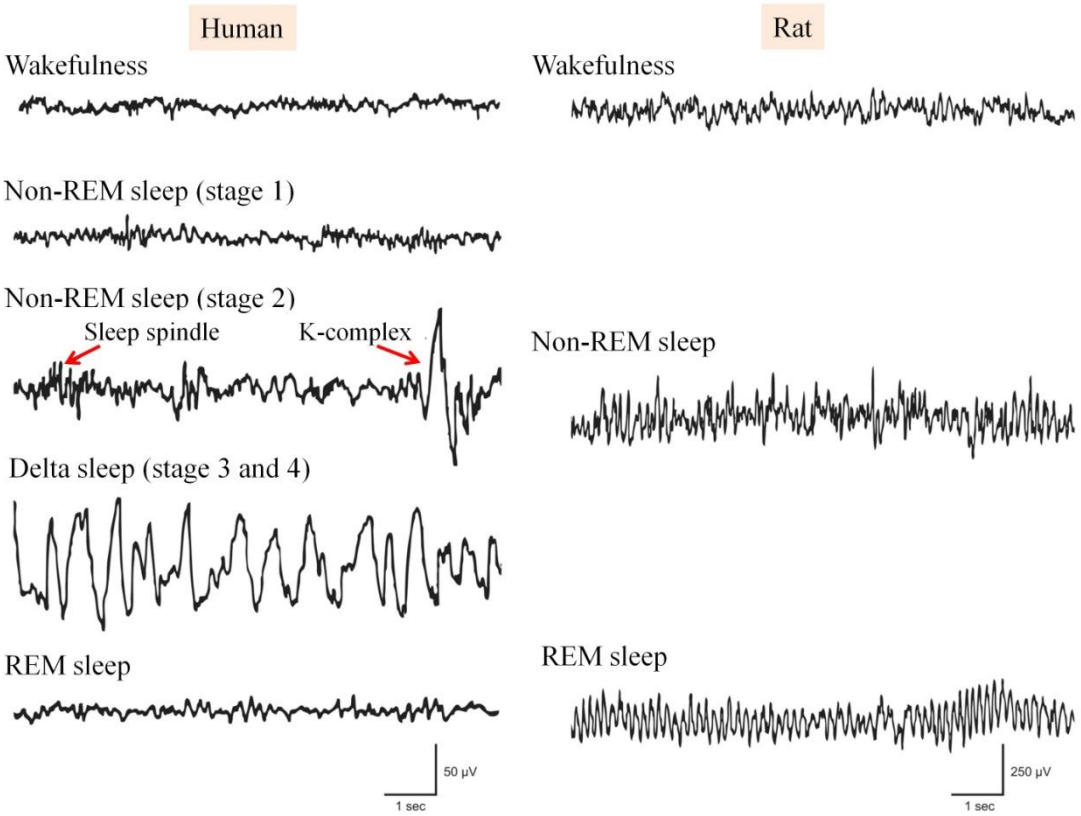

Figure 1. Electroencephalographic (EEG) recordings of different vigilance stages in human and rat. Wakefulness is characterized by desynchronized (low-amplitude and high-frequency) EEG in both human and rat. As sleep deepens, non rapid eye movement (non-REM) sleep in human can be divided into four stages, like stage 1 (superficial sleep), stage 2 (accompanied by the appearance of sleep spindles and K-complexes) as well as stage 3 and 4 (also called delta sleep together due to the high amount of high amplitude, low frequency delta waves). The EEG feature of rapid eye movement (REM) sleep is very similar to that in wakefulness (low-amplitude and high-frequency) in human. In rat, non-REM sleep is also characterized by low frequency delta waves that increase in amplitude and decrease in frequency as sleep deepens, although in most cases non-REM sleep in rat is not parsed into separate stages. In the REM sleep of rat, strong synchronous theta activity is typical, presumably generated by the hippocampus. Based on Brown et al. [5].

DOI: 10.14753/SE.2016.1869

Table 1. Basic EEG rhythms and the typical vigilance stages where the rhythms are most frequently occur in human and rat [8, 11, 12].

EEG rhythm	Frequency range (Hz)	Typical Vigilance stage	
		Human	Rat
Delta	0.5-4	non-REM III-IV	slow wave sleep
Theta	5-9	non-REM I REM sleep wakefulness	REM sleep wakefulness
Sigma (spindles)	12-14	non-REM II	deep slow wave sleep
Alpha	9-13	drowsiness	light slow wave sleep
Beta	15-30	wakefulness	wakefulness
Gamma	30<	wakefulness	wakefulness

5.1.1. Wake

The state of wakefulness is a complex manifestation of behaviours that are continually changing in response to alterations in the internal and external stimuli. This vigilance stage is characterized by high frequency, low voltage waves (desynchronized or "activated" EEG activity, see on Figure 1) with high muscular activity. These faster EEG rhythms with low amplitude comprise synchronized activity in small functionally interconnected areas. Theta rhythm, typical in wake and rapid eye movement (REM) sleep, appears over more widespread areas, and synchronizes faster, locally generated beta (15-30 Hz) and gamma (>30 Hz) rhythms (Table 1) that oscillations are considered to provide a temporal framework for higher-order brain functions such as conscious awareness, attention, representation of spatial position and memory [6]. In rat, the waking state with high theta activity corresponds to the attentive and/or psychoactive waking comprising 23% of sleep-wake cycle, while waking without theta activity represents the non-attentive waking or non-motivated motor activities, called quiet or passive wake (PW), comprising 33% of sleep-wake cycle [7]. Theta power is

presumably arising from the hippocampus [8]. More than one theta generator as well as more than one type of hippocampal theta activity has been suggested, however, the functional relevance of hippocampal theta activity is still not clear [6, 9].

5.1.2. Non rapid eye movement (non-REM) sleep

As the individual fall asleep, EEG switches to higher amplitude, slower frequency EEG signs (synchronized EEG activity) characteristic of non rapid eye movement (non-REM) sleep. Then, during non-REM sleep, the EEG slows progressively, until the EEG is dominated by high voltage, slow delta waves (0.5-4 Hz frequency, Table1). During this stage, the underlying cellular phenomenon is the slow oscillation (<1Hz), which contains an UP state, characterized by maintained depolarization and irregular neuronal firing, and a DOWN state characterized by silence in firing of cortical cells. Consequently, during non-REM sleep, cortical neurons show a firing pattern prevailed by periods of increased population activity (ON periods) intermitted by shorter periods of generalized silence (DOWN period), referring to the negative phase of EEG slow waves [10, 11].

Depending on the extent of synchronization, non-REM sleep can be subdivided into four stages in human. Stage one (non-REM I) comprises the superficial sleep, characterized by relative low amplitude theta frequency and vertex sharp waves. In stage two (non-REM II) distinctive sleep spindles (augmenting and decrementing waves at 12-14 Hz frequency) and K-complexes appear on the EEG. In stage three (non-REM III) and stage four (non-REM IV), EEG is occupied by delta waves (0.5-4 Hz) in no more than 50% and more than 50% of the EEG record, respectively. The deepest stages, like non-REM III and non-REM IV are also called slow wave sleep (SWS) or delta sleep [12], and recently not considered to be separate stages. Duration of a non-REM sleep bout typically lasts ca. 40-60 minutes in human, and about three-five minutes in rodents. Slow rolling eye movements and decreased tone of somatic musculature is typical. In rats, non-REM sleep is subdivided into two stages: light slow wave sleep (slow wave sleep 1, SWS1) is characterized by the occurrence of slow waves with increasing amplitude, while in deep slow wave sleep (slow wave sleep 2, SWS2), there

are spindles with progressively increasing amplitude and number interspersed by high-amplitude, low-frequency cortical slow waves on EEG [7].

5.1.3. Rapid eye movement (REM) sleep

During the switch from non-REM sleep to REM sleep, the slow waves are replaced by high frequency low-amplitude fast, tonically activated EEG signs. REM sleep is characterized by a distinct constellation of tonic and phasic features, namely, atony of skeletal muscles with the exception of breathing- and eye-moving muscles (tonic), and stereotyped bursts of saccadic eye movement, called rapid eye movements (phasic) observable on the electrooculogram. This sleep stage is also called paradoxical sleep due to the presence of an increased cortical activity while the arousal threshold is high. The duration of REM sleep bouts varies with species, age and heath of the individual lasting usually 1.5 h in human vs. 7-13 min in rodents (reviewed in [12-14].

During REM sleep in rodent, a rhythmic theta EEG activity, generated by the hippocampus, is a striking feature on the EEG. In theta activity, two different subtypes have been observed: the Type I (4-7 Hz) theta has been demonstrated under urethane or ether anaesthesia and during behavioural immobility, and was abolished by atropine sulphate, a muscarinic antagonist, while Type II theta (7-12 Hz) has been demonstrated during waking associated with movements and was abolished by urethane. However, during REM sleep, a combination of Type I and Type II theta can be detected [9]. In rats, REM sleep is preceded and sometimes followed by a short stage called intermediate stage of sleep (IS) characterized by high-amplitude anterior cortex spindles and low-frequency hippocampal theta rhythm [15].

In humans, although low frequency (4-7 Hz) theta activity is generated mainly from the hippocampus, the EEG is prevailed by faster and lower voltage cortical frequencies. In contrast to rats, theta in humans was not detected continuously, rather in short (1 sec) periods, moreover, it was not correlated with the occurrence of rapid eye movements [16]. In humans, the IS transitional stage has been identified as part of the non-REM II sleep [12].

DOI: 10.14753/SE.2016.1869

5.2. The role of brain structures in the regulation of sleep-wake cycle

The regulation of sleep-wake cycle is based on two independent processes: the circadian rhythm and the homeostatic drive [17]. In mammals, the circadian rhythmicity of vigilance is determined by the function of the hypothalamic suprachiasmatic nucleus (SCN), a key pacemaker that translates the light-dark information from the retina into transcriptional and translational feedback loops of clock genes, and regulates behavioural responses with a roughly 24 h period [18]. In homeostatic sleep regulation, the length and depth of sleep is driven by sleep-promoting molecules, such as adenosine, which may accumulate extracellularly as a by-product of cellular metabolism. In other words, if someone is sleep-deprived for a period of time, he/she will have an increase in the subsequent sleep-time to compensate deprivation [2, 14, 19].

Regarding the transition between different vigilance stages, a mutually inhibitory relationship between sleep- and wake-promoting systems in the brain generates a flip-flop switch that is presumed to allow a sharp transition between sleep and wakefulness [14]. However, a similar switch is thought to regulate the transition between non-REM and REM sleep through the mutually antagonistic relationship of REM-on and REM-off neuronal populations [20] (Figure 2). In the brain, the mutual inhibition is between large populations of neurons, which may also respond to other stimuli at the same time, consequently the transition will take seconds to minutes, depending on the species, and the developing behavioural state is most likely the result of the summed activity across all neurons. However, this switch ensures stable sleep and wake, thus, lesion of a single component of the sleep-wake circuitry can destabilize the sleep switches, as shown by the example of narcolepsy [14, 21].

DOI: 10.14753/SE.2016.1869

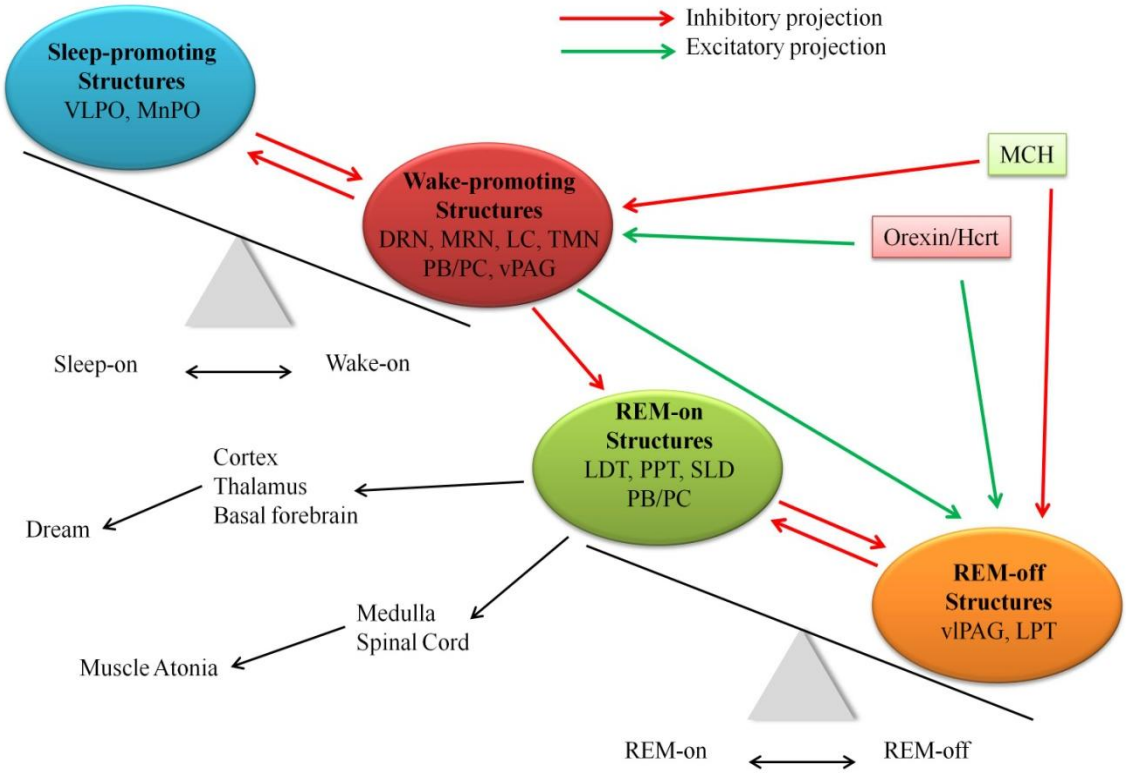

Figure 2. "Flip-flop" model of wake - sleep and REM - non-REM sleep switch, and how this cascade is stabilized by orexin/hypocretin (Hcrt) neurons (based on Saper et al. 2010 [18]). In the regulation of vigilance, the "switch" between sleep and wakefulness (at the upper left) is established by the mutually inhibitory relationship of sleep promoting structures [ventrolateral preoptic area (VLPO), median preoptic nucleus (MnPO)] and wake-promoting structures [dorsal raphe nucleus (DRN), median raphe nucleus (MRN), locus coeruleus (LC), tuberomamillary nucleus (TMN), parabrachial nucleus (PB) and the adjacent precoeruleus area (PC) and the ventral periaqueductal gray matter (vPAG)]. There is an also mutually inhibitory relationship between structures having REM-on- [laterodorsal tegmentum (LDT), pedunculopontine tegmentum (PPT), sublaterodorsal tegmentum (SLD), and PB/PC] and REM-off- [ventrolateral periaqueductal gray matter (vlPAG) and LPT] characteristic (at the lower right). The monoaminergic arousal neurons inhibit the VLPO during wakefulness, but also prevent the generation of REM sleep by inhibiting the REM-on neurons and exciting the REM-off neurons. Thus, the wake-REM sleep transition is practically impossible for normal individuals. In the stabilization of the "flip-flop switch" between non-REM and REM sleep as well as wakefulness, the orexin/hypocretin (Hcrt)- and melanin-concentrating hormone (MCH)-expressing neuron populations, intermingled in the hypothalamus, are considered to have a key role.

5.2.1. Brainstem

The importance of brainstem in the regulation of brain state and muscle tone is crucial: its extensive damage can cause coma, a state of unconsciousness and unresponsiveness. In the maintenance of wakefulness, two critical pathways originate from the brainstem (i) the ascending reticular activating system (ARAS) projecting to the thalamus, hypothalamus, basal forebrain (BF), and neocortex being important for cortical activation, and (ii) the descending pathway to the spinal cord being crucial for the maintenance of muscle tone [22] (Figure 3).

The ARAS comprises serotonergic neurons mostly from the dorsal and median raphe nuclei (DRN and MRN, respectively), noradrenergic neurons from the locus coeruleus (LC) and dopaminergic neurons from the area adjacent to the DRN, as well as cholinergic neurons from the pedunculopontine tegmental (PPT) and laterodorsal tegmental (LDT) nuclei. The ARAS also includes histaminergic neurons from the tuberomamillary nucleus (TMN), although this structure is localized in the posterior hypothalamus (PH, see later in section 5.2.4.2). The monoaminergic neurons, including DRN, LC and TMN neurons, show their highest firing rate at wakefulness, low rates during non-REM sleep while they nearly silent during REM sleep [23-25]. The relative small number of noradrenergic neurons in the LC (ca. 1500 in rat) innervates almost the entire CNS [26] and possibly has a role in generating arousal during conditions that needs high level of attention or activation of the sympathetic nervous system [23]. The importance of this structure is shown by the finding that optogenic stimulation of the noradrenergic neurons can lead to immediate awakening [27]. Moreover, noradrenergic release in the cortex is essential for the EEG desynchronization [28] (Figure 3).

The serotonergic neurons of the DRN and MRN project widely to the cortex and subcortical areas, including the BF, thalamus, hypothalamus and the preoptic area (POA). Besides its involvement in the regulation of vigilance, serotonin (5-hydroxytryptamine, 5-HT) has been shown to regulate many other aspects of behaviour such as appetite, mood, aggression and anxiety. Early studies suggested that 5-HT might promote non-REM sleep and possibly REM sleep, however, more recent studies have indicated that serotonin generally induces wakefulness and suppresses REM sleep (reviewed in [29]). In agreement with this role, agonists of the 5-HT_{1A}, 5-HT_{1B}, 5-HT_{2},

or 5-HT_3 receptors elevate wakefulness [30-33]. Of clinical relevance, increased extracellular 5-HT concentration can be elicited by the application of selective serotonin reuptake inhibitor (SSRI) antidepressants, like fluoxetine or escitalopram, that agents had been shown to increase wakefulness while suppress REM sleep in both humans and rodents [34-36].

The LDT/PPT cholinergic neurons, comprising one of the two major cholinergic cell populations, send extensive projections to subcortical regions including the thalamus, lateral hypothalamus and BF [37]. In contrast to the monoaminergic components of the ARAS, cholinergic neurons show high firing rate during both wakefulness and REM sleep [38]. Thus, the cholinergic system seems to be linked to cortical EEG desynchronization typical during wakefulness and REM sleep, but not necessarily to behavioural arousal. The impact of the PPT is suggested by the fact that lesion of the cholinergic neurons of PPT causes significant reduction in the amount of REM sleep [39].

Also glutamatergic neurons from the rostral pons, localizing in the parabrachial nucleus and the adjacent precoeruleus area, have been postulated to participate in the maintenance of wakefulness (Figure 3). These neurons have been demonstrated to send projections to the cerebral cortex, BF and the lateral hypothalamus. Although the firing pattern of these neurons have not been investigated yet, studies with the early gene product Fos (see later in section 5.3) have found mostly wake- and REM sleep -active neurons in these regions [14, 20].

5.2.2. Basal forebrain

The cholinergic neurons of the BF give the primary source of cholinergic input to the cortex and the hippocampus, and in line with this, have a role in the cortical desynchronization. These cholinergic neurons, similarly to the LDT/PPT group, show their highest firing rate during wake and REM sleep, while in non-REM sleep their neuronal activity is minimal [40-42]. The BF also contains a large group of neurons that release the inhibitory neurotransmitter γ-aminobutyric acid (GABA), which neurons may activate the cortex by decreasing the activity of inhibitory cortical interneurons [43] (Figure 3). On the contrary, recent data suggest a dual function of BF in the

modulation of cortical activation and behavioural state, namely, populations of GABA-ergic BF neurons have been shown to facilitate cortical activation by modulating gamma or theta activity, while other subgroups decrease cortical activation by modulating irregular slow oscillations that normally occur during SWS [44].

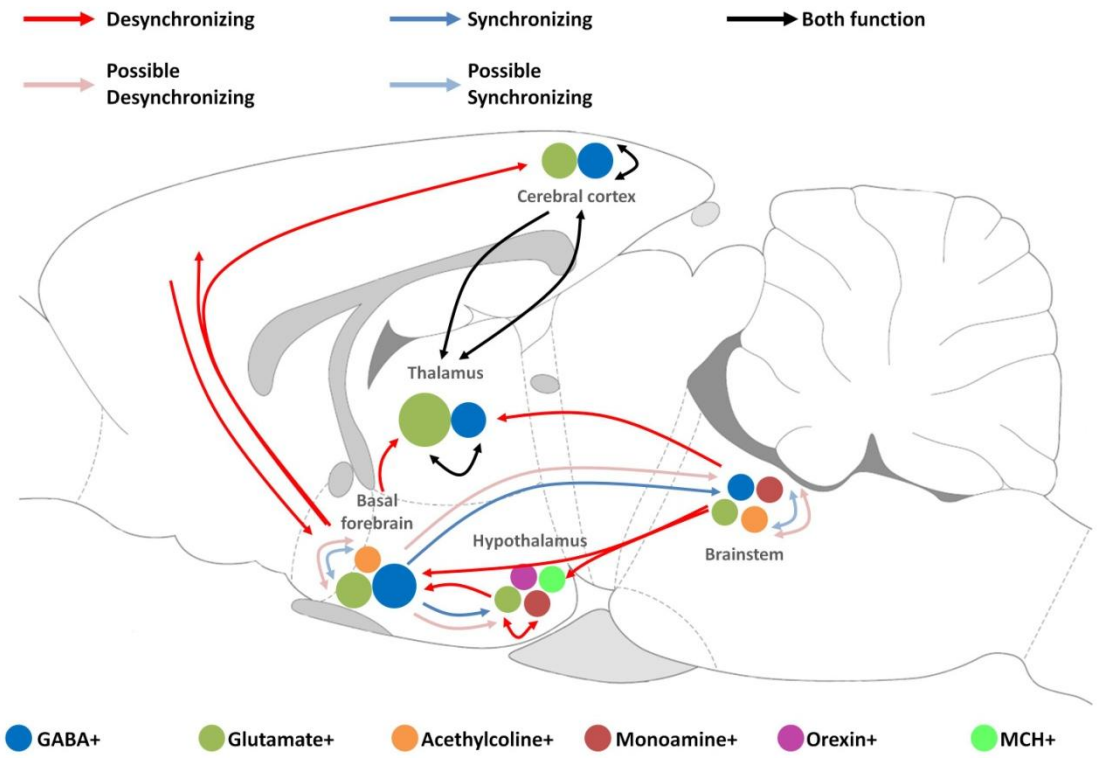

Figure 3. Schematic drawing illustrating the key circuits involved in the regulation of sleep and wakefulness in rat brain. Red and blue arrows indicate the major pathways of cortical desynchronization and synchronization, respectively. Black arrows demonstrate pathways that mediate both synchronization and desynchronization. Possible pathways of desynchronization and synchronization are shown by light red and light blue arrows, respectively. Different cell types are illustrated by coloured circles in each brain areas. Abbreviations: GABA: gamma-aminobutyric acid, MCH: melanin-concentrating hormone (Based on Lee et al., 2012) [45].

5.2.3. Thalamus and cortex

Thalamus comprises the gateway of sensory input to the cortex and can directly influence state of the cortex. The highly interconnected thalamocortical, thalamic reticular and cortical neurons comprise the thalamocortical loop which has a crucial role

in setting the global brain state and in regulating the flow of sensory information [46, 47]. Thalamic neurons show distinct modes of firing in different vigilance stages demonstrating tonic spiking in alertness and rhythmic bursting in drowsiness or non-REM sleep [48]. Delta oscillation and spindles are generated in sleep or drowsiness by the intrinsic properties of the thalamocortical and thalamic reticular neurons and through their synaptic interactions [48]. Thalamus receives strong input from the ARAS and the BF [37, 49] comprising the major pathway through which the neuromodulatory system can influence cortical function [45] (Figure 3).

Cortical neurons can also influence the global state of the brain. In non-REM sleep, slow oscillations originate in the cortex [10], and cortico-cortical connections are sufficient for the synchronization of the oscillations across different brain areas [50]. Notably, in anesthetized rat, high-frequency burst firing of a single cortical neuron has been found to be sufficient to induce transition in the global brain state, either from a synchronized to desynchronized state or *vica versa* [51]. Cortical neurons are highly interconnected with thalamic neurons and can also exert strong influences on the global brain state. Neurons from the prefrontal cortex provide strong descending inputs to the neuromodulatory circuits in the BF [52]and the brainstem [45, 53]

5.2.4. Hypothalamus

The role of hypothalamus in the regulation sleep and wakefulness was first hypothesized during the epidemic encephalitis letargica around the time of the First World War by Constantin von Economo, who reported lesions in the preoptic region around the rostral end of the third ventricle in patients suffering from profound insomnia. A smaller part of patients suffering from encephalitis letargica showed opposite symptoms: they became insomniac and slept only for a few hours each day despite being extremely tired. These patients had lesions in the anterior hypothalamus and basal ganglia [54]. Recently, the crucial role of the hypothalamus in the regulation of sleep and wakefulness has been rediscovered, shifting the focus away from the thalamocortical system and the brainstem. As a key integrator centre of the brain, the hypothalamus expresses several neuropeptides and transmitters to synchronize the regulation of basic physiological functions of the body, like food intake, temperature,

energy homeostasis, stress response and reproduction with the circadian pacemaker of the body as well as the sleep-wake cycle [55].

5.2.4.1. The preoptic area

In the POA, two neuronal populations have been identified as sleep-promoting structures: the ventrolateral preoptic area (VLPO) and the median preoptic nucleus (MnPO) [56, 57]. The key property of VLPO neurons, that they have reciprocal innervations with several components of the ARAS, including DRN and adjacent ventral periaqueductal grey matter (vPAG), TMN, LC and parabrachial nucleus [20, 58]. The dense core of the VLPO innervates the histaminergic TMN, and includes GABA- and galanin neuropeptide-containing neurons that show their highest firing rate during non-REM sleep. However, a more diffuse population of VLPO, the extended VLPO, innervates DRN and LC [59, 60]. Cell-specific lesions of the VLPO core correlated most closely with non-REM sleep decrease, while the cell loss of the extended VLPO correlated rather with the decline of REM sleep [60]. The major input of VLPO is provided by the MnPO that contains mostly sleep-active GABAergic neurons that do not contain galanin [58, 61]. In contrast to VLPO, the neurons of which increase firing rate during sleep just from sleep onset, neurons of MnPO often fire in advance of sleep, suggesting a role in accumulating sleep pressure [61]. The mutual inhibition between sleep-active neurons of VLPO-MnPO and the ARAS-lateral hypothalamus led to the proposal of a flip-flop model (see in chapter 5.2, Figure 2) for sleep-wake switches [14].

5.2.4.2. The posterior hypothalamus

The involvement of PH was postulated by the early experiments of Nauta [62] who demonstrated that large posterior hypothalamic lesions led to a continuous sleep-like state. Further research identified two arousal-related neuronal populations in the PH: a histaminergic cell group in the TMN [63] and an orexin/hypoctretin neuropeptide-containing cell population in the perifornical hypothalamic area (PFH, perifornical area and lateral hypothalamus).

Similarly to the monoaminergic components of ARAS (see before), histaminergic TMN neutrons show their maximal firing rates in wakefulness, though

silent during non-REM sleep [63, 64]. Many TMN neurons discharge robustly also during REM sleep suggesting a possibly stronger correlation with EEG desynchrony than with wakefulness itself. In line with this, axons from TMN neurons target predominantly the lateral hypothalamus, BF and the cerebral cortex, where they terminate, particularly in the prefrontal cortex [65]. Histaminergic TMN neurons, influence sleep-wake state through reciprocal interactions with sleep promoting systems in the anterior hypothalamus [66], BF and brainstem arousal systems.

5.2.4.3. The lateral hypothalamic area

The lateral hypothalamic area (LH), being an important integrator region of the brain, has been implicated in a wide variety of functions, such as energy homeostasis, regulation of motor activity as well as motivation and reward [67]. A growing body of evidence sustains the role of this area with the PH as a key centre in the regulation of vigilance [68-70]. The impact of LH in the regulation of sleep-wake cycle is shown by the fact that reversible inactivation of this area, using muscimol a $GABA_A$ agonist, completely abolishes REM sleep [71]. Moreover, neurons showing REM-specific firing pattern have been recorded from this area.

In the lateral hypothalamus and the adjacent perifornical area (PFA), just dorsal and rostral to the TMN histaminergic cell population, another arousal-related neuronal system has been identified, namely the orexin/hypocretin (Hcrt) neuropeptide-producing neurons. Hcrt neurons are essentials for the maintenance of waking, showing their highest firing rate during wakefulness, decreasing their activity in non-REM sleep, and being almost silent in REM sleep [72]. Partly intermingled (although not co-expressing) with the Hcrt neurons in the LH and PFA, the melanin-concentrating hormone (MCH)-containing neurons are localized [73, 74] playing an opposite role in the regulation of sleep-wake cycle promoting sleep, particularly REM sleep [72, 75-77]. For the connection between MCH and Hcrt neurons and their innervations, see Figure 4. Notably, MCH and Hcrt neurons send parallel projections innervating almost the entire CNS, including the cortex, amygdala, hippocampus, nucleus accumbens, thalamus, hypothalamus, ventral tegmental area (VTA), LDT/PPT nuclei, raphe nuclei and LC suggesting common, integrative roles in the central regulation of vigilance, food intake and energy expenditure [70, 73, 78-80]. All MCH-containing neurons express a relative

novel neuropeptide, the nesfatin/NUCB2, identified in 2006 [81], however, the role of this peptide in the regulation of sleep-wake cycle had not been investigated until the beginning of our experiment.

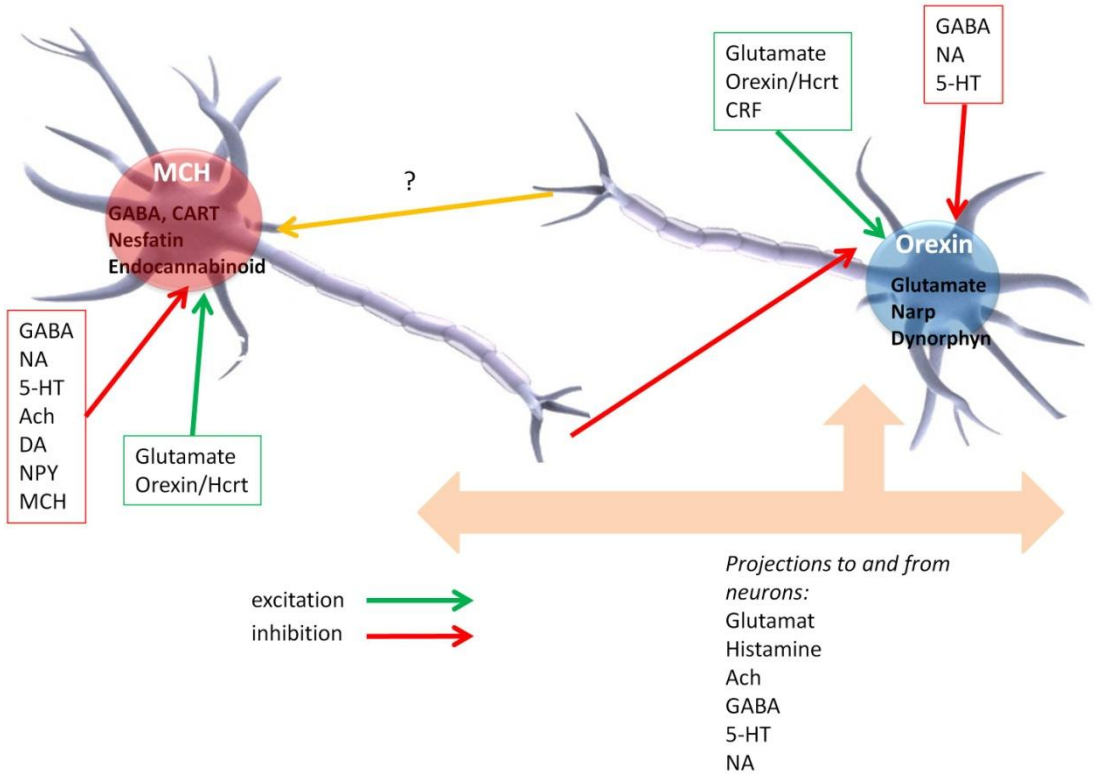

Figure 4. Schematic illustration of the connection between the orexin/hypocretin (Hcrt) and the melanin-concentrating hormone (MCH)-containing neurons and their innervations. MCH neurons contain gamma-aminobutyric acid (GABA), cocaine-amphetamine-regulated transcript (CART), nesfatin and endocannabinoids, while Hcrt neurons express neuronal activity regulated pentraxin (Narp), dynorphyn and glutamate. In the interaction between MCH and Hcrt neurons, MCH neurons inhibit Hcrt neurons, while the influence of Hcrt neurons on MCH neurons can be excitatory or inhibitory. Abbreviations: noradrenaline (NA), serotonin (5-HT), acetylcholine (Ach), dopamine (DA), neuropeptide Y (NPY), corticotropin releasing factor (CRF). Red and green arrows show inhibitory or excitatory innervations, respectively, while yellow arrow means that both inhibitory and excitatory connection can be present. Based on Konadhohe et al., 2014 [82].

5.2.4.3.1. The hypocretins /orexins

The orexin A and B, also called hypocretin-1 and 2 (Hcrt) have been discovered by two groups independently [83, 84]. The term *hypocretin* (i.e. hypothalamus-specific secretin-like peptide) comes from the fact that Hcrt-positive neuronal somata have been reported only in the PFH [83], while the term *orexin* emphasizes their obvious role in the appetite regulation [84]. The importance of the Hcrt system in the sleep-wake regulation was suggested by the discovery of decreased expression of Hcrt peptides and Hcrt receptors in the background of narcolepsy both in humans and dogs [85, 86]. Additionally, narcolepsy-like phenotype has been reported in Hcrt knock-out mice [87] and in rats with specific Hcrt-directed neurotoxic lesions [88]. Narcolepsy is characterized by the inability to sustain wakefulness, frequent state transitions and inappropriate intrusions of REM sleep-related phenomena (i.e. motor atonia) during wakefulness, suggesting the specific function of Hcrt neurons in ensuring the stability and maintenance of non-REM and REM sleep as well as wake stages [14]. Additionally, central administration of Hcrt has been shown to elevate wake and decrease non-REM and REM sleep [89], and blockade on Hcrt receptors promotes both non-REM and REM sleep at the expense of wakefulness [90]. This relative small neuron population (ca. 6700 neurons in the rat brain) [76] gives excitatory projections to all other arousal- and wake-related cell groups, including the cholinergic neurons in the BF, the histaminergic cells in the TMN as well as cholinergic and aminergic cells in the brainstem [91], suggesting the wake-executive property of Hcrt neurons in the regulation of vigilance [92]. Hcrt 1 and 2 are neuro-excitatory peptides, and binding to specific receptors (Hcrt-1R and Hcrt-2R) evoke excitatory post-synaptic effects when released from the glutamatergic Hcrt-neurons [78, 93]. In addition, nearly all Hcrt neurons also contain the neuropeptide dynorphin [94].

5.2.4.3.2. The melanin-concentrating hormone (MCH)

MCH is a 19-amino acid peptide, with a conservative structure that is identical in all mammals examined to date, including rabbits, rats, mice, and humans [95].The MCH-expressing neuronal population (ca. 10,000-12,000 in the rat brain), localizing in the zona incerta/subzona incerta (ZI), LH and the PFA [73]. A small number of MCH-containing neurons have also been demonstrated in the pontine reticular formation and

the olfactory tubercle in rat, as well as in the LDT and POA of female and lactating rats, respectively [73, 96, 97]. MCH-containing fibres are in close relationship with Hcrt neurons and *vice versa*, moreover, hypocretinergic receptors are present on MCH neurons, suggesting reciprocal synaptic contacts between MCH and Hcrt neurons as well as an important functional interaction between the two systems [98, 99]. Earlier studies have reported that Hcrt neurons increase MCH mRNA expression, directly exciting MCH neurons as well as elevating glutamate release onto them [75, 100]. However, recent optogenic data show that firing of Hcrt neurons exerts inhibitory effect on most MCH neurons via $GABA_A$ receptors, while bath-applied Hcrt caused excitation only in a minority of MCH neurons (Figure 4), providing evidence for a GABAergic microcircuit that, by a potential feed-forward loop, may stabilize the switch between sleep and wakefulness [101]. On the contrary, MCH neurons exert a unique inhibitory effect on hypocretinergic signaling as a way to fine-tune the output of these neurons [102] (Figure 4). To date, two receptor of MCH have been identified, the MCHR1 and MCHR2 that show 38% sequence homology [103, 104]. While binding of MCH to MCHR1 activates diverse intracellular signaling pathways by coupling to G_i, G_q and G_0 proteins, MCHR2 is known to couple only to G_q [104, 105]. Similarly to centrally administered Hcrt, intracerebroventricularly (icv)-injected MCH has been demonstrated to stimulate feeding [84, 106]. Targeted deletion of either the MCH gene or melanin-concentrating hormone MCH1 receptor in mice led to hypophagic lean mice [107], while overexpression of the prepro-MCH resulted in obese mice [108]. Moreover, non-peptide MCHR1 antagonist has been found to abolish the MCH-induced feeding behaviour and diminished body weight [109].

Beyond the involvement of MCH in food intake, additional physiological evidence suggests its role in the regulation of sleep and wakefulness (reviewed in [110, 111]. While Hcrt neurons have a critical role in the maintenance of wakefulness, MCH neurons increase their firing rate during slow wave sleep (SWS) and show their maximal firing rate in REM sleep [72]. The implication of MCH in sleep-regulation is strengthened by the fact that centrally administered MCH elevated the time spent in REM sleep (~200%), and to a lesser degree, the amount of SWS [112], moreover, MCHR1 antagonists dose-dependently decreased SWS2, IS as well as REM sleep, while active and passive wake have been found to increase [113]. In addition,

optogenic activation of MCH neurons promotes REM sleep [114]. Interestingly, regarding the function of MCH-containing neurons, the action of MCH neuropeptide does not seem to be as important as GABA release from these neurons, causing inhibitory post-synaptic effect [70, 114].

In accordance with its role in promoting sleep, activity of MCH-containing neurons is regulated by components of the wake-promoting system. Namely, MCHergic neurons are hyperpolarized by noradrenaline (NA), serotonin, acetylcholine [100], while dopamine reduces the excitability of MCH-containing neurons by decreasing the membrane resistance without modifying the resting potential [115] (Figure 4). Cannabinoids, being sleep-promoting neuromodulators, increase the firing rate of MCH-containing neurons by decreasing the activity of nearby GABAergic neurons via CB1 receptors [116].

In the MCH-containing cells, MCH is generated by the cleavage of the prepro-MCH precursor, which contains other neuropeptides besides MCH, such as neuropeptide EI (NEI) and neuropeptide GE (NGE) [73]. In addition to prepro-MCH-derived neuropeptides, other neurotransmitter and neuromodulators have been demonstrated to co-localize with MCH, like the anorexinergic cocaine- and amphetamine-regulated transcript (CART). In the ZI and the lateral hypothalamus of rat, 95% and 70% of the MCH-containing neurons co-express CART, respectively [117]. The MCH population, based on the CART positivity, can be separated functionally into two MCH subpopulations, namely, (i) the CART co-localizing MCH neurons sending ascending projections toward the septum and hippocampus, whereas (ii) the non-CART MCHergic neurons send descending projections toward the brainstem and spinal cord [118].

Considering physiological functions, MCH possesses an integrative role in energy conservation by decreasing metabolism and promoting sleep as well as food intake. In line with this, MCH reduces heart rate, temperature and metabolic rate by central actions, namely, it elevates the parasympathetic/sympathetic rate and diminishes the release of thyroid hormones [95]. The MCHergic system is thought to play a crucial role in special cases, when the energy conservation is indispensable. One example is hibernation, when the metabolism of the body decreases to 1-2% of the basal level.

Notably, the entrance to this stage is via SWS [119]. Another example is lactation, when activity of the MCHergic system is suggested to be high [111]. In lactation period, MCH expression in the medial preoptic area, a crucial region in the maternal behaviour, is very high [97]. Interestingly, milk ejection is preceded by EEG synchronization, and lactation period is accompanied by somnolence in rats [120]. In lactating humans also the increase of SWS has been reported [121].

According to preclinical studies, dysfunction of the MCH-system can be associated with many pathophysiological conditions. Shimida et al. [107] have reported that prepro-MCH knockout mice are anorectic and lean, while over-expression of MCH leads to obesity [108]. Wermter at al. have found association between single-nucleotide polymorphism in the MCHR1 gene and obesity investigating German children and adolescence [122]. Consequently, antagonists of the MCHR1 could be a potential therapeutic target in the treatment of obesity [123]. In addition, the involvement of MCH has also been suggested in the inflammatory processes of the intestine [124].

Regarding neuropsychiatric disorders, MCH evokes predominantly depression-like effect when injected into the DRN, while immunoneutralization of MCH had an antidepressive effect [125]. Similarly, antagonists on the MCHR1 evoked antidepressant effects in several model of depression and anxiety [109]. In line with its pro-depressive effect, MCH promotes the occurrence of REM sleep in animal studies [112], which sleep alteration is considered a characteristic feature in major depression disorder [35]. Taken together the above mentioned facts, MCHR1 antagonist can be potential drug targets in the treatment of depression and anxiety in the future.

Recent results has also associated MCH with the pathomechanism of narcolepsy. Bergman et al. have identified an autoantibody in the sera of a group of narcoleptic patients that showed a selective binding to MCH/proopiomelanocortin (POMC) in the hypothalamus, and this autoantibody, when injected centrally, altered the sleep pattern of rats similarly to the effect of MCHR1 antagonists [21].

5.2.4.3.3. The nesfatin-1/NUCB2

The 82-amino acid nesfatin-1 protein is the posttranslational product from the cleavage of the prohormone NEFA (for DNA binding/EF-hand/acidic protein)

/nucleobinding-2 (NUCB2). The structure of nesfatin-1/NUCB2 (nesfatin), showing 85% homology, is highly conserved among mammalian species. The NUCB2 polypeptide, composed of 396 amino acids, is preceded by a 24-amino acid signal peptide, which protein consists of an N-terminal signal peptide, a Leu/Ile rich region, a DNA-binding domain, a nuclear targeting signal, two Ca^{2+}-EF-hand motifs and a leucine zipper domain [126]. The suspected major fragments of processing are the nesfatin-1 (spanning residues 1-82), nesfatin-2 (residues 85-163) and nesfatin-3 (residues 166-369) [81]. Nesfatin-1 molecule consists of three domains: the N-terminal (N23), the middle part (M30) and the C-terminal (C29). Among these parts, the M30 active core seems to play the key role in physiological effects of nesfatin [81].

Nesfatin has been suggested to influence cross-binding of its presumptive receptor with various types of G protein, initially activating G_i, followed by the activation of G_s protein, although its receptor(s) has/have not been cloned yet [127].

Nesfatin has a wide distribution in the CNS, such as in the forebrain, the hindbrain, the brainstem and the spinal cord. Using immunohistochemistry (IHC), the largest nesfatin- immunoreactive (IR) population has been localized in the PFA and the lateral hypothalamus including the dorsolateral hypothalamus (DLH) and the ZI. In the hypothalamus, nesfatin-containing neurons can also be detected in the arcuate, paraventricular (PVN) and supraoptic nuclei (SON). The anterior and intermediate pituitary host a substantial number of nesfatin-positive neurons as well. Regarding areas outside the hypothalamus, nesfatin-IR neurons have been detected in the piriform and insular cortex, endopiriform and central amygdaloid nuclei, lateral septum, bed nucleus of the stria terminalis, medial preoptic area, raphe and ambiguous nuclei, ventrolateral medulla and gigantocellular reticular nucleus as well as the Purkinje cells in the cerebellum. Nesfatin-IR neurons have also been detected in the spinal cord in both sympathetic and parasympathetic preganglional neuronal groups, originating from thoracic, lumbar and sacral segments [126, 128-131].

In the LH, nesfatin is co-localized with several neuropeptides, like POMC, corticotrophin-releasing hormone (CRH), CART, neuropeptide Y (NPY), oxytocin and vasopressin [131, 132], as well as with neurotransmitters, like serotonin and NA. In the DLH and ZI, all MCH-containing neurons co-express nesfatin, and only a small portion

of nesfatin-IR neurons are MCH-negative [128]. In hypothalamic nuclei, nesfatin is also co-localized with a most recently identified peptide, the phoenixin (PNX) that shows a similar distribution like nesfatin [133]. Most of the above mentioned neuropeptides have also been involved in the regulation sleep-wake cycle, besides other roles, like stress-response or feeding, suggesting their integrative role in basic physiological functions.

Initial functional and neuroanatomical studies have supported the role of nesfatin as a satiety molecule. Central administration of the peptide has been shown to depress nocturnal food intake in rats in a dose-dependent manner. However, neither nesfatin-2 nor nesfatin-3 possesses this anorectic effect. Additionally, chronic icv infusion of nesfatin has been demonstrated to reduce body weight gain and the amount of white adipose tissue in rats [81, 130]. Beyond regulating food consumption, accumulating evidence proves that nesfatin plays an important role in the regulation of other physiological functions, like body temperature [134], blood pressure via the hypothalamus melanocortin 3/4 receptor (reviewed in [135]), operation of the reproductive axis [136], moreover, nesfatin has an anti-hyperglycaemic effect by regulating hepatic glucose production [137]. Nesfatin has also been involved in anxiety- and stress-related responses [138-141]. Acute 30-min restrain stress, involving physiological and physical stress components, has been shown to induce the activation of nesfatin-containing neurons in the PVN, SON, LC, ventrolateral medulla, NTS, DRN and rostral Raphe pallidus, although this relatively strong neuronal activation was not accompanied by an increased nesfatin level in the plasma [142, 143]. Another study has reported that icv administration of nesfatin-1 elevated the circulating level of adrenocorticotropin (ACTH) and corticosterone, indispensable elements of the hypothalamus-pituitary adrenal axis (HPA), suggesting the HPA-stimulating effect of nesfatin, moreover, bilateral adrenalectomy increase the expression of NUCB2 mRNA in the PVN [139] [143]. These data postulate nesfatin as a potential new player in the stress adaptation response, and thus, suggest the role of nesfatin in the pathology of stress-associated mood disorders, like anxiety and depression [141].

Anxiety is obviously a stress-related disorder, however, it has a profound effect on feeding behaviour as well [144]. The first evidence for the involvement of nesfatin in

anxiety has been demonstrated by Merali et al., indicating that icv administered nesfatin dose-dependently enhances anxiety- and fear-related behaviours in rat, as shown by different behavioural tests assessing the innate anxiety response and the conditioned fear response, through the activation of the melanocortin pathways [138] possibly inhibiting GABAergic neurons or hyperpolarizing NPY neurons in the nucleus arcuatus [145].

Nesfatin has also been associated with depression, that is, similarly to anxiety, also a common stress-related pathophysiology in humans with two-times higher incidence in women [146]. Ari et al. have reported a two-fold increase in plasma concentration of nesfatin in patients with major depressive disorder without any difference between genders [147]. In agreement with this, almost two-times higher NUCB2 mRNA level has been found in post mortem samples of rostroventral midbrain punches including the Edinger-Westphal nucleus of depressed suicide victims, compared to controls. In contrast to men, in female suicide victims, the expression was three-times lower, compared to female controls. Noteworthy, that basal expression of NUCB2 mRNA did not differ between males and females [148]. These finding suggest that nesfatin may play a role in the sex-specific pathobiology of depression. However, due to the limited number of studies, the causality has not been established yet [141].

From a clinical point of view, nesfatin can be a potential drug target in the treatment of depression or anxiety as well as metabolic disorders and obesity, particularly for patients taking antidepressive and antipsychotic medications, as resistance to leptin or some adipokines in these patients are common [149]. Another promising clinical application of nesfatin can be its use as a biomarker in epilepsy, since positive correlation has been found between nesfatin level in body fluids (plasma, saliva) and the course of epilepsy [150].

5.3. Fos expression as an indicator of neuronal activity

In neurobiology, Fos (also called c-Fos) protein, the product of one of the immediate early genes (IEGs) *c-fos*, is a widely used, reliable functional anatomical marker to visualize neuronal activity in the CNS. The expression of *c-fos* induces Fos

protein synthesis that returns to the nucleus after synthesis and acts as a transcription factor to regulate the expression of other genes. Synthesis of the Fos protein is induced in response to several extracellular signals such as growth factors, neurotransmitters (with the exception of GABA and gylcine), neuromodulators, drugs, thermal, visual and somatosensory stimuli [151, 152], while its level is low in the brain under basal conditions. Thus, the expression of *c-fos* (mRNA or the Fos protein) can be visualized by combining with various markers, including neuropeptides, proteins or retrograde tracers, etc. The expression of *c-fos* mRNA is induced in 20 minutes after stimulus, whereas the accumulation of Fos protein requires up to a 90-minute period [151, 153]. High levels of Fos protein are generally observed for hours and then decline progressively [154]. For instance, Fos protein reaches its peak level in the SCN in one-two hours after a five-minute light pulse and disappears within six hours [155]. Fos-induction is more effective when the stimulus is novel or when applied following a period of deprivation [151].

DOI: 10.14753/SE.2016.1869

6. Objectives

Hypothalamus, the key integrator area of several physiological functions in the brain, has a crucial role also in the regulation of sleep. Thus, the role of neuron populations expressing different neuropeptides in the regulation of sleep-wake cycle is an intensively investigated area with countless new questions.

Several data support the role of MCH in the regulation of sleep, besides other important physiological functions [99, 110, 112, 118]. Former data from our laboratory showed a positive correlation between the time spent in REM sleep during 'REM sleep rebound' and the activation of MCH-containing neurons [77], although it was not investigated how the MCH populations of different hypothalamic structures respond to 'REM sleep rebound'. It was also pending if an increased serotonergic-tone, known to suppress REM sleep even during the 'REM sleep rebound' is able to modify the activation of MCH neuron populations.

To examine this question, we applied a selective REM sleep deprivation followed by 'REM sleep rebound' to provoke increased neuronal activation of hypothalamic structures possibly involved in the regulation of REM sleep, parallel with the robust elevation in REM sleep. Neuromorphological examination of the brains enabled us to visualize the altered activation of different neuron populations as a result of 'REM sleep rebound'.

All hypothalamic/thalamic MCH neurons co-express nesfatin-1/NUCB2 (nesfatin), the neuropeptide that has an opposite effect on many physiological functions, however, a relative smaller population of hypothalamic nesfatin-positive neurons does not contain MCH. As no literature data was available about the role of nesfatin in the regulation of vigilance, we aimed to investigate this issue using immunohistochemistry and electrophysiology.

Based on the above mentioned aspects, our aims were the followings:

1. We intended to investigate if ‘REM sleep rebound’ causes any difference in the activation of MCH neurons of different hypothalamic/thalamic nuclei, such as ZI, LH and PFA.

2. Considering that escitalopram, the extracellular serotonin level-increasing antidepressant, suppresses REM sleep, even during ‘REM sleep rebound’, how escitalopram treatment influences the neuronal activation of MCH-neuron population during ‘REM sleep rebound’ in the investigated hypothalamic/thalamic nuclei?

3. How the activation of the hypothalamic/thalamic nesfatin-positive neuron population is influenced by REM sleep deprivation and the following ‘REM sleep rebound’? Is there any difference between the activation of MCH-positive and -negative nesfatin–neuron populations in different hypothalamic/thalamic nuclei?

4. How the exogenously (icv) administered nesfatin-1 peptide injected in the passive phase affects the architecture of sleep-wake cycle?

5. Does the icv injected nesfatin-1 alter the quantitative EEG spectra of different vigilance stages in passive phase?

6. Is there any similarity in the EEG spectral effect of icv-injected nesfatin-1 vs. 2 or 10 mg/kg escitalopram, suggesting a possible serotonergic component in the action of nesfatin-1 on vigilance?

DOI: 10.14753/SE.2016.1869

7. Materials and methods

7.1. Housing of the animals

Experiments and housing conditions were performed according to the international regulations [European Communities Council Directive of 24 November 1986 (86/609/EEC)] and the "Principles of Laboratory Animal Care" (National Institute of Health). All experiments were approved by the National Scientific Ethical Committee on Animal Experimentation, and permitted by the government (Food Chain Safety and Animal Health Directorate of the Central Agricultural Office, Permit Number: 22.1/1375/7/2010).

Male Wistar rats (from the Semmelweis University, Animal Facility, Budapest, Hungary) weighing 300–350 g were used. Animals were kept under controlled environmental conditions, with light-dark cycle of 12:12 h (10:00 A.M.-10:00 P.M, daylight type fluorescent tubes, 18 W, approximately 300 lx) at room temperature (21±1°C), and had free access to standard rodent chow and tap water. Animals were habituated to the conditions in the experimental room at least for two weeks. All efforts were made to minimize pain and suffering during the experiments.

7.2. Neuromorphological studies: *Experiment 1 and 2*

7.2.1. REM sleep deprivation (flower pot) method

For REM sleep deprivation in *Experiment 1 and 2*, we used the classic flower pot (platform on water) method set up earlier in our laboratory [112, 156, 157]. Briefly, animals were placed onto small round platforms (∅=6.5 cm, called 'small pot') situated in the middle of a round water tank (∅=41 cm) for 72 h, at lights on. The surface of the platform was 0.5 cm above the water level. The control rats were kept single undisturbed in their single home cages ('HC controls'). As lack of the muscle tone is typical in REM sleep, animals on the platforms fall into the water immediately as they switch to REM sleep. Following the 72h-long deprivation, one group of the animals had

been replaced into their singe cages and kept undisturbed for a 3h-long 'REM sleep rebound'.

Rats on the platforms were fed *ad libitum* without restriction using a waterproof food supplier unit at a distance easy to approach. Body weight change and food intake of rats during the time spent on the platforms were measured.

7.2.2. Immunohistochemistry (IHC)

Following the procedure, rats anesthetized with sodium pentobarbital (Nembutal, 35 mg/kg, i.p.; CEVA-Phylaxia) were sacrificed by transcardial perfusion using 4% paraformaldehyde in 0.1 M phosphate buffered saline, pH = 7.4 (PBS). Fixed tissue was postfixed at 4 °C overnight and cryoprotected in 20% sucrose in 0.1M phosphate buffer pH = 7.4 (PB) overnight before freezing. Then, hypothalami were cut into 50-µm-thick serial coronal sections on a frigomobile (Frigomobile; Reichert-Jung, Vienna, Austria) for immunohistochemical procedure.
The morphometrical analysis in *Experiment 1 and 2* was performed in the following hypothalamic areas (Paxinos and Watson 2007):

- zona incerta/subzona incerta (ZI)
- lateral hypothalamic area (LH)
- perifornical area (PFA)

7.2.2.1. Experiment 1. - MCH/Fos double immunostaining and morphometry analysis

First, sections were permeabilized with 0.5 % Triton X-100 for 1 h. The endogenous peroxidase activity and the nonspecific antigen binding sites were blocked with the incubation of the sections in 3 % hydrogen-peroxide solution and in 10% normal goat serum for 15 min and for 1 h, respectively. For immunostaining, solutions were dissolved in PBS and the primary antibodies were applied for 2 days at 4 °C; all the other incubations were performed at room temperature for 1h. Between the incubation steps, sections were washed for 3×10 min in PB.

Following these steps, the sections were incubated in rabbit anti-Fos (1:30,000, in PB; Santa Cruz Biotechnology, Inc., Heidelberg, Germany) primary antibody, and then in biotinylated goat anti-rabbit IgG (1:1,000) and in avidin–biotin–peroxidise

complex (ABC, 1:500) for 1 h in both solutions (both from Vector Laboratories, Burlingame, CA, USA). The immunostaining was visualized by nickel-enhanced diaminobenzidine (NiDAB) chromogen resulting in a dark-blue reaction product. Then, MHC immunostainings were performed in the same way as the first one, but in this case using rabbit anti-MCH as primary antibody (1:10,000 in 3 % BSA/0.5 % Triton X-100 from Phoenix Europe GmbH, Karlsruhe, Germany) and DAB, with chromogen resulting a brown reaction product. Finally, the sections were collected on gelatin-coated slides, dehydrated, and mounted with DPX Mountant (Sigma-Aldrich, Budapest, Hungary) mounting medium.

During the morphomety analysis, we determined the quantity of total number of the MCH-immunoreactive (MCH-IR or MCH-positive) neurons and the total amount of the Fos-immunoreactive (Fos-IR or Fos-positive) nuclei as well as the total amount of the MCH/Fos double positive neurons bilaterally in the areas of interest. For that we used at least five 50-µm-thick coronal sections per animal between bregma −2.5 and −3.5 mm caudally to bregma using a Visopan microscope (No. 361977; Reichert, Austria). In each section, four randomly selected non-overlapping areas were quantified (0.64 mm^2 altogether) under a 40× objective by the same observer in all cases. Finally, the number of cells was calculated to cells per square millimeter values. For further analysis, we calculated the ratio of the activated (Fos-positive) portion of the MCH-immunoreactive (MCH-IR or MCH-positive) neurons, namely the percent of the MCH/Fos double positive neurons.

7.2.2.2. Experiment 2. - MCH/nesfatin/Fos triple immunolabeling and morphometry analysis

The starting steps of this immunostaining was performed similarly to Experiment 1, including blocking the endogenous peroxidase activity and non-specific binding sites (here in 1% BSA), increasing permeability of the cell membranes and diluting primary and other antibodies. Sections were washed 3×5 min in PBS following each incubation step. To block peroxidase enzyme used for visualization previously, and to prevent species cross-reactions caused by primary antibodies raised in the same hosts, sections were microwave-treated in 0.1 M citric-acid (pH = 6.0) for 5 min after each immunostaining [158]. Fos immunostaining was performed using rabbit anti-Fos primary antibody (1:30,000, Santa Cruz Biotechnology, Inc., Santa Cruz, CA, USA)

and anti-rabbit IgG polymer-HRP (Millipore, Budapest, Hungary) secondary antibody. The immunostaining was visualized by FITC-conjugated tyramide according to manufacturer's instructions (Invitrogen, Budapest, Hungary). Next, sections were incubated in rabbit anti-nesfatin (1:24,000, Phoenix Pharmaceuticals, Inc., Burlingame, CA, USA) and again in anti-rabbit IgG polymer-HRP (Millipore). The second immunostaining was developed by tyramide-conjugated Alexa Fluor 568 (Invitrogen). In case of triple immunostainings for Fos, nesfatin and MCH, rabbit anti-MCH was applied (1:10,000, Phoenix Europe GmbH), followed by incubation in biotinylated anti-rabbit IgG as secondary antibody (1:1,000, Vector Laboratories, Inc., Burlingame, CA, USA) and in extravidine-peroxidase (1:1,000, Sigma). The MCH antigen was visualized by tyramide-conjugated biotin (Invitrogen) and Streptavidin-Cy5 (1:1000, Jackson ImmunoResearch Europe Ltd, Newmarket, Suffolk, UK). Sections were mounted on non-coated slides, air - dried and coverslipped with DPX (Sigma).

For morphometry analysis, images were captured bilaterally using a 20X objective (S Fluor 20X/0.75, ∞/0.17, WD1.0) on 3–5 sections per animal by a Nicon Eclipse E800 microscope attached to a Bio-Rad Radiance 2100 Rainbow confocal scanning system by sequential scanning. Cell counts and determination of co - localization were made using the AnalySIS Pro 3.2 program (Olympus, Soft Imaging Solutions GmbH, Münster, Germany), by simultaneous examination of the greyscale images of the separated channels and the coloured overlay picture. To identify neurons in the pictures, a numbered grid of the same size was placed over the overlay picture and the greyscale pictures of the separated channels. Only neurons with visible cell nuclei were counted.

For further analysis, we calculated the percentage of (i) the nesfatin/MCH double positive neurons among the nesfatin positive ones, (ii) the Fos-positive nesfatin neurons within the single nesfatin and (iii) the Fos/nesfatin/MCH within the nesfatin/MCH double positive subpopulations, per animal.

7.2.3. Drug treatment

In order to investigate how an increased serotonergic tone influences the neuronal activation of MCH- and nesfatin-positive neuron populations, we applied 10 mg/kg escitalopram-oxalate (dissolved in saline, provided by EGIS Plc., Hungary) the

highly selective serotonin reuptake inhibitor (SSRI) antidepressant, in acute intraperitoneal (ip) injection. Escitalopram (or saline) was injected prior to 'REM sleep rebound' ('rebound') period in *Experiment 1*.

7.2.4. Experimental groups

The following groups were used in
Experiment 1 (Figure 5, A)*:*

- **Small pot rebound – vehicle group (SPR-veh)**: sacrificed after spending 72h on small platform followed by a 3h-long 'REM sleep rebound' (3h after light on, on Day 4); injected with vehicle (saline) prior to 'rebound' period, (n=9)
- **Home cage – vehicle group (HC-veh):** kept undisturbed in the home cages, and sacrificed at the same time like SPR groups (3h after light on, on Day 4); injected with vehicle (saline), (n=7)
- **Small pot rebound – SSRI group (SPR-SSRI):** sacrificed after spending 72h on small platform followed by a 3h-long 'REM sleep rebound'(3h after light on, on Day 4); injected with SSRI prior to 'rebound' period (n=9)
- **Home cage – SSRI group (HC-SSRI):** kept undisturbed in the home cages, and sacrificed at the same time like SPR groups (3h after light on, on Day 4); injected with SSRI, (n=7)

Experiment 2 (Figure 5, B):

- **Small pot deprived group (SPD)**: sacrificed after spending 72h on small platform (at light on), (n=5)
- **Small pot rebound group (SPR)**: sacrificed after spending 72h on small platform followed by a 3h-long 'REM sleep rebound'(3h after light on), (n=5)
- **Home cage group (HC):** kept undisturbed in their home cages, and sacrificed at the same time like SPR group (3h after light on), (n=5)

DOI: 10.14753/SE.2016.1869

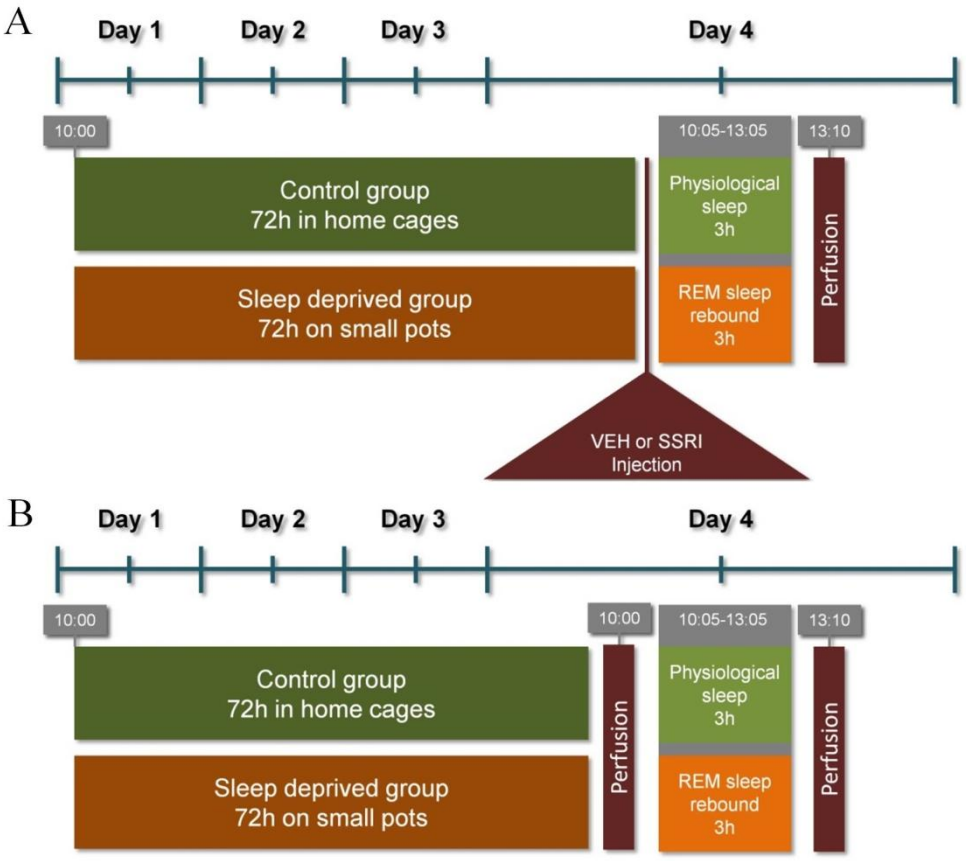

Figure 5. Schematic illustration of the flower pot sleep deprivation method in *Experiment 1* and *Experiment 2* (A-B). In *Experiment 1* (A), rats were injected with 10 mg/kg ip SSRI (escitalopram) or vehicle (VEH, saline) just prior to the 3h-long sleep. Following the 72h-long REM sleep deprivation or home cage stay (in case of controls) during Day 1 – Day 3, animals were allowed to sleep in their own cages for 3h on Day 4. The 'REM sleep rebound' and home cage animals were sacrificed at the same time (ca. 13:10 h). In *Experiment 2* (B), one subgroup of the sleep deprived animals was sacrificed immediately following the 72 h deprivation (ca. 10:00), and another subgroup of them was sacrificed after the 3h 'rebound sleep' (ca. 13:10 h). Home cage animals were sacrificed at the same time with 'REM sleep-rebound' rats. All animals were perfused transcardially for immunohistochemical procedure.

7.3. Electroencephalography (EEG): *Experiment 3 and 4*

In order to investigate the effect of exogenously administered nesfatin-1 on the EEG pattern of sleep-wake cycle and the quantitative EEG power spectra, as well as to

compare the quantitative power spectra of nesfatin-1 and escitalopram, we performed EEG study.

7.3.1. EEG surgery

Rats (n=6/group) were equipped chronically with electroencephalographic (EEG) and electromyographic (EMG) electrodes for EEG recordings, as described earlier (Kantor, 2004). Stereotaxic surgery was performed under 2% halothane anesthesia (using Fluotec 3 halothane vaporizer). Briefly, stainless steel screw electrodes were implanted epidurally over the left frontal motor cortex (coordinates: anterior-posterior (A-P): 2.0 mm from bregma, lateral (L): 2.0 mm to the midline, [159] the left parietal cortex (A-P: 2.0 mm from lambda, L: 2.0 mm) for fronto-parietal EEG recordings, and a ground electrode was placed over the cerebellum. In addition, EMG electrodes (stainless steel spring electrodes embedded in silicon rubber, Plastics One Inc., Roanoke, VA, USA) were placed into the muscles of the neck. To record motor activity of the animal, electromagnetic transducers were used in which potentials were generated by movement of the recording cable [160].

In case of *Experiment 3*, during the surgery, for the icv injections, we implanted a plastic cannula into the right lateral ventricle (coordinates: A-P: −0.8 mm to the bregma level, L: 2.0 mm, and ventral: 4.0 mm below the skull surface). The cannula and the EEG electrodes were anchored to the skull with dental cement (Spofa Dental a.s., Markova, Czeh Republic). A stainless steel obturator was inserted into the guide cannula and was kept patent until use. The placement of the cannula was verified at the end of the study by injecting 10 nM/3 µl of angiotensin II icv [161-163]. Only animals reacting with an intensive (3 ml water intake in 30 min) drinking response were included in the study.

After surgery, rats were kept in single cages in the recording chamber, and were allowed to recover for 7 days. Animals were then habituated to the recording conditions for five days before experiment started by attaching them to the polygraph using a flexible recording cable and an electric swivel, fixed above the cages, permitting free movements for the animal. During the recovery and the habituation period to the recording conditions, animals were also handled daily to minimize future experimental stress, as described earlier [164].

DOI: 10.14753/SE.2016.1869

7.3.2. EEG data acquisition

The signals were amplified (amplification factors ca. 5,000 for EEG and motor activity, 20,000 for EMG), conditioned by analogue filters (filtering below 0.50 Hz and above 60 Hz at 6dB octave^{-1}) and subjected to analogue to digital conversion with a sampling rate of 128 Hz. The digitalized signals are stored on the computer for further analysis.

7.3.3. Design of *Experiment 3 and 4*

7.3.3.1. Experiment 3. – Effect of centrally administered nesfatin-1 on the EEG

On the day of the experiment, 25 pmol/5 µl of nesfatin-1 dissolved in physiological saline was injected into the lateral ventricle of rats at light onset (at 10:00 am.). Control rats received 5 µl physiological saline icv. After injections, animals returned to their home cages and EEG, EMG, motility and video was recorded for 24 h. Considering the possible effect of stress on vigilance, caused by the icv - procedure, despite former habituation, the 1st h of all EEG recordings has been excluded from the analysis. Thus, the 2nd-6th h of passive (light) phase, as well as the first six hours of active (dark) phase (13th-18th h) have been included in the sleep analysis. See the experimental design on Figure 6.

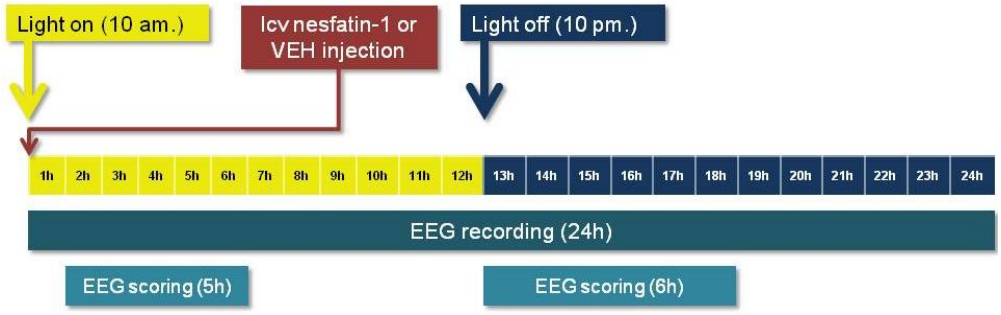

Figure 6. Experimental design of the electroencephalographic (EEG) study in *Experiment 3*: the effect of nesfatin-1 on the sleep-wake cycle and EEG spectra. EEG recording was performed for 24h following the intracerebroventricular (icv) administration of nesfatin-1 or vehicle (VEH, saline) in the passive phase at light on (10:00 h). Scoring of the EEG recordings were performed during the 2nd-6th h of passive phase and the first 6 h of active phase (13th-18th h).

7.3.3.2. Experiment 4. – Effect of two doses of intraperitoneally injected escitalopram on EEG

On the day of the experiment, 2 or 10 mg/kg escitalopram-oxalate dissolved in vehicle [solution of 10% (2-hydroxypropyl)-β-cyclodextrin, Sigma-Aldrich] was injected ip at light onset (at 10:00 am.). Control rats received vehicle ip. in the same volume (1ml/kg body weight). After injections, animals returned to their home cages and EEG, EMG, motility as well as video were recorded for 24 h. The quantitative EEG spectra of the first three hours were evaluated, compared to control.

The following experimental groups were used:

- Escitalopram 2 mg/kg (n=13)
- Escitalopram 10 mg/kg (n=12)
- Vehicle (n=9)

7.3.4. Sleep scoring

The vigilance states were classified by SleepSign for Animal sleep analysis software (Kissei Comtec America, Inc., USA) for 4 sec periods using conventional criteria [160, 165] followed by visual supervision of an expert scorer who was blind to experimental treatment. We differentiated the following vigilance stages:

1) **Wakefulness**; EEG is characterized by low amplitude activity at beta (14–30 Hz), alpha (8–13 Hz) and theta (5–9 Hz) frequencies; according to high or low EMG and motor activity, wakefulness can be subdivided into active- (AW) and passive wakefulness (PW), respectively

2) **REM sleep**; low amplitude and high frequency EEG activity with regular theta waves (5–9 Hz) accompanied by silent EMG and motor activity with occasional twitching

3) **Intermediate stage of sleep (IS)**; a brief stage just prior to REM sleep and sometimes just after it, characterized by unusual association of high amplitude spindles (mean 12.5 Hz) and low-frequency (mean 5.4 Hz) theta rhythm

4) **Non-REM sleep**; slow cortical waves (0.5–4 Hz) accompanied by reduced EMG and motor activity. Depending on the amount delta power non-REM sleep can be subdivide into light and deep slow wave sleep (SWS1 and SWS2, respectively) [160].

In sleep analysis after icv nesfatin-1 treatment, the following vigilance parameters were calculated: time spent AW and PW, REM sleep, SWS1 and SWS2 per hour. Additionally, specific parameters were calculated, namely, the number and the average duration of episodes in REM sleep, IS, SWS1 and SWS2. An episode of any vigilance stages was defined as an item lasting at least 4 sec and not interrupted by any other vigilance stages for longer than 4 sec. Sleep fragmentation was defined as the number of wake epochs (AW, PW) after a sleep stage (SWS1, SWS2, REM and IS).

7.3.5. EEG power spectra analysis

EEG power spectra (quantitative EEG spectra, qEEG) were computed for consecutive 4s epochs in the frequency range of 0.25-60 Hz (using fast Fourier transformation routine, Hanning window; frequency resolution 0.25 Hz). Adjacent 0.25 Hz bins were summed into 1 Hz bins. Bins are marked with their upper limits; therefore, e.g. 2 Hz refers to 1.25-2.00 Hz. Epochs with artifacts were omitted from the EEG power analysis. The EEG power values of the consecutive epochs were averaged in the summarized 2^{nd}-3^{rd} h of passive/light phase to obtain the power density values for the following vigilance stages: AW, PW, SWS1, SWS2 and REMS. To reduce individual differences, we normalized data dividing the EEG power values at each Hz of frequency by the summed whole spectra (0.25-60 Hz) in case of each animal.

7.3.6. Heat map spectra

To compare the spectral distribution of EEG power of different vigilance stages in the nesfatin- and escitalopram-treated groups in the summarized 2^{nd}-3^{rd} h of passive phase, we adapted ‘state space analysis technique’ (modified after Diniz-Behn et al. [166]). We plotted EEG power values of each epoch (4s interval) as Ratio 1 (6.5-9/0.5-9 Hz) on the abscissa and Ratio 2 (0.5-20/0.5-60 Hz) on the ordinate, which defined 2-dimensional spectra separating three clusters, correspond to the conventionally determined vigilance stages, namely REM sleep, non-REM sleep and wake. Ratio 1 was determined to emphasize high theta (6.5-9 Hz) activity which dominates REM sleep in rodents. Although this range is slightly different from that considered generally as theta range in rat (5-9 Hz), we used the 6.5-9 Hz range, as cluster-separation was more

efficient using this one. Ratio 2 (0.3-20/0.3-55 Hz) was developed to separate non-REM sleep and wake [166]. We adopted this range with little modification (0.5-20/0.5-60 Hz), as our setup measures the frequency range of 0.5-60 Hz. To visualize not only the dispersion but also the density of EEG power data of clusters, we created a heat map with centroids, where red colour shows higher, while blue colour shows lower density of epochs at a given point. The general positions of 'state space clusters' associated with REM sleep, non-REM sleep and wake stages is considered to be conserved [21]. We marked the stage cluster centroids with white and black dots in the control and the treated groups, respectively, to visualize both the direction and the degree of the shift from the 'control position' as a result of treatment, demonstrating the alteration of EEG power density. Centroids were calculated by averaging EEG power data (arithmetic mean calculated from the x and y coordinates of each epoch) of animals within control and (nesfatin-1- or escitalopram-) treated groups in passive phase. To perform heat map spectra from EEG power data Matlab software was used.

DOI: 10.14753/SE.2016.1869

7.4. Statistics

We used STATISTICA 7.0 program (Statsoft Inc., Tulsa, OK, USA) to perform statistics. For the evaluation of the IHC data, one-way analysis of variance (ANOVA) or (in case of inhomogeneous variances) one-way ANOVA on Ranks were used, followed by all pairwise comparisons with Dunn's or Tukey's method, respectively. Data in all figures are expressed as mean ± standard error of mean (SEM).

Sleep data of different vigilance stages, summarized hourly, were evaluated by two-way ANOVA for repeated measures (repeated factor: time). In case of inhomogeneous variances of the experimental groups, repeated measures ANOVA on Ranks was performed. For post hoc analysis, Tukey HSD was used.

The effect of nesfatin-1 and (2 or 10 mg/kg) escitalopram on the power spectra, compared to vehicle, was analysed in each vigilance stage, during the summarized 2^{nd}-3^{rd} h using repeated measure two-way ANOVA with two main factors: 'treatment' and 'frequency bands' (repeated factor). For multiple post hoc comparisons, Holm-Sidak method was used. We indicated significant multiple comparison results even if the RM ANOVA had no significant main effect, as Holm-Sidak method is not restricted to use as a follow-up test after ANOVA [167].

Regarding the heat map spectra, shifts in the centroids were evaluated with two-tailed unpaired t-tests (nesfatin-1-treated group vs. control) as well as with one-way ANOVA followed by Tukey's multiple comparison test or (in case of inhomogeneous variances) Kruskal-Wallis test followed by Dunn's multiple comparison (2 mg/kg and 10 mg/kg escitalopram-treated groups vs. control). To test the equal variances Brown-Forsythe test was used. The results are presented as mean ± (SEM).

DOI: 10.14753/SE.2016.1869

8. Results

8.1. Immunohistochemistry

8.1.1. *Experiment 1*: Activation of MCH neuron population as a result of 'REM sleep rebound' in different hypothalamic/thalamic nuclei

We found that in the vehicle-treated small-pot REM sleep-deprived group, 'REM sleep rebound' (SPR-veh) caused a significant increase in the neuronal (Fos) activation of the MCH-containing neurons in different hypothalamic/thalamic structures, like the ZI, the LH and the PFA including the perifornical nucleus itself (Figure 7, A, B, C, respectively), compared to vehicle-treated home cage (HC-veh) group. In the SPR-veh group, the ratio of Fos-positivity in the MCH-IR neurons was 65.69±6.98% in the ZI, 64.99±5.47% in the LH and 56.24±7.15% in the PFA. In the HC-veh group, the Fos-positive rate of MCH-containing neurons was quite low (less than 2 % in all the investigated areas). The effect of Tukey's *post hoc* comparisons following significant one-way ANOVA results (see later) are indicated on Figure 7, A, B, C.

We also investigated whether an increased serotonergic tone is able to influence this strong neuronal activation of the MCH-positive neurons. For that, escitalopram, a highly selective SSRI antidepressant was applied in acute ip injections (or vehicle for controls) prior to the beginning of the 3h-long 'REM sleep rebound' (for experimental design, see Figure 5, A in Methods). According to our results, escitalopram significantly decreased the rate of activated MCH-containing neurons in the ZI, LH and PFA. In the SPR-SSRI group, the Fos-ratio of MCH-neurons was the following: ZI: 56.33±11.32%, LH: 52.03±8.52% and PFA: 46.08±9.79%.

One-way ANOVA results for the comparison of the four experimental groups (SPR-veh, SPR-SSRI, HC-veh and HC-SSRI) in the investigated areas are the following: ZI: $F_{(3,28)}=187.3$, $p<0.0001$; LH: $F_{(3,28)}=271.8$, $p<0.0001$; PeF: $F_{(3,28)}=161.3$, $p<0.0001$. Tukey's *post hoc* results (depicted on Figure 7.) show that escitalopram markedly reduced the rate of MCH/Fos in the SPR-SSRI group in all the investigated areas, compared to the SPR-veh group.

DOI: 10.14753/SE.2016.1869

On the contrary, we did not find any difference in the neuronal activation of MCH-positive neurons between the HC-SSRI and HC-veh groups in any of the investigated structures (Figure 7, A, B and C). On the other hand, two-way ANOVA showed a significant interaction between the 'REM sleep rebound' and escitalopram treatment in the ratio of MCH/Fos in both the LH ($F_{(1,28)}$=15.37, p<0.001) and the PFA ($F_{(1,28)}$=4.459, p<0.05), although in the ZI, we found only a tendency ($F_{(1,28)}$=3.875, p=0.0590). However, the total number of MCH-IR neurons (Fos–positive and –negative together) was not affected by the experimental procedures (Figure, 7, D). Representative figures about the MCH/Fos immunostainings investigating three hypothalamic structures in the four experimental groups are depicted on Figure 8.

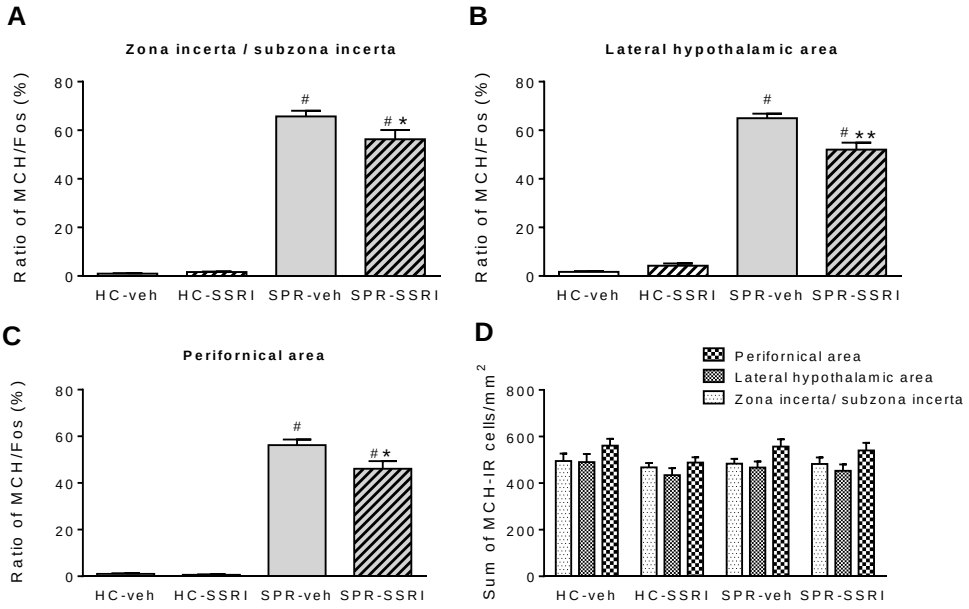

Figure 7. The neuronal (Fos) activation of the melanin-concentrating hormone (MCH)-containing neuronal cell population of different hypothalamic/thalamic structures as a result of 'REM sleep rebound' and selective serotonin reuptake inhibitor (SSRI) treatment and their combination. The ratio of MCH/Fos in the (A) zona incerta/subzona incerta, (B) the lateral hypothalamic area and (C) the perifornical area in the vehicle- and SSRI-treated home cage [HC-veh (n=7) and HC-SSRI (n=7), respectively] and 'REM sleep rebound' [SPR-veh (n=9) and SPR-SSRI (n=9), respectively] groups. The total amount of MCH-immunoreactive (IR) neurons per mm^2 (D) was not influenced by the experimental procedure in the investigated nuclei. Note, that Fos-positivity of MCH neurons was significantly increased by 'REM sleep rebound', however, SSRI-treatment decreased it in all the investigated structures. Results of *post hoc* comparisons: *: p<0.05 and **: p<0.01 compared to SPR-veh, #: p<0.05 compared to HC-veh.

DOI: 10.14753/SE.2016.1869

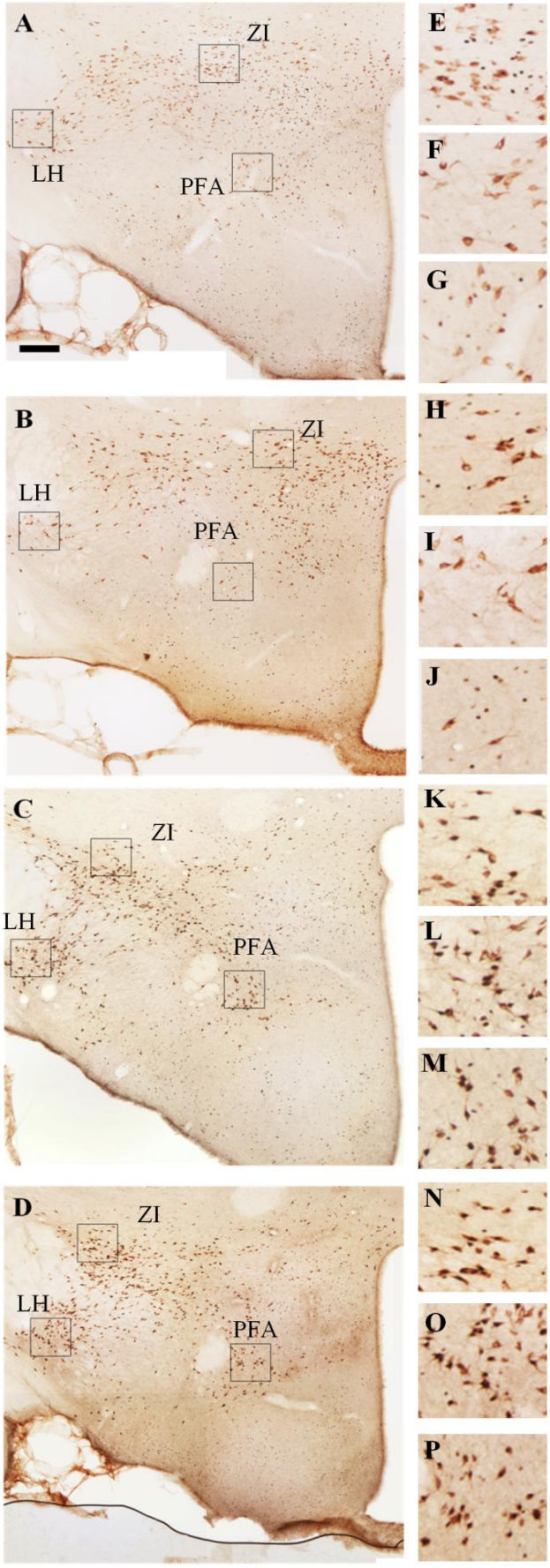

Figure 8. Illustrative pictures about the MCH/Fos double immunostaining visualizing the neuronal (Fos, bluish nuclei) activation of the melanin-concentrating hormone (MCH)-expressing neurons (brown cytoplasmatic staining) in different hypothalamic nuclei in four experimental groups as a result of 'REM sleep rebound' and combined SSRI-treatment (A-P). A-D, Lower magnification pictures of the presented sections in the experimental groups (A, vehicle-treated home cage; B, SSRI- treated home cage; C, vehicle-treated 'small pot REM sleep-rebound'; SSRI-treated 'small pot REM sleep-rebound'). Higher magnification of the boxed zones on A, B, C and D pictures show the areas of interest: ZI: zona incerta/subzona incerta (on E, H, K and N panels), LH: lateral hypothalamic area (on F, I, L and O panels) and PFA: perifornical area (on G, J, M and P panels). Note the high rate of MCH/Fos double-labeled cells in the 'REM sleep rebound' groups (C, D as well as K-M and N-P). However, the decrease in MCH/Fos ratio caused by escitalopram-treatment (panel D and N-P vs. panel C and K-M) is not apparent at this magnification (D and N-P). In the HC groups, MCH/Fos double-labeled cells among MCH-immunoreactive neurons are almost absent (A-M). Scale bar = 100 μm. The boxed zones are 100 μm×100 μm.

DOI: 10.14753/SE.2016.1869

8.1.2. *Experiment 2*: Activation of nesfatin-containing neurons in different hypothalamic/thalamic structures as a result of 'REM sleep rebound'

Regarding data in the literature, namely, (i) all MCH-positive neurons co-express the neuropeptide nesfatin-1/NUCB2 (nesfatin), (ii) but only a portion of nesfatin-IR neurons co-express MCH [128], moreover, (iii) there is a strong connection between the activation of MCH-neuronal population and REM sleep, we aimed to investigate how the MCH-positive and -negative nesfatin-IR neuronal cell populations respond to 'REM sleep rebound'.

First, we determined the degree of co-localization of MCH and nesfatin in HC controls. The rate of co-localization showed slight differences in the investigated areas: ZI: 81.9±1.7%, LH: 75.4±2.1%, PFA: 66.2±4.8% and these ratios were not affected by the 'REM sleep rebound'.

Investigating the MCH/nesfatin co-expressing neuron populations in the ZI, LH and PFA, we found that neuronal (Fos) activation was minimal (less than 0.5%) both in HC controls and the SPD group. However, 'REM sleep rebound' caused a significant elevation in the rate of neuronal activation regardless of the area investigated (ZI, 86.9±2.9%, $H=11.04$, $p<0.01$; LH: 79.0±1.8%, $H=9.673$, $p<0.01$ and PFA: 78.3±2.7%, $F_{(2,12)}=818.1$, $p<0.0001$, Figure 9, A).

However, the MCH-negative nesfatin neurons showed higher activity in HC and SPD groups, particularly in the PFA (24±8.1% and 39.4±7.4% in HC and SPD groups, respectively). 'REM sleep rebound' caused an increase in the Fos positivity, although it reached the level of statistical significance only in the LH (SPR: 37.6±4.8% vs. HC: 6±2.4%, $F_{(2,12)}=21.12$, $p<0.01$, Figure, 9, B). For the illustration of nesfatin/MCH/Fos triple immunostaining, see Figure 10. The results of Tukey's or Dunn's *post hoc* tests are shown on Figure 9, A and B.

DOI: 10.14753/SE.2016.1869

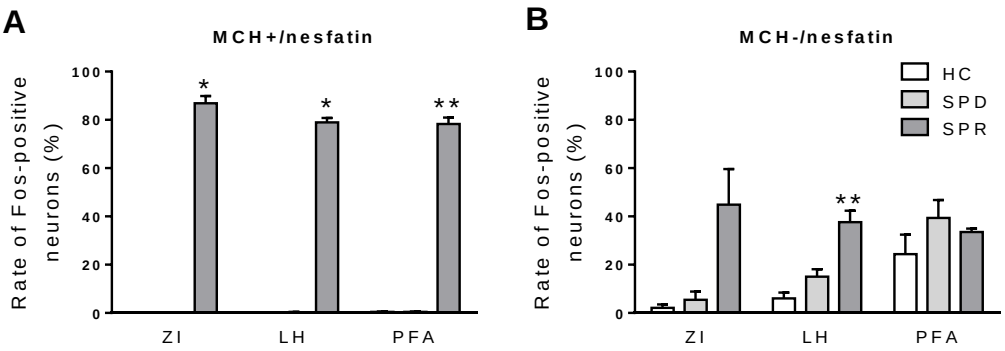

Figure 9. The neuronal (Fos) activation of the melanin-concentrating hormone (MCH)-positive and MCH-negative nesfatin cell populations of different hypothalamic/thalamic structures as a result of REM sleep deprivation and 'REM sleep rebound' (A-B). The following experimental groups were used: small pot REM sleep deprived (SPD, n=5), small pot 'REM sleep rebound' (SPR, n=5) and home cage controls (HC, n=5). Regarding the MCH-positive nesfatin-population (A), minimal (<0.5%) neuronal activation was detected in HC and SPD groups, while 'REM sleep rebound' caused a markedly elevated Fos activation in the zona incerta/subzona incerta (ZI), the lateral hypothalamic area (LH) and in the perifornical area (PFA). In the MCH-negative nesfatin population (B), in HC and SPD groups, a higher Fos activity was detected, particularly in the PFA. However, 'REM sleep rebound' caused a significant elevation in Fos-positivity only in the LH. Results of *post hoc* comparisons: *: $p<0.05$, **: $p<0.01$ compared to HC controls.

Similarly to the effect of escitalopram on the Fos-positivity of the MCH-IR neuron-population, escitalopram also decreased the rate of neuronal activation in the nesfatin-positive neuron population. The average reduction of nesfatin/Fos was 12.2% (n=3), however, due to the small number of cases we did not have enough statistical power to evaluate the effect of escitalopram in this case.

DOI: 10.14753/SE.2016.1869

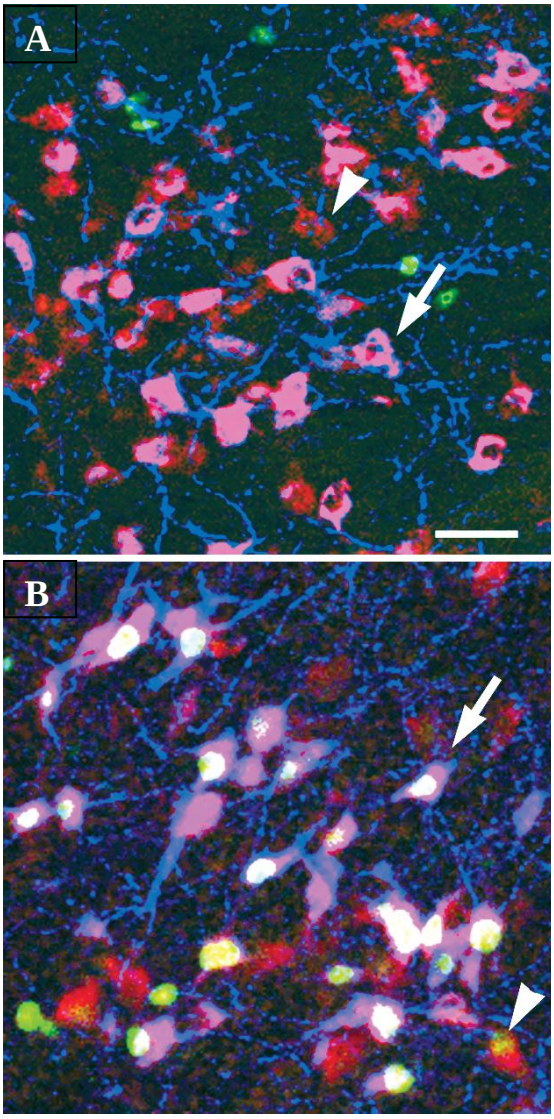

Figure 10. Photomicrographs illustrating the results of triple fluorescent immunostaining, visualizing the melanin-concentrating hormone (MCH)-positive and –negative nesfatin-1/NUCB2 (nesfatin) neurons in the lateral hypothalamic area of home cage (A) and 'REM sleep rebound' group (B). The staining was the following: blue for MCH, red for nesfatin and green for Fos. On the pictures, nesfatin/MCH double-positive neurons are pink (arrows), MCH - negative nesfatin neurons are red (arrowheads). Activated nesfatin/MCH neurons show white nuclei, activated nesfatin - positive, but MCH - negative neurons have yellow nuclei. Note, that the majority of the MCH - positive nesfatin neurons (arrows) are activated by rebound (Fos - positive), while only a few of the MCH - negative nesfatin neurons (arrowheads) showed Fos - positivity. Scale bar: 100 μm. Data are shown as mean ± SEM, n = 5.

DOI: 10.14753/SE.2016.1869

8.2. Electroencephalography (EEG)

8.2.1. The effect of exogenously administered nesfatin-1 on the architecture of sleep-wake cycle

The high neuronal activity of the MCH/nesfatin-co-expressing cell population, as a result of 'REM sleep rebound', raised the question, whether nesfatin-1 neuropeptide, the N-terminal fragment of the nucleobindin 2 protein (NUCB2) itself, can influence sleep-wake cycle or not. To investigate this question, we injected 25 pmol nesfatin-1 icv at the beginning of passive phase, and analysed the architecture of sleep-wake cycle (i) during the 2^{nd}-6^{th} h after injection, and (ii) for the possible rebound effect, at the beginning of the active phase (13^{th}-18^{th} h, see chapter 8.2.1.2.).

8.2.1.1. Passive phase: 2^{nd}-6^{th} hours following central injection

We found that icv nesfatin-1 significantly elevated sleep fragmentation, namely the number of awakenings ($F_{(1,10)}$=5.1046, $p<0.05$). However, the amount of total sleep time showed only a tendency to decrease during the five investigated hours of passive phase ($p = 0.0587$).

Regarding the effect of nesfatin-1 on different stages of sleep-wake cycle, we observed the most apparent change in REM sleep. It decreased the time spent in REM sleep significantly ($F_{(1,10)} = 18.99$, $p<0.001$), compared to controls. This reduction was approximately 60% in the 2^{nd} h, but in the next three hours, the decrease in REM sleep reached an approximate value of 90%, while in the 6^{th} h it was ca. 70% (Fig. 11, A). Due to the REM sleep-suppressing effect of nesfatin-1, we could calculate REM sleep data of only four animals in the nesfatin-1-treated group. The amount of IS showed a similar decrease, with the lowest value in the 3^{rd} h ($F_{(1,10)} = 11.04$, $p<0.01$, Fig. 11, B).

Considering the time spent in non-REM sleep, we differentiated light slow wave sleep (SWS1) and deep slow wave sleep (SWS2). In SWS1, a significant time × treatment interaction ($F_{(2,20)} = 4.092$, $p<0.05$) was found, when repeated measure ANOVA was performed including the 2^{nd}, 3^{rd} and 4^{th} hours only. The significant results

DOI: 10.14753/SE.2016.1869

of the *post hoc* comparisons are shown on Fig. 11, C. In SWS2, we found no alteration in any investigated hours, compared to control (Fig. 11, D).

In wakefulness, the amount of PW elevated markedly ($F_{(1,10)} = 8.955$, $p<0.05$, Fig. 11, E), while the time spent in AW revealed no alteration (Fig. 11, F).

DOI: 10.14753/SE.2016.1869

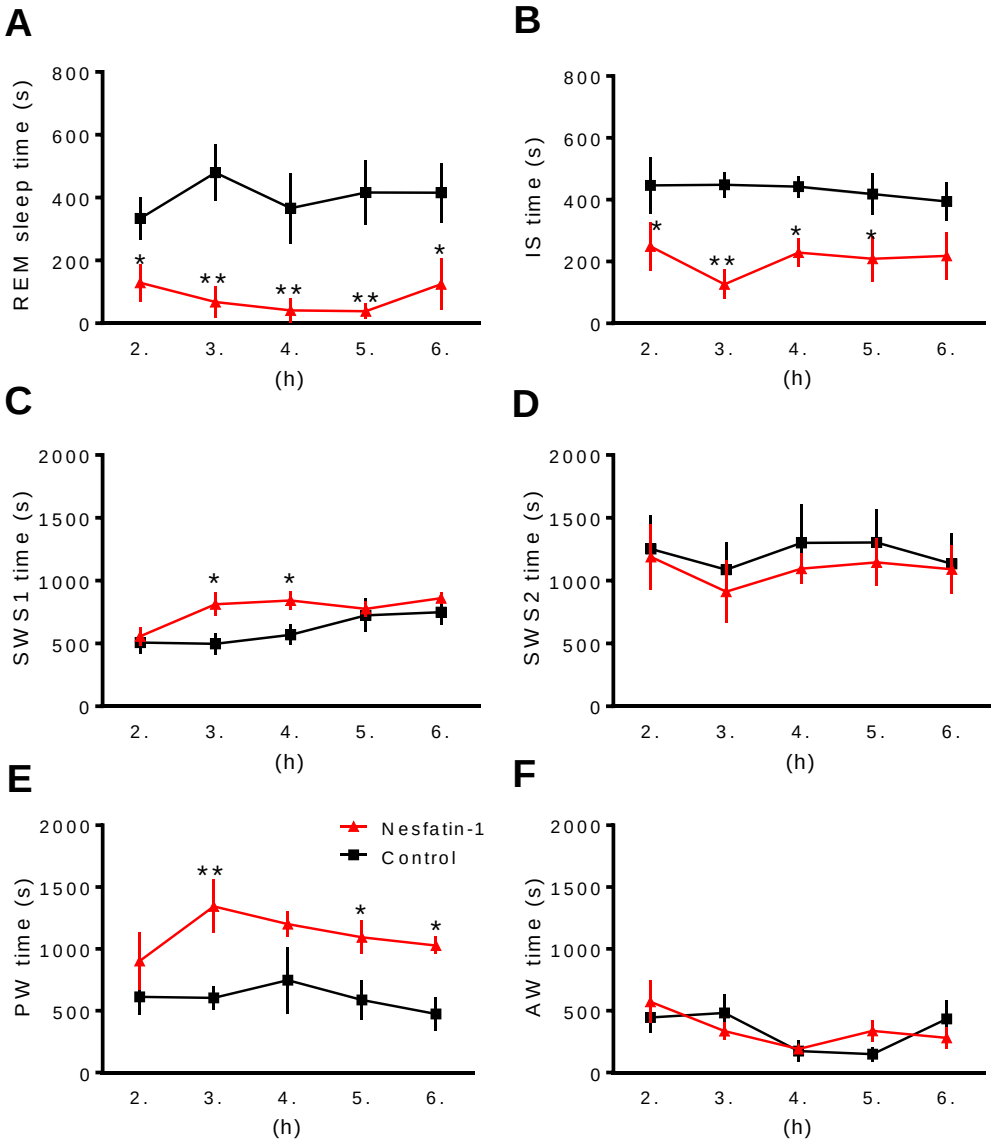

Figure 11. The effect of intracerebroventricularly (icv) administered nesfatin-1 on the architecture of sleep-wake cycle (A-F). (A, B) The time spent in rapid eye movement (REM) sleep and intermediate stage of sleep (IS), (C, D) light and deep slow wave sleep (SWS1 and SWS2, respectively), as well as (E, F) active and passive wake, respectively in the 2nd–6th hours of passive (light) phase, compared to (icv vehicle) control group. Note, that nesfatin-1 affected REM sleep, PW and IS markedly and SWS1 for a short time, while SWS2 did not show any alteration. Data are presented as mean ± SEM, n = 6 per group, p*<0.05, p**<0.01. Due to the REM-suppressing effect of nesfatin-1, in the nesfatin-1-treated group, REM amount was calculated using only n=4 data.

DOI: 10.14753/SE.2016.1869

The REM sleep- and IS-declining effect of nesfatin-1 seemed to be apparent also in the number and the average duration of the episodes in both REMS ($F_{(1,10)}$ = 10.45, $p<0.01$ and $F_{(1,10)}$ = 12.81, $p<0.01$, Fig. 12, A and B, respectively) and IS ($F_{(1,10)}$ = 7.18, $p<0.05$ and $F_{(1,10)}$ = 6.99, $p<0.05$, Fig. 12, C and D, respectively).

Noteworthy, that the increase of SWS1 and PW (Figure 11, C and E) was parallel to the elevation of episode-numbers generally ($F_{(1,10)}$ = 9.87, $p<0.05$, Fig. 13, A and ($F_{(1,10)}$ = 6.46, $p<0.05$, Fig. 12, E, respectively), although the average episode-durations of these stages were unaffected (Fig. 13, B and 12, F, respectively). However, the time spent in SWS2 showed no alteration despite the significant increase in the number of episodes in the 4th h (Fig. 13, C).

DOI: 10.14753/SE.2016.1869

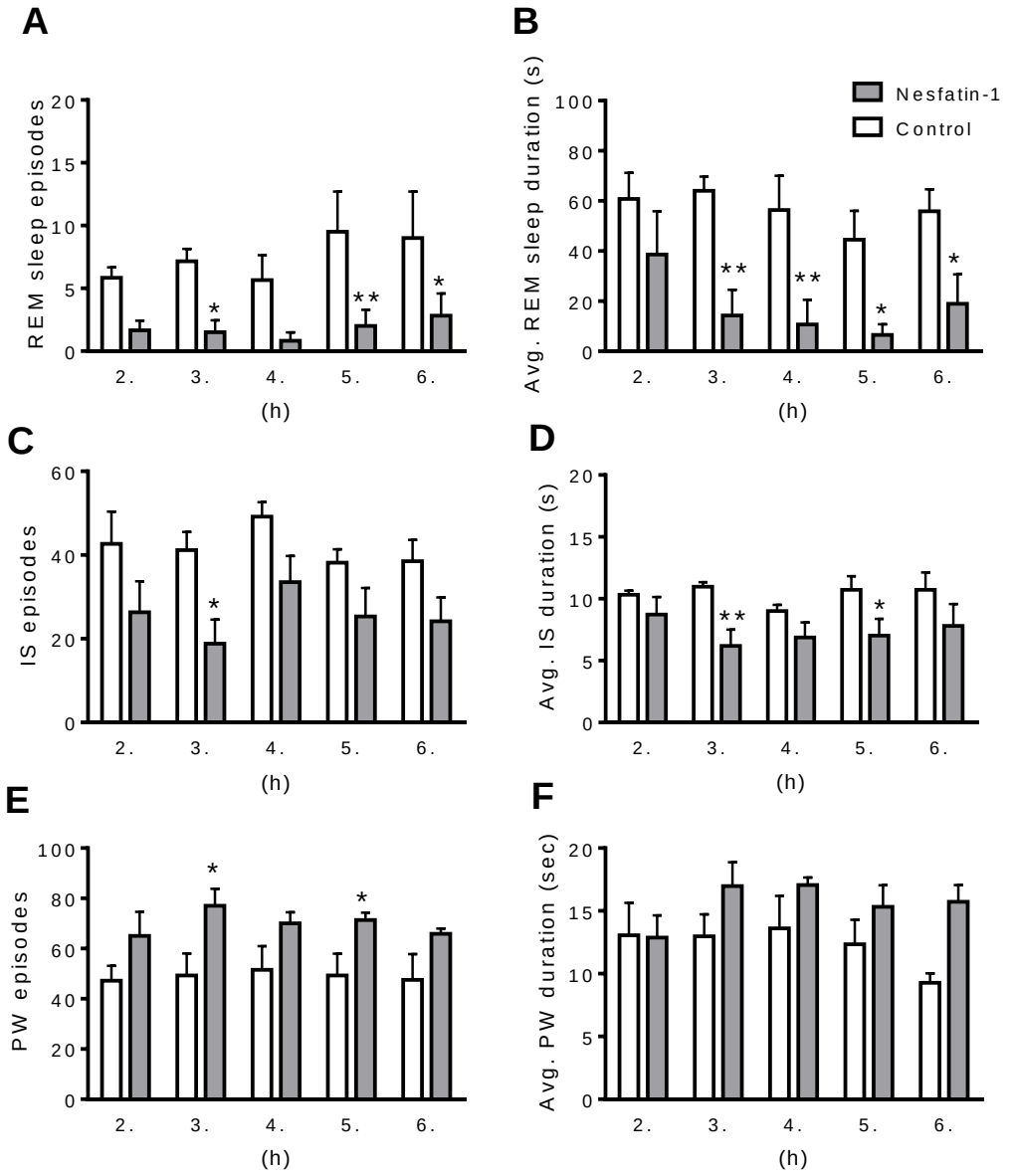

Figure 12. The effect of intracerebroventricularly (icv) administered nesfatin-1 on the number and average duration of episodes in different vigilance stages during the 2nd-6th h of passive (light) phase (A-F). The number of episodes in rapid eye movement (REM) sleep (A), intermediate stage of sleep (IS, C) and passive wake (PW, E), as well as the average duration (Avg. duration) of episodes in REM sleep (B), IS (D) and PW (F) vigilance stages, compared to (icv vehicle) control group. Note the definite decreasing effect of nesfatin-1 on both the number and average duration of REM sleep and IS episodes, while in case of PW, nesfatin-1 influenced only the number of episodes. Data are presented as mean ± SEM, n = 6 per group, p*<0.05, p**<0.01. Due to the REM-suppressing effect of nesfatin-1, in the nesfatin-1-treated group, REM data were calculated only using n=4 data.

DOI: 10.14753/SE.2016.1869

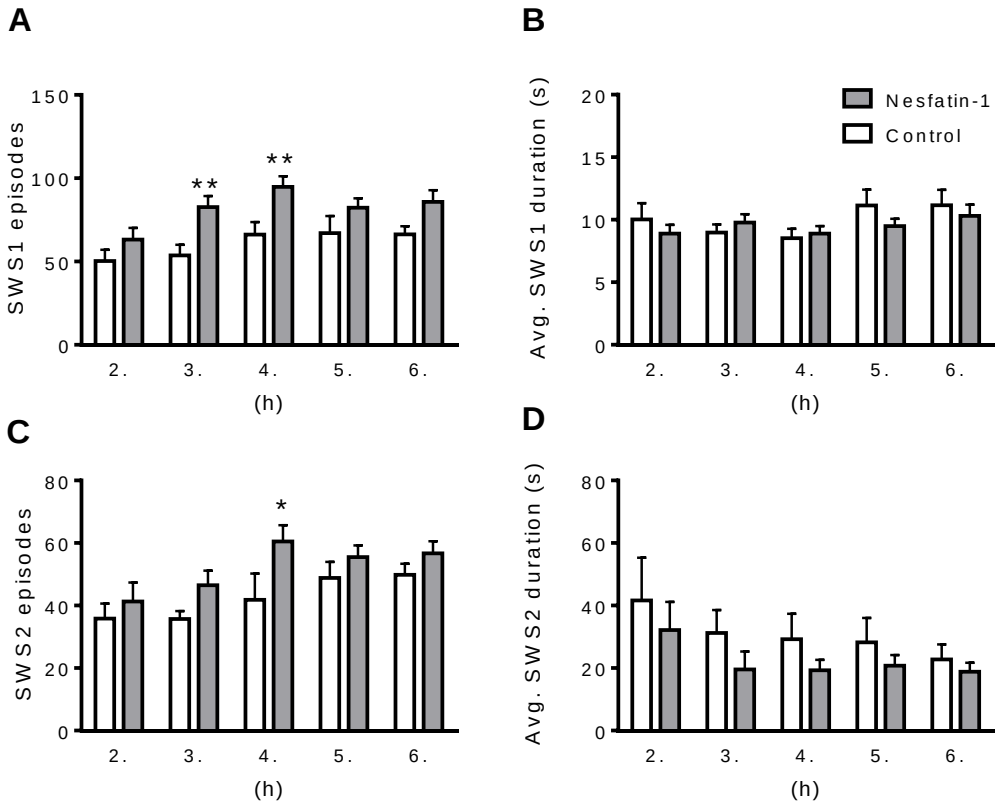

Figure 13. The effect of intracerebroventricularly (icv) administered nesfatin-1 on the number and average duration of episodes in non-REM vigilance stages during the 2nd-6th h of passive (light) phase (A-D). The number of episodes in light and deep slow wave sleep (SWS1 and SWS2, A and C, respectively), and the average duration (Avg. duration) of SWS1 and SWS2 episodes (B and D, respectively), compared to (vehicle) control group. Note that despite the increasing effect of nesfatin-1 on the episode number in both SWS1 and SWS2, the average duration of the episode was not changed. Data are presented as mean ± SEM, n = 6 per group, p*<0.05, p**<0.01.

8.2.1.2. Active phase: 13th-18th hours following central injection

In contrast to the alterations of sleep time in passive phase, we found no significant change in the time spent in different vigilance stages in the active phase after 25 pmol icv nesfatin-1 (Fig. 14).

DOI: 10.14753/SE.2016.1869

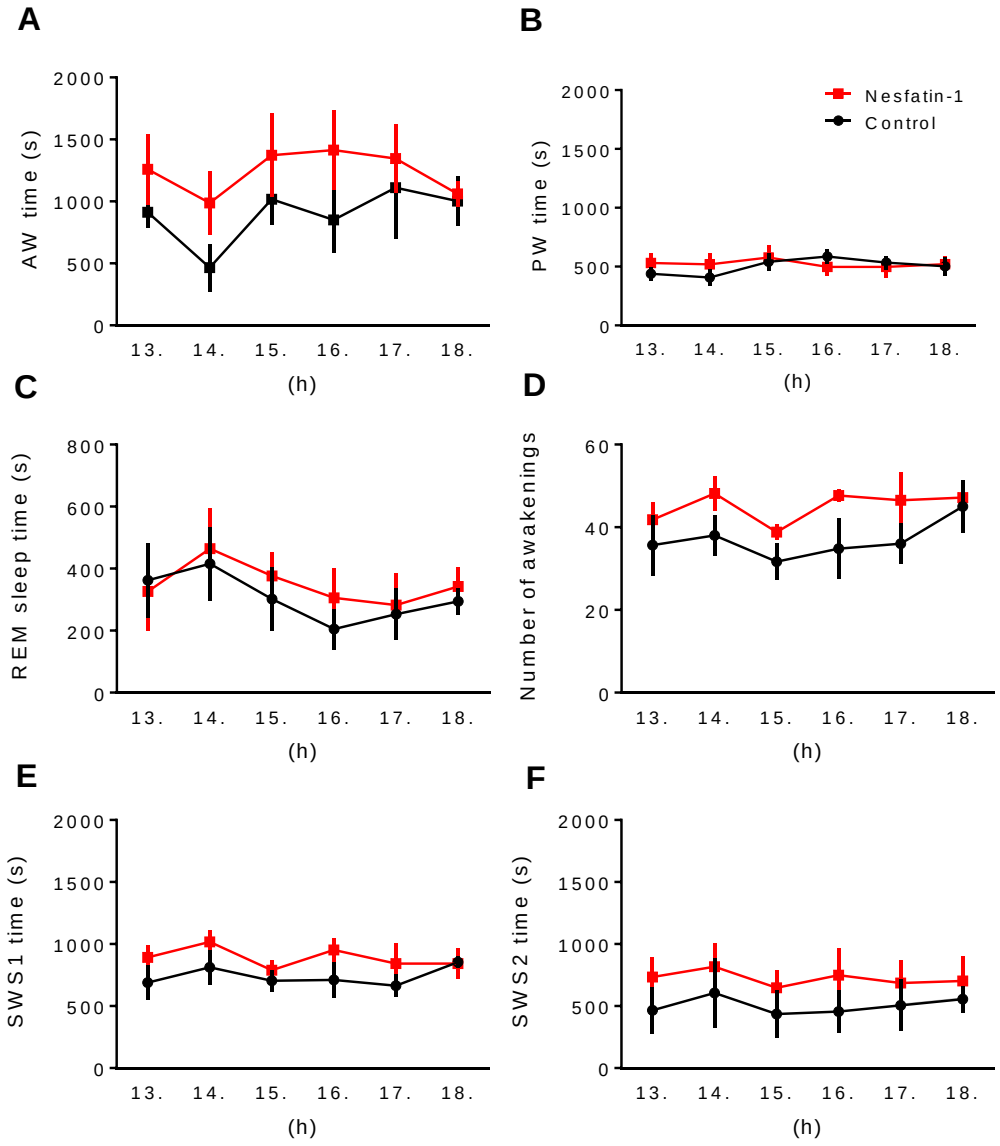

Figure 14. The effect of intracerebroventricularly (icv) administered nesfatin-1 on the architecture of sleep-wake cycle in the active (dark) phase (13-18 h after injection, A-F). The time spent in active and passive wake (A and B), rapid eye movement (REM) sleep (C), light and deep slow wave sleep (SWS1 and SWS2, E and F, respectively), as well as number of awakenings (i.e. sleep fragmentation, D) during the 13-18 hours, compared to (vehicle) control group. Note that nesfatin-1 did not affect any of the vigilance stages significantly 13-18 h after the icv injection. Data are presented as mean ± SEM, n = 6 per group.

DOI: 10.14753/SE.2016.1869

8.2.2. Comparison of the EEG power spectral data of nesfatin-1 and escitalopram using 'state space analysis'

Based on the strong REM sleep-decreasing and passive wake-increasing effect of nesfatin-1 in our study, as well as literature data [143] have reported that icv nesfatin-1 elevates the neuronal (Fos) activation of DRN and MRN serotonergic neurons, we raised the question whether the effect of icv nesfatin-1 can be associated with the serotonergic system or not. To address this issue, we investigated the possible similarities between the effect of nesfatin-1 and escitalopram, the selective SSRI antidepressant that is known to increase the serotonergic tone even after acute dosing. For this comparison, we used a relative new method [21], the 'state space analysis' technique (partly modified after Diniz-Behn et al. [166]).

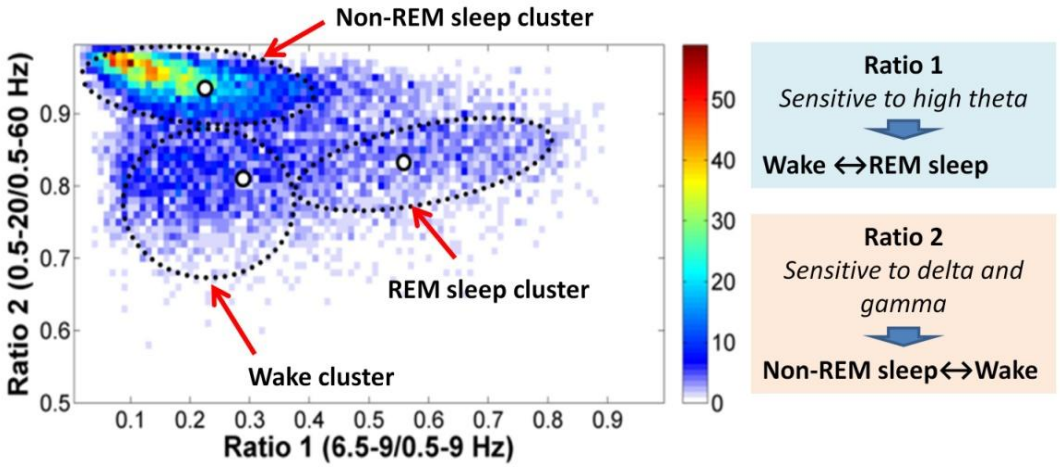

Figure 15. Demonstration of the basic concept of 'state space analysis' (modified after Diniz Behn et al. 2010 [170]. Each point on the plot represents a 4s-period (one epoch) of the sleep-wake cycle. Ratio 1 [6.5-9/0.5-9 Hz] and Ratio 2 [0.5-20/0.5-60 Hz], calculated from the Fast Fourier Transformed EEG spectral data for each epoch, determines the position of each epoch, defining a 2D heat map. Ratio 1 (on the abscissa) is sensitive to high theta content, thus, it will effectively separate 'REM sleep cluster' from 'wake cluster' (with greater and lower amount of high theta power, respectively), while Ratio 2 separates 'non-REM sleep cluster' and 'wake cluster' based on the delta (0.5-4 Hz) and gamma power (30-60 Hz) content of epochs. White circles show the centroid of each cluster calculated from the arithmetic mean of the coordinates of EEG data points. The alteration in the extension, shape, density and centroid position of wake, non-REM and REM sleep clusters suggests changes in the EEG spectra as a result of treatment.

This technique enables visualization of the ‘topography’ of different vigilance stages using heat map spectra, moreover, can provide a way to observe general EEG spectral changes (‘shifts’) that are visible easily to the naked eye; and since the ‘topography’ of non-REM, REM sleep and wake stages is based on their power spectral content, ‘state space analysis technique’ can be performed without sleep scoring (Figure 15). However, in this chapter, I also demonstrate the traditional way of evaluation of EEG spectral data to reinforce results of ‘state space analysis technique’.

To visualize the spectral distribution of EEG power data in different vigilance stages, we plotted EEG power data as Ratio 1 (6.5-9/0.5-9 Hz, on the *x* axis) and Ratio 2 (0.5-20/0.5-60 Hz, on the *y* axis) defining two-dimensional spectra in the passive phase (Figure 16), in both the control and nesfatin-1-treated groups.

These ratios separated EEG power data into clusters, corresponding to the conventionally determined vigilance stages, namely REM sleep, non-REM sleep and total wake (TW). To visualize not only the dispersion but also the density of power data, we created heat maps. The distribution of ‘state space clusters’ shows that nesfatin-1 treatment significantly diminished the extent of the cluster corresponds to the REM sleep stage, compared to vehicle (Figure 16, C and A, respectively), reinforcing the REM sleep-inhibiting effect of icv nesfatin-1 (chapter 8.2.1.1.). The result of unpaired t-test indicated a significant shift in the centroid position of ‘REM sleep cluster’ ($t=2{,}337$, $df=8$, $p=0.0476$), but we note, that due to the REM suppressing effect of nesfatin-1, REM sleep data were evaluated using only n=4 REM data (Figure 16, C).

Since in the spectral analysis of passive phase, the most remarkable alteration was found in wakefulness, we demonstrated the heat map of TW separately (control and nesfatin-1-treated groups, Figure 16, B and D, respectively). These figures show that nesfatin-1 treatment caused a significant shift ($p=0.0283$, $t=2.563$, $df=10$) in the position of centroids (black circles) of the cluster corresponds to wake, compared to control (Figure 16, D and B, respectively). This shift to the left visualizes the significant theta power-reducing effect of nesfatin-1 in wakefulness. As Figure 16, C shows, icv nesfatin-1 caused no alteration in the centroid position of non-REM sleep evaluated with the ‘state space analysis’ technique.

DOI: 10.14753/SE.2016.1869

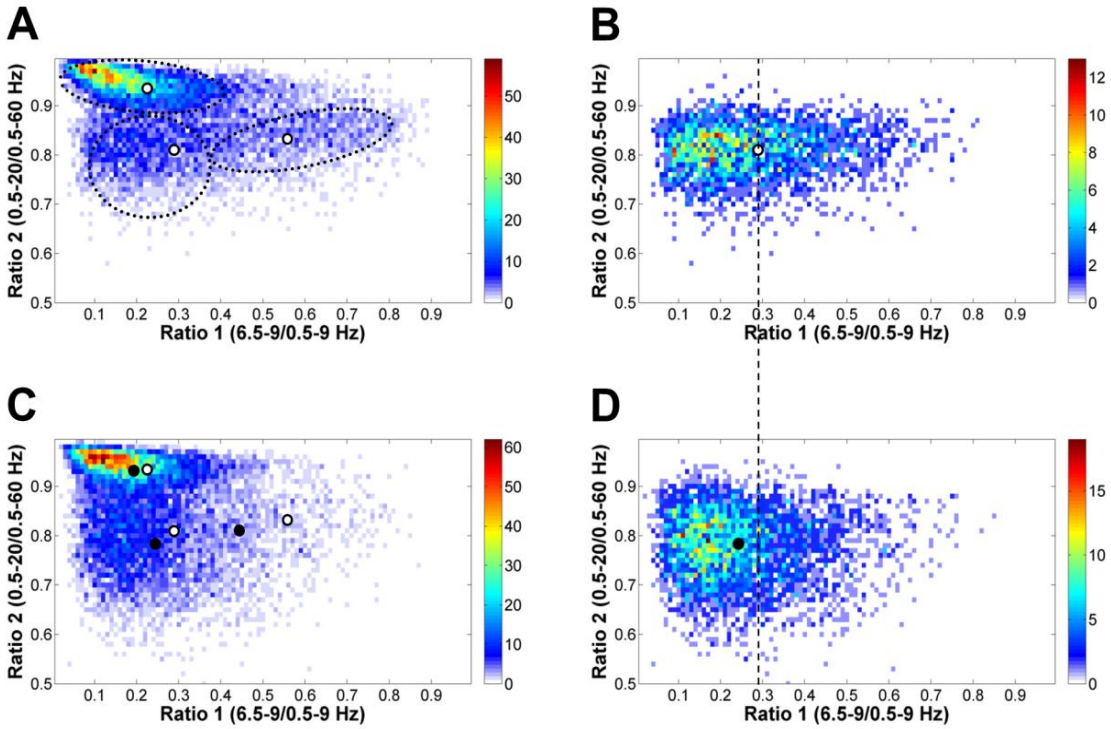

Figure 16. Demonstration of the effect of icv-injected vehicle (A and B) or nesfatin-1 (C and D) on the distributions and density of EEG power in passive (light) phase on a 2-dimensional 'state space' heat map (modified after Diniz Behn et al. 2010 [170]). Plotting the spectral ratios of EEG power data (Ratio 1 [6.5-9/0.5-9 Hz] on the abscissa and Ratio 2 [0.5-20/0.5-60 Hz] on the ordinate) separated three distinct clusters of EEG power points: rapid eye movement (REM) sleep: right, non-REM sleep: upper left and total wake: lower left (circled on Fig. A). Each plot represents EEG power data (including n=6 animals per groups) of the 2-3h of recordings on colour-coded density maps (digits on the scale show the number of overlapping epochs on a given area). Note the obvious alterations in the distribution of clusters in the nesfatin-1-treated group (C) compared to the control group (A). Apparently, the cluster corresponds to REM sleep is significantly sparser, than that in the control. (B and D) Heat map spectra to visualize the alteration of EEG power in total wake in the nesftain-1-treated group separately (D), compared to control (B). Note that besides the higher density of wake epochs in the nesfatin-1-treated group, the centroid of wake is shifted to the left, compared to vehicle, possibly due to the decreased theta power in wake. Centroids (arithmetic mean of the given cluster) of the nesfatin-1- and vehicle-treated group are shown by black and white circles, respectively. The shift in the position of centroids as a result of nesfatin-1 treatment in TW, compared to control is shown by the dotted line. We note, that due to the REM sleep-inhibiting effect in the nesfatin-1-treated group, REM sleep data were evaluated only from n=4 data.

DOI: 10.14753/SE.2016.1869

In the active phase, we did not find significant shift in the centroid position of REM, non-REM sleep and wake stages versus control (data not shown).

To compare the effect nesfatin-1 on ‘state space’ heat map spectra with the effect of a serotonergic-tone-increasing agent, we used 2 and 10 mg/kg escitalopram in ip injections at the beginning of passive phase. Figure 17 demonstrates that both the distribution and the density of the REM sleep-cluster shows a decrease after 2 and 10 mg/kg escitalopram, compared to control (Figure 17, C, E and A, respectively). In case of the 10 mg/kg escitalopram-treated group, the area correspond to the ‘REM sleep cluster’ barely can be seen due to the strong REM sleep-inhibiting effect of escitalopram in this dose (Figure 17, E).

DOI: 10.14753/SE.2016.1869

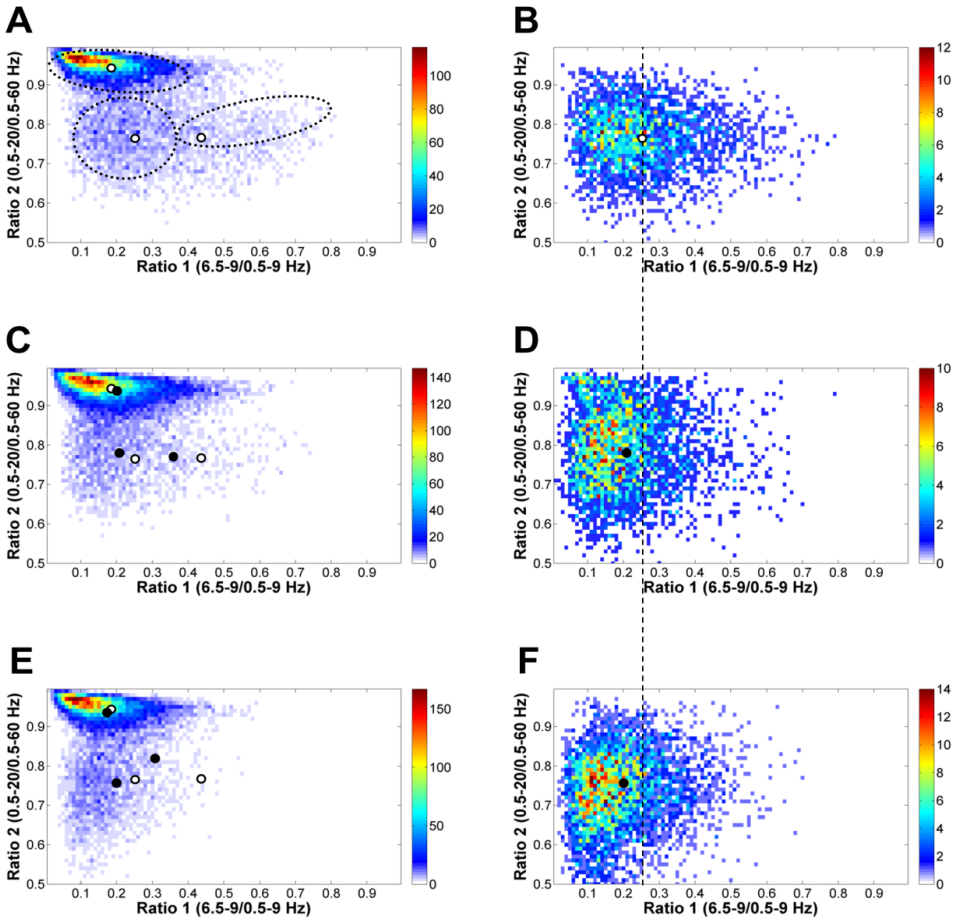

Figure 17. Demonstration of the effect of 2 and 10 mg/kg escitalopram or vehicle (of the summarized 2nd-3rd h) on the distributions and density of EEG power in passive (light) phase on a 2-dimensional 'state space' heat map (modified after Diniz Behn et al. 2010 [166]). Plotting the spectral ratios of EEG power data (Ratio 1 [6.5-9/0.5-9 Hz] on the *abscissa* and Ratio 2 [0.5-20/0.5-60 Hz] on the *ordinate*) separated three distinct clusters of EEG power points: rapid eye movement (REM) sleep: right, non-REM sleep: upper left and wake: lower left. Each plot represents EEG power data of 2 h recordings during the 2nd-3rd h on colour-coded density maps (digits on the scale show the number of overlapping epochs on a given area). REM sleep cluster show a dose-dependent decrease in density and a definite shift to the left in the centroid-position of the clusters in the 2 and 10 mg/kg escitalopram-treated groups (C and E, respectively) vs. control (A). The enlarged 'wake clusters' are shown in the 2 and 10 mg/kg escitalopram-treated groups (D and F, respectively) vs. control (B). The centroids of the vehicle- or the escitalopram-treated groups are indicated by white and black circles, respectively. The experimental groups included n=9 in the vehicle-treated group, n=13 in the 2mg/kg and n=12 rats in the 10 mg/kg escitalopram-treated groups, respectively. In case of the 10 mg/kg escitalopram-treated group, heat map spectrum for REM sleep was calculated from n=10 data, as two animals had no REM sleep data in the investigated 2h period.

DOI: 10.14753/SE.2016.1869

In REM sleep stage, the shift in the centroid position was significant (Kruskal-Wallis test: H=9.778, p=0.0075). However, Dunn's multiple comparisons test showed that only the 10 mg/kg escitalopram treatment caused significant shift in the centroid position, compared to control (Fig. 18, A).

On the contrary, the cluster corresponds to TW ('wake cluster') becomes apparently more populated in the 2 and 10 mg/kg escitalopram-treated groups, compared to vehicle (Fig. 17, C, E and A, respectively). We also can observe a notable shift to the left in the distribution and the centroid-position in both the 2 and 10 mg/kg escitalopram-treated groups, compared to vehicle (Fig. 17, D, F and B, respectively). According to one-way ANOVA, escitalopram caused a significant shift in the centroid-position of TW ($F_{(2,31)}$=6.732, p=0.0037). Tukey's *post hoc* test showed significant shifts in the centroid position of TW cluster in both the 2 and 10 mg/kg-escitalopram-treated groups, compared to control (Fig. 18, B).

Besides the changes in the heat map spectra of TW and REM sleep in the escitalopram-treated groups, in non-REM stage, we did not find any alteration in the centroid positions (Figure 17, C and E vs. A, Figure 18, C).

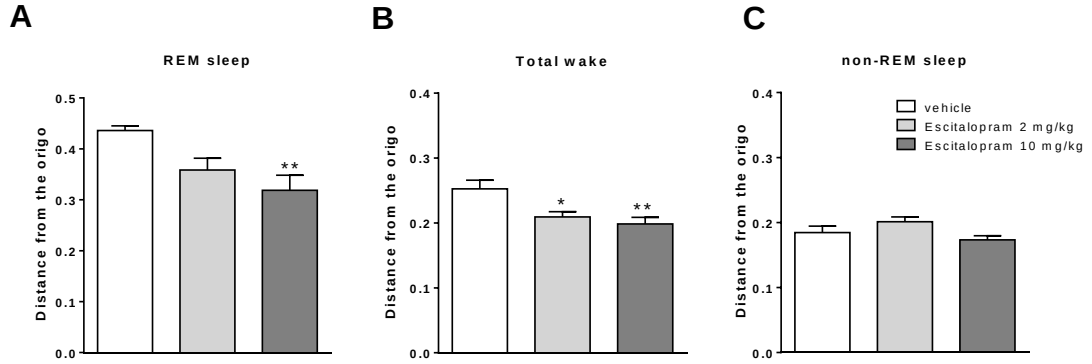

Figure 18. Demonstration of the shifts in the centroid-positions (distance from the origo on x axis) in REM sleep, total wake (TW), and non-REM sleep vigilance-stages on the 'heat map spectra' performed using 'state space analysis technique' in 2 (n=13) and 10 mg/kg (n=10-12) escitalopram-treated groups, compared to vehicle controls (n=9). Note that 10 mg/kg escitalopram caused a significant shift in both (rapid eye movement) REM sleep and wake stages (A and B), while in case of the 2 mg/kg escitalopram, the shift was significant exclusively in TW, compared to control. However, in non-REM sleep, no alteration was found in any of the experimental groups (C). Data are presented as mean ± SEM. p*<0.05, p**<0.01.

DOI: 10.14753/SE.2016.1869

As a short summary, ‘state space analysis’ indicated a shift to the left in the centroid positions on the *x*-axis of TW in the nesfatin-1- and escitalopram-treated groups, as well as in REM sleep in the escitalopram-treated groups, that suggests a possible decrease in theta power, as Ratio 2 is sensitive to the high theta-range (6.5-9 Hz).

8.2.3. Comparison of the EEG power spectra of nesfatin-1 and escitalopram using conventional spectral analysis

As ‘state space’ analysis revealed similarities between the effect of nesfatin-1 and escitalopram on the heat map spectra of wake, REM and non-REM sleep stages, I further investigated the EEG spectra in more detail using the traditional quantitative EEG spectral analysis (qEEG), separating AW and PW, REM sleep as well as SWS1 and SWS2 stages. In this case, I depicted the normalized EEG power data of the summarized 2^{nd}-3^{rd} hours in the nesfatin-1- and escitalopram-treated groups, compared to their appropriate (vehicle) control groups.

On Figure 19, the EEG power spectra from 1 to10 Hz is depicted, including the theta (5-9 Hz) and delta (1-4 Hz) range in TW, AW and PW stages. In case of nesfatin-1- and both doses of escitalopram-treated groups, we found a decrease in theta power (5-9 Hz) in TW. In the nesfatin-1-treated group, two-way repeated measure (RM) ANOVA showed a significant treatment × frequency interaction ($F_{(4,10)}$=3.958, p=0.0135), while regarding the treatment effect, we found only a tendency (p=0.0535). The same was true for both doses of escitalopram: significant interaction effects (2 mg/kg: $F_{(4,80)}$=3.175, p=0.0179, 10 mg/kg: $F_{(4,76)}$=3.390, p=0.0132;) were found. Interestingly, *post hoc* results demonstrated significant alteration at 7 Hz in the nesfatin-1-treated group, while in the escitalopram-treated groups, at 8 Hz frequency (Figure 19, A and B, respectively).

DOI: 10.14753/SE.2016.1869

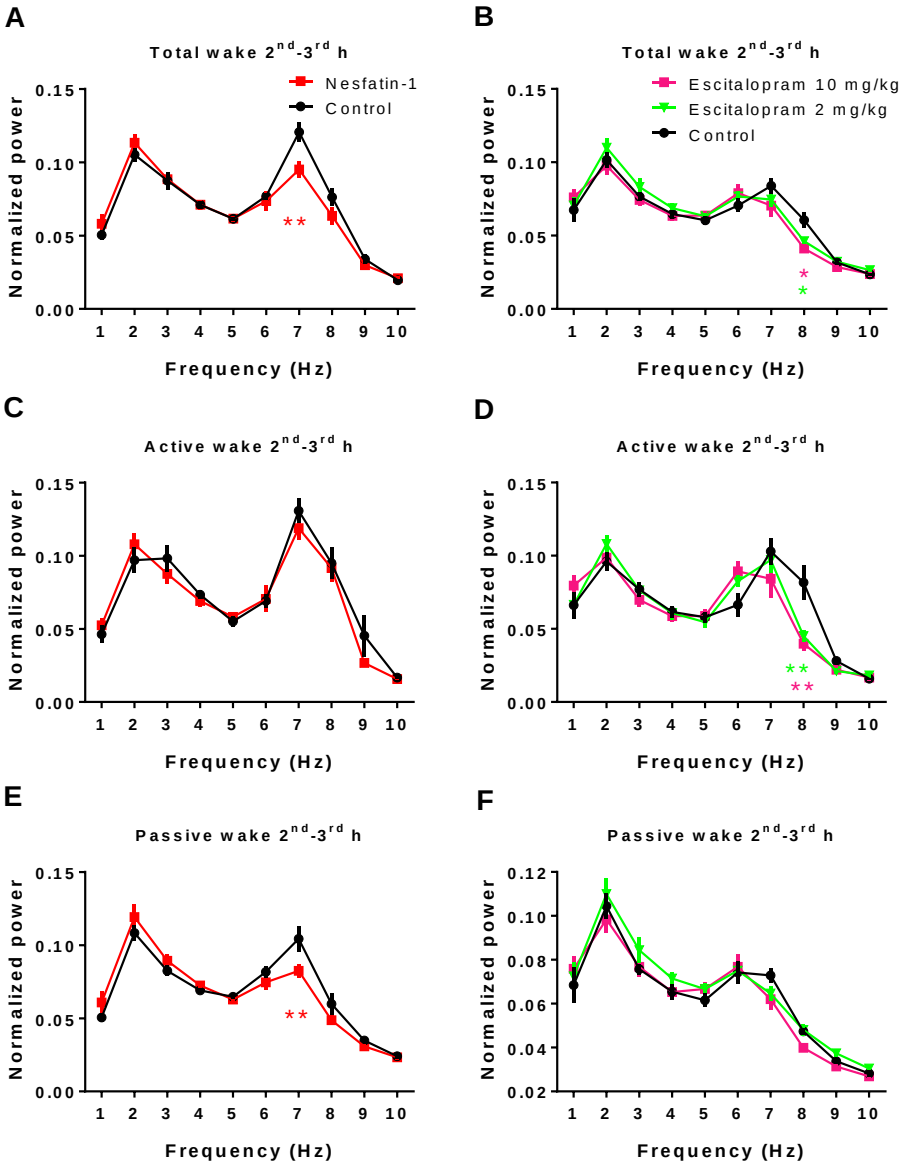

Figure 19. Effect of nesfatin-1 and two doses (2 and 10 mg/kg) of escitalopram on the EEG power of total-, active- and passive wake (TW, AW and PW, respectively) during the 2nd-3rd h of passive (light) phase (A-F). In TW, normalized theta power (5-9 Hz) decreased in the nesfatin-1-treated group and in both escitalopram-treated groups (A and B, respectively). In AW, only the escitalopram-treated groups showed a reduction in theta power (D), while in PW, the theta power was diminished only in the nesfatin-1-treated group (E), compared to control. AW in nesfatin-1-treated group as well as PW in the escitalopram-treated groups did not show any alteration (C and F, respectively). Normalized EEG power data are presented as mean ± SEM, (2 and 10 mg/kg escitalopram-treated groups, n=13 and 12, respectively, nesfatin-1-treated group, n = 6 per group). p*<0.05, p**<0.01, significant results of the Holm-Sidak's multiple comparisons test.

In the theta power of AW, RM ANOVA showed a significant treatment effect in the 2 mg/kg escitalopram-treated group ($F_{(1,20)}$=4.944, p=0.0379) and a treatment × frequency interaction only in the escitalopram-treated groups: (2 mg/kg: $F_{(4,80)}$=4.356, p=0.0031; 10 mg/kg: $F_{(4,76)}$=4.605, p=0.0022). *Post hoc* results were significant in both escitalopram-treated groups, at 8 Hz frequency (Figure 19, D). In the nesfatin-1-treated group, theta range showed no alteration, compared to control (Figure 19, C).

In contrast to AW, in PW the nesfatin-1-treated group showed a decrease in theta power (RM ANOVA 'treatment effect': $F_{(1,10)}$=6.994, p=0.0245), while the escitalopram-treated groups revealed no alteration in the theta power in PW (Figure 19, E and F, respectively). The *post hoc* comparisons showed significant result in the nesfatin-1-treated group at 7 Hz frequency (Figure 19, E).

Regarding REM sleep, both nesfatin-1 and escitalopram caused a definite decrease in the relevant theta power. In the nesfatin-1-treated group we found a significant treatment × frequency interaction ($F_{(4,32)}$=2.858, p=0.0393) with a significant *post hoc* result at 8 Hz frequency (Figure 20, A). Although it needs to be noted that due to the REM sleep-inhibiting effect of nesfatin-1, qEEG data of REM sleep were calculated only from data of four animals. In the 2 mg/kg escitalopram-treated group, we found a significant treatment × frequency interaction ($F_{(4,80)}$=3.021, p=0.0225), with a significant *post hoc* result at 8 Hz frequency (Figure 20, B). However, the 10 mg/kg escitalopram-treated group showed a significant treatment × frequency interaction ($F_{(4,64)}$=3.109, p=0.0211), without any significant *post hoc* result (Figure 20, B).

DOI: 10.14753/SE.2016.1869

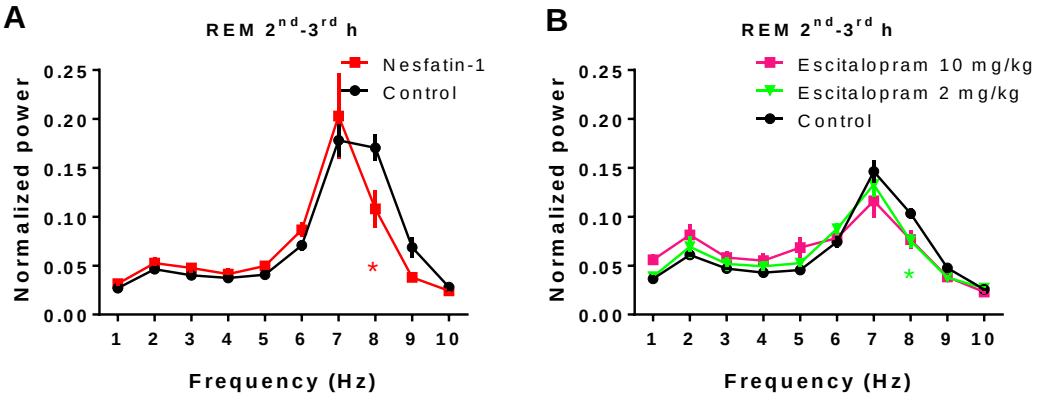

Figure 20. Effect of nesfatin-1 and two doses (2 and 10 mg/kg) of escitalopram on the EEG power of rapid eye movement (REM) sleep during the 2nd-3rd h of passive (light) phase, compared to vehicle control. Normalized theta power (5-9 Hz) decreased in both escitalopram-treated groups (B). Notably, theta power also showed a reduction in the nesfatin-1-treated group, although the amount of REM sleep data was only n=4. Normalized EEG power data are presented as mean ± SEM, (control, 2 and 10 mg/kg escitalopram-treated groups, n=9, n=13 and 12, respectively; control as well as nesfatin-1-treated group, n = 6 and 4, respectively). p*<0.05, significant results of the Holm-Sidak's multiple comparisons test.

Considering non-REM sleep, we did not find any spectral alteration in SWS1 and SWS2 in the investigated nesfatin-1- and escitalopram-treated groups, compared to their control (Figure 21).

DOI: 10.14753/SE.2016.1869

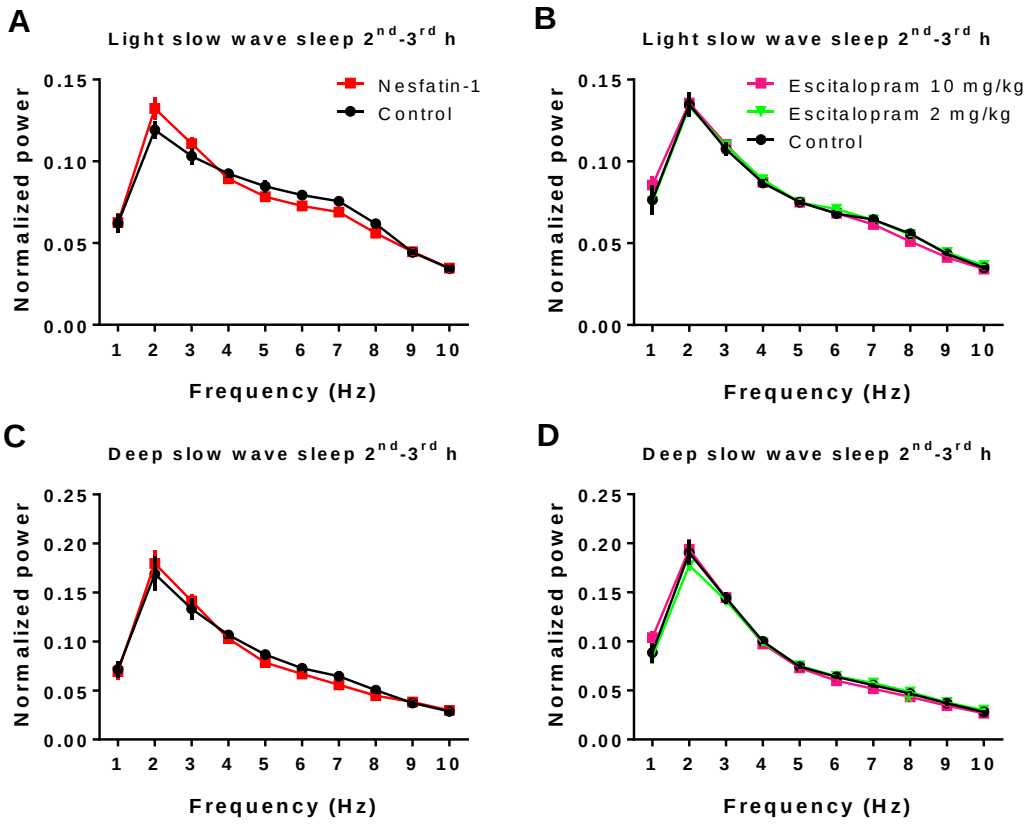

Figure 21. Effect of nesfatin-1 and two doses (2 and 10 mg/kg) of escitalopram on the EEG power of light- and deep slow wave sleep (SWS1 and SWS2, respectively) during the 2nd-3rd h of passive (light) phase (A-D). Delta power (1-4 Hz) in SWS1 and SWS2 showed no alteration either in the nesfatin-treated group (A and C, respectively) or in the escitalopram-treated groups (B and D, respectively). Normalized EEG power data are presented as mean ± SEM, (vehicle and 2 and 10 mg/kg escitalopram-treated groups, n=9, n=13 and 12, respectively, nesfatin-1-treated group and controls, n = 6 per group).

As a short summary, beyond similarities in the effect of nesfatin-1 and escitalopram, namely, the alteration in theta power in REM sleep and TW, comparison of AW and PW data reveals differences. While nesfatin-1 decreases the theta power solely in PW, escitalopram affected theta power of AW, causing a deceleration in the theta oscillation (reduction in the peak of theta power), rather than in the total power. In TW and PW, both doses of escitalopram shift the peak frequency of theta power from 7 Hz to 6 Hz, while in AW this shift was observed only in the 10 mg/kg-treated group. In the nesfatin-1-treated group, theta peak was unaffected.

DOI: 10.14753/SE.2016.1869

9. Discussion

This work is aimed to summarize our immunohistochemical and electroencephalographical findings regarding the role of two neuropeptides, the MCH and the nesfatin in the regulation of sleep and wakefulness.

We found markedly increased activation in the MCH neurons as a result of 'REM sleep rebound' ('rebound') in all the investigated hypothalamic/thalamic structures, such as the ZI, LH and PFA, and this activation was reduced by previous (10 mg/kg) escitalopram treatment. The MCH/nesfatin/Fos triple-immunostaing revealed a strong neuronal activation of MCH/nesfatin population as a result of 'rebound', while the MCH-negative nesfatin neurons showed increased Fos positivity only in the LH, compared to controls. The involvement of endogenous nesfatin in sleep regulation was further investigated by exogenously (icv)-administered nesfatin on vigilance, demonstrating a mostly REM sleep-suppressing and PW-increasing effect. The comparison of EEG spectral effect of nesfatin and escitalopram (2 and 10 mg/kg) showed similarities, like reduction of theta power in TW and REM sleep, although a more detailed spectral analysis revealed differences between nesfatin and escitalopram. While nesfatin decreased theta in PW, escitalopram diminished it in AW, and shifted theta peak to a lower value. In the EEG spectral analysis, we also demonstrated the application of 'state space analysis', a relative new method, that provides a quick topographical depiction of vigilance to visualize shifts in the EEG spectral content of different stages of sleep-wake cycle without visual EEG scoring.

To examine the association between the hypothalamic/thalamic neuropeptides and REM sleep, we used the classic 'flower pot' REM sleep-deprivation method to provoke the forced activation of neuronal populations possibly involved in the regulation of REM sleep. This 72 h-long procedure leads to a ca. 6-7-times increase in the amount of REM sleep during the 3 h-long 'REM sleep rebound' [36]. This type of REM sleep deprivation methods utilizes one of the key features of REM sleep, namely the absence of muscle tone. Briefly, rats are kept on single 'small platforms' surrounded by water, and when they switch to REM sleep, they fall into the water and awaken [168]. Besides, I mention that using 'large pot' kept animals (LP) as 'stress controls',

the effect of REM sleep deprivation can be differentiated from the unavoidable stress, since due to the larger surface of the pot, these animals are able to sleep, although they undergo the same stress like 'small pot' kept (SP) rats [157, 169, 170]. The similar stress-level is confirmed by the likewise elevated ACTH and corticosterone levels in the plasma, as well as the increased CRH in the hypothalamic PVN and the negative energy balance of both SP and LP animals, suggesting a similarly increased activity of the hypothalamic-pituitary adrenal axis [170, 171]. Despite the presence of a moderate SWS deprivation besides the total REM sleep deprivation on the 'small pots', this technique is considered a highly selective REM sleep deprivation method causing an increased amount of REM sleep, even compared to LP controls [36, 112, 156, 157, 172].

Based on our earlier findings, demonstrating a positive correlation between the neuronal (Fos) activation of the hypothalamic MCH neurons as a result of 'rebound', first, we performed a more detailed morphometrical analysis investigating the activated portion of the MCH neurons in different hypothalamic/thalamic nuclei. According to our results, 'REM sleep rebound' produced a markedly elevated activation of MCH neurons in all the investigated areas, such as the ZI, the LH and the PFA. The LH and the PFA have been implicated in the control of several physiological functions, including feeding, energy homeostasis, cardiovascular regulation, locomotor activity and the regulation of sleep and wakefulness [173]. However, ZI, "the zone of uncertainty", is considered to be the main centre in the diencephalon for the generation of direct visceral, arousal, attention and posture/locomotion responses to somatic or visceral stimuli [174]. To date, hardly any functional studies have investigated the role of ZI in sleep-wake cycle [174, 175], however, more recent data in narcoleptic mice have demonstrated that Hcrt gene transfer into the ZI was able to suppress muscular paralysis [176].

However, cell groups of ZI are contiguous and neurochemically identical with neuron populations of the hypothalamus, suggesting a close structural and functional connection between ZI and hypothalamus [174]. The ZI has been shown to possess only 18% of MCH neurons [177], however, this small MCH neuron population revealed a considerable activation as a result of REM sleep rebound in our study. This high level of activation during 'rebound' and the fact that 43% of neurons recorded from the ZI

were most active during REM sleep [178], suggests the functional role of ZI in the regulation of REM sleep. Regarding the PFH, 35% of neurons recorded from this structure showed their maximal firing rate during REM sleep suggesting the impact of also this area in the regulation of REM sleep [178]. Koyama et al. also recorded neurons from these areas that showed activity during both REM sleep and wake (ZI and PLH: 23% and 12.3% of all the investigated neurons, respectively), while during SWS, only 10% or less of neurons showed maximal firing rates in these areas. The role of PFH and ZI is notable especially in the regulation of phasic events, rather than the maintenance of REM sleep, moreover, these areas are considered to be involved also in the maintenance wake. However, ZI seems to be more closely involved in the induction of REM sleep and the generation of phasic motor or autonomic events during this stage, than PFH, namely, rapid eye movements, respiratory irregularities and blood pressure fluctuations [178]. Taken together, the high-level activity of MCH cells during 'REM sleep rebound', in line with earlier findings, further supports the strong relationship between REM sleep and the MCH system, moreover, suggests the involvement of ZI, PFA and LH in the regulation of REM sleep.

The therapeutic effect of escitalopram, the SSRI antidepressant, is linked to its extracellular serotonin level-increasing effect as a result of 5-HT reuptake inhibition. Since neuronal pathways and receptors involved in the therapeutic effect of SSRIs are largely overlapped with those in sleep regulation, these medications influence sleep, however, escitalopram is considered to be the less disruptive to sleep architecture among SSRIs [35, 179]. Yet, with increasing the serotonergic tone, escitalopram reduces the time spent in REM sleep in humans and rodents as well [35, 180]. This REM sleep-suppressing effect has been shown to prevail even in 'small pot-deprived' animals, when the ca.6-7-fold increased amount of REM sleep reduced by half [36]. In accordance with this, we observed a decrease in the activation of the MCH neurons following the 3 h 'REM sleep rebound' in all the investigated structures, despite the fact that Fos-positivity of MCH neurons was well above the physiological level. This decrease in the Fos-positivity of the MCH neurons can be the attributable to a direct postsynaptic inhibition effect of 5-HT [100] caused by the increased serotonergic tone evoked by escitalopram. In contrast to these *in vitro* findings, Kumar et al. have found increased Fos-IR in MCH neurons as a result of 5-HT given locally by unilateral

perfusion into the PF-LHA, possibly due to the reduction of inhibitory influences of GABAergic neurons by 5-HT [181]. Another possible explanation for the decrease of Fos-positivity of MCH neurons and REM-suppression can be the inhibition of the cholinergic neurons in the LDT/PPT, a core structure in the promotion of REM sleep. This inhibition is probably mediated through $5HT_{1A}$ receptors, as in $5HT_{1A}$ receptor knockout mice, the REM sleep-suppressing effect of citalopram has not been detected [34], moreover, the selective $5HT_{1A}$ receptor agonist ipsapirone is a strong REM sleep-suppressor in human [182]. However, MCH neurons have projections, among others, toward the LDT/PPT and the DRN [111], raising the possibility of a bidirectional interaction among the two systems.

On the other hand, escitalopram treatment was not able to diminish the activation of MCH neurons in the control (HC-SSRI) group, despite its definite REM-suppression detected in these rats [36]. It can be interpreted (i) by a floor-effect, as MCH/Fos was below 1-2% in the HC-SSRI group. On the other hand, (ii) although MCH neurons have primarily been involved in REM sleep generation, their function has also been suggested in the regulation of non-REM sleep, which stage was not inhibited by escitalopram, and other physiological functions as well, such as feeding [112, 113] [111].

The remarkable association between REM sleep and MCH directed our attention to nesfatin, the neuropeptide that is co-expressed by all MCH-containing neurons in the hypothalamus and ZI [128]. To investigate the nesfatin- and MCH-positive neuron populations at the same time, we performed MCH/nesfatin/Fos triple immunostaining. The MCH-nesfatin co-expression rate was the highest in the ZI, lower in the LH and the lowest in the PFA, similarly to literature data [128]. The ‘REM sleep rebound’ evoked a strong Fos expression in large percent of MCH-positive nesfatin neurons in all the investigated areas, like ZI, LH and PFA. However, MCH-negative nesfatin cells showed a moderate but significant increase in activation only in the LH, compared to controls, suggesting that nesfatin-IR cells exclusively in the LH can be associated with regulation of REM sleep, while other populations of MCH-negative nesfatin cells are possibly under a different regulation. However, the highly increased activation of MCH/nesfatin

co-expressing neurons suggests a strong association with REM sleep of all the investigated areas.

The association between nesfatin expression and REM sleep regulation is strengthened by our *in situ* hybridization and ELISA findings showing a decreased nesfatin expression a result of REM sleep deprivation, while during 'REM sleep rebound' these expressions returned to the control levels [171]. In line with these data, Jego et al. have found a positive correlation between the (Fos) activation of nesfatin neurons and the amount of REM sleep quantities, although they applied a shorter (6 h) REM sleep-deprivation and a shorter (2 h) rebound time [183].

Considering that nesfatin has been shown to influence food intake as an anorexigen [134], it is crucial to clarify that despite negative energy balance during the REM sleep-deprivation, the cumulative food intake was not changed significantly, compared to HC and LP controls [171].

To further examine the suggested link between endogenous nesfatin-expression and REM sleep, we examined the effect of exogenously (icv)-administered nesfatin-1 on the architecture of sleep-wake cycle and the quantitative EEG spectra of different vigilance stages. The applied 25 pmol dose of nesfatin-1 was established based on previous studies [81, 134, 139]. As icv procedure - despite the former habituation - is usually accompanied by increased plasma ACTH and corticosterone levels in the first 30 and 60 min, respectively [139, 143], we omitted the first hour and evaluated EEG data from the beginning of the 2^{nd} to the end of the 6^{th} hours (as part of passive phase), as well as the 13^{th}-18^{th} hours (as part of active phase) to investigate the possible prolonged or rebound effect. The most striking influence of icv nesfatin-1 on the pattern of sleep-wake cycle was the IS- and REM sleep-decreasing effect that lasted 5–6 hours following administration. Decrease in both the number and the average duration of REM sleep and IS episodes seemed to be implicated in this effect, suggesting that neurons responsible for the induction and maintenance of IS and REM sleep may be influenced. We also showed a remarkable alteration in PW: the increase in this stage was still significant in the 6^{th} hour, although AW revealed no alteration in any hour. However, sleep fragmentation (the number of awakenings) also increased significantly. The decline of REM sleep and IS was probably associated with a short-time increase of

SWS1 in the 3rd and 4th hours, however, the amount of SWS2 was unaffected. The total sleep time showed only a tendency for decrease. Regarding active (dark) phase, we did not find any prolonged or rebound effect of icv nesfatin-1.

The precise mechanism of action regarding the effect of nesfatin in the sleep-wake regulation needs a refinement in the future. Enhanced activity of different component of the ARAS, like the serotonergic, noradrenergic, and/or reduction in the arousal threshold of the midbrain reticular formation by nesfatin-1 directly or indirectly, could be one explanation. This hypothesis is in line with the results of Yoshida et al., namely that icv injected nesfatin-1 induced neuronal activity (Fos expression) in serotonergic cells of the DRN and MRN as well as in the noradrenergic neurons in the LC [143], structures comprising parts of the ARAS, subsequently enhancing the activation of vlPAG and the adjacent lateral pontine tegmentum. These latter regions are expected to function as REM-off structures giving inhibitory GABAergic innervation to the SLD, that possesses REM-on function [14, 184]. However, icv nesfatin-1 injection also caused (Fos) activation of neurons in the PVN, the nucleus of the solitary tract and the SON [143]. As these structures have been related to stress, their activation consequently may alter sleep architecture too [185-187]. Increase in the time spent in PW by nesfatin, similarly to escitalopram, suggests an increased serotonergic tone, as in contrast to other wake-related neuromodulatory systems, serotonergic neurons support a state of quiet or relaxed wakefulness [188].

However, beyond the similarities in the effect of nesfatin-1 and the serotonergic-tone increasing escitalopram, like reducing the amount of REM sleep, decreasing the number and average duration of REM episodes as well as increasing PW and SWS1 amount, there are also differences, namely, while nesfatin decreases IS amount and episode numbers, escitalopram caused an increase in this stage [180].

The IS sleep stage, that usually precedes or follows REM sleep, is characterized by high-amplitude anterior cortex spindles as well as low-frequency hippocampal theta oscillation. This stage is suggested to correspond to a brief functional disconnection of the forebrain and the brainstem as a result of the massive decrease of brainstem ascending influences [15]. The mental content of IS, namely “feeling of indefinable discomfort, anxious perplexity and harrowing worry” was reported in normal subjects

when behaviourally awakened from this stage. This mental content was presumably linked to the transient suppression of the brainstem ascending influences, leading to uncontrolled higher nervous processes. The discrepancy in the IS effect of nesfatin and escitalopram may be explained by their different effect on the ascending brainstem influences, or on the GABAergic influences, leading to hyperpolarisation of thalamocortical neurons, the degree of which is very high during IS. However, literature data regarding the neuroanatomical regulation of IS are very sparse [15].

Thus, despite the considerable overlap between the influence of nesfatin and escitalopram, we cannot explain the effect of icv nesfatin-1 on vigilance with an increased serotonergic tone exclusively. To clarify the mechanism how nesfatin influences sleep-wake cycle, and to prove the involvement of a serotonergic component in the effect of nesfatin, further studies are needed.

In contrast to our results, Jego et al. have reported REM sleep-increasing effect of icv nesfatin-1, but this effect was significant only when injecting 250 pmol dose, and when cumulating REM sleep quantities over the 8h post-treatment. They did not detect any change in the average duration of REM sleep episodes, non-REM sleep and wakefulness [114]. (i) One feasible explanation for this discrepancy is that Jego et al. have examined the effect of icv nesfatin-1 in active phase, when rats spend most of their time with activity, and accordingly, the global state of the brain is different from that in the passive phase, when rats mostly sleep. (ii) Another cause of the difference can be that they applied a 10-times higher dose of nesfatin-1 than us. It is possible that the effect of icv nesfatin-1 on vigilance shows a biphasic U- or J-shaped dose-response curve, a widely observed phenomena, where inhibition can be seen only when the agent is present in low concentration, while at higher concentrations, the inhibitory effect is lost and a stimulatory effect can be observed [189]. (iii) Another interesting point to note is the molecular mechanism of nesfatin, namely, this neuropeptide may influence cross-binding of the receptor with various types of G protein, initially activating G_i, followed by the activation of G_s protein which could also be an explanation for this inverse effect in different concentrations [127].

In view of the relationship of nesfatin and MCH, it is interesting to note their opposite effect in the regulation of vigilance. Unlike nesfatin-1, MCH has been

demonstrated to induce a dose-dependent increase of REM sleep and to a minor extent an elevation of SWS, when injected icv [112]. Consistently, MCHR1 antagonist compounds have been found to decrease REM sleep, IS and SWS2, while increased wakefulness [113]. According to Verret et al., MCH may promote REM sleep indirectly by inhibiting neurons themselves suppress the REM-executive neurons during wake and SWS, namely the monoaminergic neurons in the brainstem and histaminergic neurons of the PH [112]. However, GABAergic REM-off neurons originating from the vlPAG inhibit the sublaterodorsal nucleus (SLD), the structure that contains glutamatergic REM-executive ('REM-on') neurons [14, 184]. It would be logical to assume that the co-expressing nesfatin may act on the same neurons compensating the effect of MCH. Another possibility, that nesfatin modulates the amount of REM sleep via an excitatory action on the intermingled orexinergic neurons that are active during wakefulness, but silent in REM sleep. It would not be surprising given the putative somasomatic, axosomatic and axodendritic connection between orexin and nesfatin-containing MCH neurons [75].

Moreover, on food intake and energy expenditure, the effect of MCH and nesfatin are also opposing [81, 106, 134]. Chronic icv infusion of MCH has been reported to increase body weight in mice, particularly when mice were fed with moderately high-fat diet [190], while continuous infusion of nesfatin to the 3rd ventricle diminishes body mass [130]. In agreement with the sleep-promoting and energy conserving effect of MCH, it decreases body temperature, heart rate and metabolic rate by enhancing the ratio of parasympathetic/sympathetic tone [95], while centrally administered nesfatin-1 causes a dose-dependent elevation in temperature [134], increases blood pressure [191] as well as ACTH and corticosterone levels [143].

Co-localization of MCH with other neuropeptides having opposite effect is not unique. A high percent of the orexigenic MCH neurons (ZI: 95%, LH: 70%) co-localizes with the anorexigenic CART [117], that divides MCH population into two functionally divergent clusters: the CART-positive MCH neurons send ascending projections toward the septum and the hippocampus, while the CART-negative population sends descending projections toward the brainstem and spinal cord [118].

Furthermore, regarding synaptic action of MCH, it has a predominantly inhibitory effect at pre- and postsynaptic levels [192] and diminishes the activation of N-, L- and P/Q-type calcium channels [193], while nesfatin-1 has been shown to rise intracellular Ca^{2+} concentrations, by facilitating Ca^{2+} entry through N-, L- and P/Q-type voltage-activated calcium channels. The nesfatin-caused Ca^{2+} elevation was abolished by pertussis toxin, suggesting that nesfatin is a ligand of a metabotropic, $G_{i/o}$-coupled protein. Inconsistently, nesfatin has been indicated to increase the level of protein kinase A, which is unusual, as the effect of G_i protein would be the inhibition of adenyl cyclase, causing a reduction of the cAMP-concentration, and consequently the inhibition of protein kinase A. As an explanation for this issue, Brailiou et al. have suggested that nesftain-1 may influence cross-binding of the receptor with various types of G-proteins [127]. Since receptor(s) for nesfatin-1 has/have not been cloned yet, the precise mechanism of nesfatin's action remains to be clarified.

To further elucidate the role of nesfatin in sleep and wakefulness, we also investigated its effect on the quantitative EEG spectra, with other words, how it affects oscillations, the composition of which is characteristic in different vigilance stages. Spectral analysis of EEG data is a more sensitive manner of evaluation than conventional visual scoring of vigilance stages, providing a better resolution and unveils features that cannot be detected visually [7]. The EEG-power composition of different vigilance stages can be revealed by evaluating EEG spectrum using Fast Fourier transformation (FFT) [194, 195]. Although, there is no consensus about the adaptability of rodent to human quantitative EEG, an increasing amount of evidence suggests that the neuroanatomical projections and cellular basis are relatively conserved.

Supposing a serotonergic component in the effect of nesfatin, we compared also the EEG spectral data of nesfatin with two doses (2 and 10 mg/kg) of escitalopram. We concluded to evaluate the summarized 2^{nd}-3^{rd} hours of the recordings (at the beginning of passive phase) based on our sleep-time data, since in these two hours, the effect of both icv nesfatin-1 and ip escitalopram injection is maximal. For the comparison we used a relative new method, the 'state space analysis technique'.

This technique depicts global changes in the EEG spectra, providing a quick global overview, a topographical heat map about the architecture of sleep-wake cycle

without the need to score vigilance stages, thus, this technique is considered unbiased, i.e. free from human mistakes. Moreover, in contrast to conventional scoring, it describes different vigilance stages as a continuum, rather than discrete states, providing higher dimensional information about sleep and wakefulness and also visualizes transitions between stages, namely the variations in the depth of sleep as well as intensity of wakefulness. However, this technique is quantifiable calculating the 'centroids' (that is the arithmetic mean) of clusters, thus statistical analysis can be performed [21, 166].

Using the 'state space analysis technique', we found a significant shift to the left on the *x* axis in the centroid position of the 'REM sleep cluster' in both the nesfatin- and 10 mg/kg escitalopram-treated groups. A similar shift was observed in the centroid position of 'wake cluster' in the nesfatin- and both the 2 and 10 mg/kg escitalopram-treated groups. As *x*-axis position of the epochs is sensitive to the high theta (6.5-9 Hz) content of the EEG spectra, shift to the left of the REM sleep and wake clusters suggests a decrease in theta power. However, in non-REM sleep stage, we did not find any alteration on the heat map spectra in either the nesfatin- or the escitalopram-treated groups, showing that delta power, typical in non-REM sleep, was unaffected by the treatments, suggesting that slow wave stage, the resting part of sleep was not altered.

To verify these similarities in the EEG effect of nesfatin and escitalopram, we performed 'conventional' EEG spectral analysis for the same interval, in more detail. Our data showed that both nesfatin and the two different doses of escitalopram decreased theta power (5-9 Hz) in TW and REM sleep, in complete agreement with the results of 'state space analysis technique'. In TW, while nesfatin decreased theta at 7 Hz, both doses of escitalopram decreased it at 8 Hz frequency. However, their effect on AW and PW showed differences: while nesfatin diminished theta power in PW, both doses of escitalopram reduced it in AW. Moreover, the 2 and 10 mg/kg escitalopram reduced theta peak from 7 Hz to 6 Hz in TW (and the 10 mg/kg in AW), while nesfatin did not caused such an alteration. In REM sleep, nesfatin and both doses of escitalopram caused a decrease in theta power at 8 Hz, while deceleration of theta rhythm was not observed.

Theta EEG rhythm is linked to tasks requiring attention or memory in human, while in rats, theta rhythm occurs mostly during wake associated with various types of locomotor activity [8, 196] and in REM sleep [197]. Theta provides a temporal code for pyramidal/granule cell firing that facilitates synaptic plasticity, crucial for spatial navigation and the formation of episodic memory [198]. The generation of theta oscillation has been attributed mostly to the septo-hippocampal-entorhinal system and several subcortical nuclei, like the DRN, the ventral tegmental nucleus of Gudden and the anterior thalamic nuclei [6].

Two distinct types of hippocampal theta rhythm have been reported in behaving animals [6]. In rats, type I theta (4–7 Hz), appears in wakefulness, beginning several hundred milliseconds before particular behaviours, "voluntary", "preparatory", "orienting" and "exploratory" or when animals are immobile or during repetitive acts such as sniffing or whiskers movements [6, 196, 199, 200], while the second type characterized by higher frequency (7–10 Hz) occurs mostly during REM sleep in rats [201] and in response to acute stressors in rats [202]. In addition, the power of theta oscillation has also been used as an index for anxiety, and blockade of theta rhythm is applied to evaluate the efficacy of anxiolytics [203].

In our study, theta reduction caused by icv nesfatin-1 at 7 and 8 Hz frequency in wake and REM sleep, respectively, was very similar to that caused by escitalopram treatment, suggesting that an increased serotonergic tone is involved also in the theta-suppressing effect of nesfatin-1, similarly to its effect on the pattern of sleep-wake cycle. This is in agreement with the increased Fos activity of Raphe nuclei as a result of icv nesfatin injection, see above [143], moreover, with the finding that GABAergic interneurons of the medial septum – diagonal band of Broca, being crucial in the generation of theta rhythm, are innervated by serotonergic pathways from the MRN which afferents suppress the generation of hippocampal theta oscillations. These afferents are able to desynchronize hippocampal theta but also can modulate stress response [204, 205].

In physiological conditions, theta reduction can also be the result of an indirect effect if we consider the close relationship between Hcrt- and MCH-positive or -negative nesfatin expressing neuron populations in the DLH. The role of Hcrt in theta

modulation is shown by the fact that antagonist at Hcrt receptors have been demonstrated to suppress the footshock-induced theta waves, additionally, injection of Hcrt 1 or 2 into the MRN significantly increases theta power [206]. It also cannot be excluded that nesfatin-1 has a neuromodulatory effect on MCH neurons. MCH-containing neurons innervate medial septum strongly, suggesting their role also in the generation of theta during REM sleep [207]. In line with this, Jego et al. demonstrated a theta-increase as a result of optogenic enhancement of MCH neurons, while optogenic silencing decreased that [114].

However, serotonin hyperpolarizes MCH neurons via direct postsynaptic manner *in vitro* [100], moreover, acutely administered escitalopram, increasing the serotonergic tone, decreases Fos expression in MCH cells [36], reinforcing the inhibiting effect of serotonin in REM sleep generation via the inhibition of MCH cells.

While during REM sleep, nesfatin and both doses of escitalopram treatment led to a reduction in theta power similarly, we found differences in their theta-effect during wake. Namely, nesfatin-1 caused a theta reduction in PW, while the two doses of escitalopram treatments reduced theta power during AW, suggesting the involvement of different components in the effect of nesfatin and escitalopram. Generally, in AW, all of the medullary serotonergic neurons have been found to be activated during activities like treadmill-induced locomotion in cat, and a strong positive correlation was found between the speed of locomotion and neuronal activation [188]. Theta decrease in AW can be accomplished by the elevated serotonergic tone as a result of escitalopram, evoking an inhibiting effect on the LDT/PPT cholinergic neurons that are crucial in the generation of theta oscillation. This serotonergic input, originates mostly from the MRN, inhibits theta rhythm by desynchronizing hippocampal theta activity [204, 208, 209]. On the contrary, theta decrease in PW, as a result of nesfatin, can be explained by an increased neuronal activation, reported after icv nesfatin administration, not only in Raphe nuclei, but also in other nuclei e.g. LC and PVN, suggesting a more complex mechanism of nesfatin, in which serotonergic system can be a component. However, we have to note that basal theta power after icv administered vehicle was seemingly higher compared to ip-injected vehicle that may be attributable to the stress and anxiety due to the icv procedure. This elevated basal theta level was reduced by icv administered

nesfatin in PW, which effect may suggest an anti-anxiety effect, since suppression of hippocampal theta rhythm has been concluded to be a new reliable test of anxiolytic drug action, whether they act as a $5HT_{1A}$ agonist, a $GABA_A$ receptor agonist or a SSRI [203]. The link between nesfatin and anxiety as well as stress is also suggested by the fact, that restraint stress has been shown to induce Fos expression in nesfatin-IR neurons in the PVN, SON, the nucleus of the solitary tract, LC, DRN without altering plasma-concentration of nesfatin-1[143].

Moreover, we also found difference in theta decrease, namely it was detected at 7 Hz as a result of nesfatin, while at 8 Hz after both doses of escitalopram, although the impact of the distinct frequencies during theta range has not been clarified so far.

Taken together, we hypothesize that nesfatin-1, as a potential novel element of sleep-wake regulation, may suppress REM sleep and theta rhythm generation in wake and REM sleep most likely via an increase of the serotonergic tone or other components of the ARAS, or more hypothetically by the effect of MCH and/or Hcrt neurons in the DLH. The MCH-positive nesfatin population in the ZI, LH and PFA showed a strong connection with the augmented REM sleep amount during the 'REM sleep rebound', while MCH-negative nesfatin cells revealed increased Fos activation as a result of 'REM sleep rebound' only in the LH, suggesting that MCH-negative nesfatin cells are under a different regulation. In the EEG spectral analysis, the results of 'state space analysis technique' provided a quick global picture depicting alterations in the EEG spectra as a result of treatments, moreover, the results evaluated with its quantification were in agreement with the conventional EEG spectral analysis. As theta power is associated with cognitive functions, like spatial navigation, attention, memory formation and synaptic plasticity, decrease in theta power as a result of nesfatin can deteriorate these cognitive functions. On the other hand, theta decreasing property of nesfatin, considered an important aspect in the effect of anxiolytic medications, may promote its potential use as a target to seek for antidepressant or anxiolytic medications.

DOI: 10.14753/SE.2016.1869

10. Conclusions

The markedly elevated activation of MCH/nesfatin-co-expressing neurons in the ZI, LH and PFA as a result of 'REM sleep rebound' suggests a close association between the regulation of REM sleep and the MCH/nesfatin-neuronal populations of these structures. This activation of MCH neurons was reduced by escitalopram, the selective serotonin reuptake inhibitor antidepressant, in the ZI, LH and PFA, suggesting a direct or indirect inhibitory effect of serotonin on these neurons, in line with the REM sleep suppressing effect of escitalopram. While MCH-positive nesfatin neurons show strong connection with REM sleep regulation as a result of 'REM sleep rebound' in the ZI, PFA and LH, the MCH-negative nesfatin neurons can be associated with REM sleep exclusively in the LH, suggesting that MCH-negative nesfatin neurons of the ZI and PFA may be under a different regulation.

Nesfatin can be a potential new element in the regulation of sleep-wake cycle. Possessing a mostly REM-suppressing and PW-increasing effect, without altering non-REM sleep considerably, nesfatin alters sleep pattern similarly to several antidepressant. Centrally injected nesfatin reduced theta power (5-9 Hz) in passive wake and REM sleep, that may affect functions associated with this oscillation, like attention or memory formation, however, delta power in non-REM sleep, namely the resting part of sleep was unaffected.

The comparison of EEG spectral effect of nesfatin and (2 and 10 mg/kg) escitalopram showed similarities, like reduction of theta power in TW and REM sleep, although a more detailed spectral analysis revealed differences, namely, while nesfatin decreased theta in PW, escitalopram diminished it in AW, suggesting a different influence on the generation of theta power, however, increase in the serotonergic tone can be a potential component.

To clarify the mechanism how nesfatin influences sleep-wake cycle and EEG spectra, as well as to prove the involvement of a serotonergic or other components in the effect of nesfatin-1 further studies are needed. The REM sleep and theta power reducing effect of nesfatin can suggest its potential role in the pathomechanism of depression and anxiety.

DOI: 10.14753/SE.2016.1869

11. Summary

In this work, we investigated the role of two neuropeptides, the melanin-concentrating hormone (MCH) and the nesfatin-1/NUCB2 (nesfatin) in the regulation of vigilance, using neuromorphology and electrophysiology. Though the role of MCH in the regulation of sleep is known, the involvement of nesfatin, the co-expressing neuropeptide, and their expression in different hypothalamic/thalamic nuclei has not been examined until the start of this work. To study the link between these neuropeptides and sleep, we used 'flower pot' REM sleep-deprivation method to provoke the REM sleep-associated activation of neuron populations during the 3 h 'REM sleep rebound' ('rebound'). The activation of MCH- and nesfatin-positive neurons was investigated using double and triple immunostainings. To examine the influence of the serotonergic system on this activation, escitalopram, a serotonergic-tone-increasing antidepressant was injected prior to 'rebound' [36]. The effect of nesfatin on both vigilance and EEG spectra was investigated by the intracerebroventricular administration (icv) of the peptide [171]. Supposing a serotonergic component in the effect of nesfatin, we compared the EEG spectra of nesfatin and escitalopram, using 'state space analysis' visualizing shifts in the topography of the main vigilance stages on heat maps. To verify these results, we performed also 'conventional' EEG spectral analysis in more detail [180].

The most important results: (1) 'rebound' activated the MCH/nesfatin neuron population in the zona incerta (ZI), lateral hypothalamic area (LH) and perifornical area (PFA) and (2) this activation was reduced by increased serotonergic tone, however, (3) the MCH-negative nesfatin-population was activated only in the LH. (4) Icv nesfatin decreased REM-sleep, increased passive wake, and (5) reduced theta power in total wake and REM, similarly to escitalopram, although (6) nesfatin and escitalopram diminished theta power differently in active and passive wake.

Our results suggest a link between REM sleep and MCH/nesfatin-neuronal populations of the ZI, LH and PFA, as well as the involvement of nesfatin in the regulation of both vigilance and theta oscillation in REM sleep and wakefulness, possessing a presumed serotonergic component in this effect.

DOI: 10.14753/SE.2016.1869

12. Összefoglalás

Munkám során két neuropeptid, a melanin-koncentráló hormon (MCH) és a nesfatin-1/NUCB2 (nesfatin) alvás-ébrenlét szabályozásában betöltött szerepét vizsgáltam neuromorfológiai és elektrofiziológiai módszerekkel. Az MCH alvásszabályozásában foglalt jelentősége ma már tény, míg a vele ko-expresszálódó nesfatin szerepét, valamint különböző hypothalamicus/thalamicus magvakban történő expresszsiójukat kísérleteink megkezdéséig még nem vizsgálták. E neuropeptidek alvásszabályozásban betöltött szerepének tanulmányozására a ’virágcserép’ REM alvásmegvonás módszerrel 3 órás ’REM alvás visszacsapást’ (’rebound’) idéztünk elő, mellyel a REM alvással összefüggést mutató neuron populációk fokozott aktivációját váltottuk ki. Ezt kettős és hármas immunfestéssel vizsgáltuk. A ’rebound’-által megnövelt neuronális aktiváció és a szerotonerg rendszer kapcsolatát előzetes escitalopram (szerotonerg-tónust növelő antidepresszáns) kezeléssel vizsgáltuk [36]. A nesfatin alvásmintázatra és EEG spektrumra kifejtett hatását a neuropeptid agykamrába történő (icv) injektálásával vizsgáltuk [171]. A nesfatin hatásában szerotonerg komponenst feltételezve, a nesfatin és escitalopram EEG spektrumát egy hőtérkép-elemzésen alapuló módszerrel hasonlítottuk össze, mely a főbb vigilancia-állapotok topográfiájában bekövetkezett eltolódásokat teszi szemléletessé. Az így kapott eredmények igazolására elvégeztük a ’konvencionális’, részletesebb EEG spektrumanalízist is [180]. A legfontosabb eredmények: (1) a ‘rebound’ az MCH/nesfatin neuron populáció aktivációját váltotta ki a zona incerta (ZI), a laterális hypothalamicus area (LH) és a perifornicalis area (PFA) területén, (2) mely aktivációt emelkedett szerotonerg tónus csökkentette, míg (3) az MCH-negatív nesfatin-populáció csupán a LH területén aktiválódott. (4) Icv nesfatin a REM alvást csökkentette, a passzív ébrenlétet növelte, valamint (5) a téta EEG teljesítményt ébrenlétben és REM-ben csökkentette, az escitalopramhoz hasonlóan, noha (6) a nesfatin és az escitalopram aktív és passzív ébrenlétben különbségeket mutatott a téta teljesítmény mérséklésében.

Eredményeink a ZI, LH és PFA MCH/nesfatin neuron populációinak REM alvással való összefüggését valószínűsítik, valamint a nesfatin alvás-ébrenléti ciklus és EEG oszcillációk szabályozásában betöltött szerepét mutatják REM-ben és ébrenlétben, a hatásban szerotonerg komponenst valószínűsítve.

13. Bibliography

1. Krueger, J.M.,F. Obal, (1993) A neuronal group theory of sleep function. J Sleep Res. 2(2): 63-69.
2. Krueger, J.M., D.M. Rector, S. Roy, H.P. Van Dongen, G. Belenky, J. Panksepp, (2008) Sleep as a fundamental property of neuronal assemblies. Nat Rev Neurosci. 9(12): 910-9.
3. Gervasoni, D., S.C. Lin, S. Ribeiro, E.S. Soares, J. Pantoja, M.A. Nicolelis, (2004) Global forebrain dynamics predict rat behavioral states and their transitions. J Neurosci. 24(49): 11137-47.
4. Buzsaki, G., (2004) Large-scale recording of neuronal ensembles. Nat Neurosci. 7(5): 446-51.
5. Brown, R.E., R. Basheer, J.T. McKenna, R.E. Strecker, R.W. McCarley, (2012) Control of sleep and wakefulness. Physiol Rev. 92(3): 1087-187.
6. Buzsaki, G., (2002) Theta oscillations in the hippocampus. Neuron. 33(3): 325-40.
7. Gottesmann, C., (1992) Detection of seven sleep-waking stages in the rat. Neurosci Biobehav Rev. 16(1): 31-8.
8. Vanderwolf, C.H., (1975) Neocortical and hippocampal activation relation to behavior: effects of atropine, eserine, phenothiazines, and amphetamine. J Comp Physiol Psychol. 88(1): 300-23.
9. Kramis, R., C.H. Vanderwolf, B.H. Bland, (1975) Two types of hippocampal rhythmical slow activity in both the rabbit and the rat: relations to behavior and effects of atropine, diethyl ether, urethane, and pentobarbital. Exp Neurol. 49(1 Pt 1): 58-85.
10. Steriade, M., A. Nunez, F. Amzica, (1993) Intracellular analysis of relations between the slow (< 1 Hz) neocortical oscillation and other sleep rhythms of the electroencephalogram. J Neurosci. 13(8): 3266-83.
11. Vyazovskiy, V.V., C. Cirelli, G. Tononi, (2011) Electrophysiological correlates of sleep homeostasis in freely behaving rats. Prog Brain Res. 193: 17-38.
12. Datta, S., (2010) Cellular and chemical neuroscience of mammalian sleep. Sleep Med. 11(5): 431-40.

13. Trachsel, L., I. Tobler, P. Achermann, A.A. Borbely, (1991) Sleep continuity and the REM-nonREM cycle in the rat under baseline conditions and after sleep deprivation. Physiol Behav. 49(3): 575-80.
14. Saper, C.B., P.M. Fuller, N.P. Pedersen, J. Lu, T.E. Scammell, (2010) Sleep state switching. Neuron. 68(6): 1023-42.
15. Gottesmann, C., G. Gandolfo, C. Arnaud, P. Gauthier, (1998) The intermediate stage and paradoxical sleep in the rat: influence of three generations of hypnotics. Eur J Neurosci. 10(2): 409-14.
16. Cantero, J.L., M. Atienza, R. Stickgold, M.J. Kahana, J.R. Madsen, B. Kocsis, (2003) Sleep-dependent theta oscillations in the human hippocampus and neocortex. J Neurosci. 23(34): 10897-903.
17. Borbely, A.A., (1982) A two process model of sleep regulation. Hum Neurobiol. 1(3): 195-204.
18. Jin, X., L.P. Shearman, D.R. Weaver, M.J. Zylka, G.J. de Vries, S.M. Reppert, (1999) A molecular mechanism regulating rhythmic output from the suprachiasmatic circadian clock. Cell. 96(1): 57-68.
19. Benington, J.H.,H.C. Heller, (1995) Restoration of brain energy metabolism as the function of sleep. Prog Neurobiol. 45(4): 347-60.
20. Lu, J., D. Sherman, M. Devor, C.B. Saper, (2006) A putative flip-flop switch for control of REM sleep. Nature. 441(7093): 589-94.
21. Bergman, P., C. Adori, S. Vas, Y. Kai-Larsen, T. Sarkanen, A. Cederlund, B. Agerberth, I. Julkunen, B. Horvath, D. Kostyalik, L. Kalmar, G. Bagdy, A. Huutoniemi, M. Partinen, T. Hokfelt, (2014) Narcolepsy patients have antibodies that stain distinct cell populations in rat brain and influence sleep patterns. Proc Natl Acad Sci U S A. 111(35): E3735-44.
22. Jones, B.E.,T.Z. Yang, (1985) The efferent projections from the reticular formation and the locus coeruleus studied by anterograde and retrograde axonal transport in the rat. J Comp Neurol. 242(1): 56-92.
23. Aston-Jones, G.,F.E. Bloom, (1981) Activity of norepinephrine-containing locus coeruleus neurons in behaving rats anticipates fluctuations in the sleep-waking cycle. J Neurosci. 1(8): 876-86.

24. Kocsis, B., V. Varga, L. Dahan, A. Sik, (2006) Serotonergic neuron diversity: identification of raphe neurons with discharges time-locked to the hippocampal theta rhythm. Proc Natl Acad Sci U S A. 103(4): 1059-64.
25. Takahashi, K., J.S. Lin, K. Sakai, (2006) Neuronal activity of histaminergic tuberomammillary neurons during wake-sleep states in the mouse. J Neurosci. 26(40): 10292-8.
26. Berridge, C.W., (2008) Noradrenergic modulation of arousal. Brain Res Rev. 58(1): 1-17.
27. Carter, M.E., O. Yizhar, S. Chikahisa, H. Nguyen, A. Adamantidis, S. Nishino, K. Deisseroth, L. de Lecea, (2010) Tuning arousal with optogenetic modulation of locus coeruleus neurons. Nat Neurosci. 13(12): 1526-33.
28. Constantinople, C.M.,R.M. Bruno, (2011) Effects and mechanisms of wakefulness on local cortical networks. Neuron. 69(6): 1061-8.
29. Datta, S.,R.R. Maclean, (2007) Neurobiological mechanisms for the regulation of mammalian sleep-wake behavior: reinterpretation of historical evidence and inclusion of contemporary cellular and molecular evidence. Neurosci Biobehav Rev. 31(5): 775-824.
30. Dzoljic, M.R., O.E. Ukponmwan, P.R. Saxena, (1992) 5-HT1-like receptor agonists enhance wakefulness. Neuropharmacology. 31(7): 623-33.
31. Dugovic, C., A. Wauquier, J.E. Leysen, R. Marrannes, P.A. Janssen, (1989) Functional role of 5-HT2 receptors in the regulation of sleep and wakefulness in the rat. Psychopharmacology (Berl). 97(4): 436-42.
32. Ponzoni, A., J.M. Monti, H. Jantos, (1993) The effects of selective activation of the 5-HT3 receptor with m-chlorophenylbiguanide on sleep and wakefulness in the rat. Eur J Pharmacol. 249(3): 259-64.
33. Kostyalik, D., Z. Katai, S. Vas, D. Pap, P. Petschner, E. Molnar, I. Gyertyan, L. Kalmar, L. Tothfalusi, G. Bagdy, (2014) Chronic escitalopram treatment caused dissociative adaptation in serotonin (5-HT) 2C receptor antagonist-induced effects in REM sleep, wake and theta wave activity. Exp Brain Res. 232(3): 935-46.
34. Monaca, C., B. Boutrel, R. Hen, M. Hamon, J. Adrien, (2003) 5-HT 1A/1B receptor-mediated effects of the selective serotonin reuptake inhibitor,

citalopram, on sleep: studies in 5-HT 1A and 5-HT 1B knockout mice. Neuropsychopharmacology. 28(5): 850-6.

35. Wilson, S.,S. Argyropoulos, (2005) Antidepressants and sleep: a qualitative review of the literature. Drugs. 65(7): 927-47.
36. Katai, Z., C. Adori, T. Kitka, S. Vas, L. Kalmar, D. Kostyalik, L. Tothfalusi, M. Palkovits, G. Bagdy, (2013) Acute escitalopram treatment inhibits REM sleep rebound and activation of MCH-expressing neurons in the lateral hypothalamus after long term selective REM sleep deprivation. Psychopharmacology (Berl). 228(3): 439-49.
37. Hallanger, A.E., A.I. Levey, H.J. Lee, D.B. Rye, B.H. Wainer, (1987) The origins of cholinergic and other subcortical afferents to the thalamus in the rat. J Comp Neurol. 262(1): 105-24.
38. Steriade, M., S. Datta, D. Pare, G. Oakson, R.C. Curro Dossi, (1990) Neuronal activities in brain-stem cholinergic nuclei related to tonic activation processes in thalamocortical systems. J Neurosci. 10(8): 2541-59.
39. Shouse, M.N.,J.M. Siegel, (1992) Pontine regulation of REM sleep components in cats: integrity of the pedunculopontine tegmentum (PPT) is important for phasic events but unnecessary for atonia during REM sleep. Brain Res. 571(1): 50-63.
40. Metherate, R., C.L. Cox, J.H. Ashe, (1992) Cellular bases of neocortical activation: modulation of neural oscillations by the nucleus basalis and endogenous acetylcholine. J Neurosci. 12(12): 4701-11.
41. Lee, M.G., I.D. Manns, A. Alonso, B.E. Jones, (2004) Sleep-wake related discharge properties of basal forebrain neurons recorded with micropipettes in head-fixed rats. J Neurophysiol. 92(2): 1182-98.
42. Lee, M.G., O.K. Hassani, A. Alonso, B.E. Jones, (2005) Cholinergic basal forebrain neurons burst with theta during waking and paradoxical sleep. J Neurosci. 25(17): 4365-9.
43. Henny, P.,B.E. Jones, (2008) Projections from basal forebrain to prefrontal cortex comprise cholinergic, GABAergic and glutamatergic inputs to pyramidal cells or interneurons. Eur J Neurosci. 27(3): 654-70.

44. Manns, I.D., A. Alonso, B.E. Jones, (2000) Discharge profiles of juxtacellularly labeled and immunohistochemically identified GABAergic basal forebrain neurons recorded in association with the electroencephalogram in anesthetized rats. J Neurosci. 20(24): 9252-63.
45. Lee, S.H.,Y. Dan, (2012) Neuromodulation of brain states. Neuron. 76(1): 209-22.
46. Castro-Alamancos, M.A., (2004) Dynamics of sensory thalamocortical synaptic networks during information processing states. Prog Neurobiol. 74(4): 213-47.
47. Sherman, S.M., (2005) Thalamic relays and cortical functioning. Prog Brain Res. 149: 107-26.
48. McCormick, D.A.,T. Bal, (1997) Sleep and arousal: thalamocortical mechanisms. Annu Rev Neurosci. 20: 185-215.
49. Bickford, M.E., A.E. Gunluk, S.C. Van Horn, S.M. Sherman, (1994) GABAergic projection from the basal forebrain to the visual sector of the thalamic reticular nucleus in the cat. J Comp Neurol. 348(4): 481-510.
50. Amzica, F.,M. Steriade, (1995) Disconnection of intracortical synaptic linkages disrupts synchronization of a slow oscillation. J Neurosci. 15(6): 4658-77.
51. Li, C.Y., M.M. Poo, Y. Dan, (2009) Burst spiking of a single cortical neuron modifies global brain state. Science. 324(5927): 643-6.
52. Zaborszky, L., R.P. Gaykema, D.J. Swanson, W.E. Cullinan, (1997) Cortical input to the basal forebrain. Neuroscience. 79(4): 1051-78.
53. Jodo, E.,G. Aston-Jones, (1997) Activation of locus coeruleus by prefrontal cortex is mediated by excitatory amino acid inputs. Brain Res. 768(1-2): 327-32.
54. Economo, C.v., (1930) Sleep as a problem of localization. The Journal of Nervous and Mental Disease. 71(n°3).
55. Mignot, E., S. Taheri, S. Nishino, (2002) Sleeping with the hypothalamus: emerging therapeutic targets for sleep disorders. Nat Neurosci. 5 Suppl: 1071-5.
56. Sherin, J.E., P.J. Shiromani, R.W. McCarley, C.B. Saper, (1996) Activation of ventrolateral preoptic neurons during sleep. Science. 271(5246): 216-9.
57. Szymusiak, R.,D. McGinty, (2008) Hypothalamic regulation of sleep and arousal. Ann N Y Acad Sci. 1129: 275-86.

58. Chou, T.C., A.A. Bjorkum, S.E. Gaus, J. Lu, T.E. Scammell, C.B. Saper, (2002) Afferents to the ventrolateral preoptic nucleus. J Neurosci. 22(3): 977-90.
59. Sherin, J.E., J.K. Elmquist, F. Torrealba, C.B. Saper, (1998) Innervation of histaminergic tuberomammillary neurons by GABAergic and galaninergic neurons in the ventrolateral preoptic nucleus of the rat. J Neurosci. 18(12): 4705-21.
60. Lu, J., M.A. Greco, P. Shiromani, C.B. Saper, (2000) Effect of lesions of the ventrolateral preoptic nucleus on NREM and REM sleep. J Neurosci. 20(10): 3830-42.
61. Uschakov, A., H. Gong, D. McGinty, R. Szymusiak, (2007) Efferent projections from the median preoptic nucleus to sleep- and arousal-regulatory nuclei in the rat brain. Neuroscience. 150(1): 104-20.
62. Nauta, W.J., (1946) Hypothalamic regulation of sleep in rats; an experimental study. J Neurophysiol. 9: 285-316.
63. Ko, E.M., I.V. Estabrooke, M. McCarthy, T.E. Scammell, (2003) Wake-related activity of tuberomammillary neurons in rats. Brain Res. 992(2): 220-6.
64. Steininger, T.L., M.N. Alam, H. Gong, R. Szymusiak, D. McGinty, (1999) Sleep-waking discharge of neurons in the posterior lateral hypothalamus of the albino rat. Brain Res. 840(1-2): 138-47.
65. Lin, J.S., (2000) Brain structures and mechanisms involved in the control of cortical activation and wakefulness, with emphasis on the posterior hypothalamus and histaminergic neurons. Sleep Med Rev. 4(5): 471-503.
66. Saper, C.B., T.C. Chou, T.E. Scammell, (2001) The sleep switch: hypothalamic control of sleep and wakefulness. Trends Neurosci. 24(12): 726-31.
67. Bernardis, L.L.,L.L. Bellinger, (1996) The lateral hypothalamic area revisited: ingestive behavior. Neurosci Biobehav Rev. 20(2): 189-287.
68. Saper, C.B., T.E. Scammell, J. Lu, (2005) Hypothalamic regulation of sleep and circadian rhythms. Nature. 437(7063): 1257-63.
69. Luppi, P.H., D. Gervasoni, L. Verret, R. Goutagny, C. Peyron, D. Salvert, L. Leger, P. Fort, (2006) Paradoxical (REM) sleep genesis: the switch from an aminergic-cholinergic to a GABAergic-glutamatergic hypothesis. J Physiol Paris. 100(5-6): 271-83.

70. Adamantidis, A.,L. de Lecea, (2008) Sleep and metabolism: shared circuits, new connections. Trends Endocrinol Metab. 19(10): 362-70.
71. Lin, J.S., K. Sakai, G. Vanni-Mercier, M. Jouvet, (1989) A critical role of the posterior hypothalamus in the mechanisms of wakefulness determined by microinjection of muscimol in freely moving cats. Brain Res. 479(2): 225-40.
72. Hassani, O.K., M.G. Lee, B.E. Jones, (2009) Melanin-concentrating hormone neurons discharge in a reciprocal manner to orexin neurons across the sleep-wake cycle. Proc Natl Acad Sci U S A. 106(7): 2418-22.
73. Bittencourt, J.C., F. Presse, C. Arias, C. Peto, J. Vaughan, J.L. Nahon, W. Vale, P.E. Sawchenko, (1992) The melanin-concentrating hormone system of the rat brain: an immuno- and hybridization histochemical characterization. J Comp Neurol. 319(2): 218-45.
74. Broberger, C., L. De Lecea, J.G. Sutcliffe, T. Hokfelt, (1998) Hypocretin/orexin- and melanin-concentrating hormone-expressing cells form distinct populations in the rodent lateral hypothalamus: relationship to the neuropeptide Y and agouti gene-related protein systems. J Comp Neurol. 402(4): 460-74.
75. Bayer, L., G. Mairet-Coello, P.Y. Risold, B. Griffond, (2002) Orexin/hypocretin neurons: chemical phenotype and possible interactions with melanin-concentrating hormone neurons. Regul Pept. 104(1-3): 33-9.
76. Modirrousta, M., L. Mainville, B.E. Jones, (2005) Orexin and MCH neurons express c-Fos differently after sleep deprivation vs. recovery and bear different adrenergic receptors. Eur J Neurosci. 21(10): 2807-16.
77. Kitka, T., C. Adori, Z. Katai, S. Vas, E. Molnar, R.S. Papp, Z.E. Toth, G. Bagdy, (2011) Association between the activation of MCH and orexin immunorective neurons and REM sleep architecture during REM rebound after a three day long REM deprivation. Neurochem Int. 59(5): 686-94.
78. Sakurai, T., (2007) The neural circuit of orexin (hypocretin): maintaining sleep and wakefulness. Nat Rev Neurosci. 8(3): 171-81.
79. Elias, C.F., L.V. Sita, B.K. Zambon, E.R. Oliveira, L.A. Vasconcelos, J.C. Bittencourt, (2008) Melanin-concentrating hormone projections to areas involved in somatomotor responses. J Chem Neuroanat. 35(2): 188-201.

80. Torterolo, P., S. Sampogna, M.H. Chase, (2009) MCHergic projections to the nucleus pontis oralis participate in the control of active (REM) sleep. Brain Res. 1268: 76-87.

81. Oh, I.S., H. Shimizu, T. Satoh, S. Okada, S. Adachi, K. Inoue, H. Eguchi, M. Yamamoto, T. Imaki, K. Hashimoto, T. Tsuchiya, T. Monden, K. Horiguchi, M. Yamada, M. Mori, (2006) Identification of nesfatin-1 as a satiety molecule in the hypothalamus. Nature. 443(7112): 709-12.

82. Konadhode, R.R., D. Pelluru, P.J. Shiromani, (2014) Neurons containing orexin or melanin concentrating hormone reciprocally regulate wake and sleep. Front Syst Neurosci. 8: 244.

83. de Lecea, L., T.S. Kilduff, C. Peyron, X. Gao, P.E. Foye, P.E. Danielson, C. Fukuhara, E.L. Battenberg, V.T. Gautvik, F.S. Bartlett, 2nd, W.N. Frankel, A.N. van den Pol, F.E. Bloom, K.M. Gautvik, J.G. Sutcliffe, (1998) The hypocretins: hypothalamus-specific peptides with neuroexcitatory activity. Proc Natl Acad Sci U S A. 95(1): 322-7.

84. Sakurai, T., A. Amemiya, M. Ishii, I. Matsuzaki, R.M. Chemelli, H. Tanaka, S.C. Williams, J.A. Richarson, G.P. Kozlowski, S. Wilson, J.R. Arch, R.E. Buckingham, A.C. Haynes, S.A. Carr, R.S. Annan, D.E. McNulty, W.S. Liu, J.A. Terrett, N.A. Elshourbagy, D.J. Bergsma, M. Yanagisawa, (1998) Orexins and orexin receptors: a family of hypothalamic neuropeptides and G protein-coupled receptors that regulate feeding behavior. Cell. 92(5): 1 page following 696.

85. Kilduff, T.S.,C. Peyron, (2000) The hypocretin/orexin ligand-receptor system: implications for sleep and sleep disorders. Trends Neurosci. 23(8): 359-65.

86. Thannickal, T.C., R.Y. Moore, R. Nienhuis, L. Ramanathan, S. Gulyani, M. Aldrich, M. Cornford, J.M. Siegel, (2000) Reduced number of hypocretin neurons in human narcolepsy. Neuron. 27(3): 469-74.

87. Chemelli, R.M., J.T. Willie, C.M. Sinton, J.K. Elmquist, T. Scammell, C. Lee, J.A. Richardson, S.C. Williams, Y. Xiong, Y. Kisanuki, T.E. Fitch, M. Nakazato, R.E. Hammer, C.B. Saper, M. Yanagisawa, (1999) Narcolepsy in orexin knockout mice: molecular genetics of sleep regulation. Cell. 98(4): 437-51.

88. Gerashchenko, D., M.D. Kohls, M. Greco, N.S. Waleh, R. Salin-Pascual, T.S. Kilduff, D.A. Lappi, P.J. Shiromani, (2001) Hypocretin-2-saporin lesions of the lateral hypothalamus produce narcoleptic-like sleep behavior in the rat. J Neurosci. 21(18): 7273-83.

89. Hagan, J.J., R.A. Leslie, S. Patel, M.L. Evans, T.A. Wattam, S. Holmes, C.D. Benham, S.G. Taylor, C. Routledge, P. Hemmati, R.P. Munton, T.E. Ashmeade, A.S. Shah, J.P. Hatcher, P.D. Hatcher, D.N. Jones, M.I. Smith, D.C. Piper, A.J. Hunter, R.A. Porter, N. Upton, (1999) Orexin A activates locus coeruleus cell firing and increases arousal in the rat. Proc Natl Acad Sci U S A. 96(19): 10911-6.

90. Brisbare-Roch, C., J. Dingemanse, R. Koberstein, P. Hoever, H. Aissaoui, S. Flores, C. Mueller, O. Nayler, J. van Gerven, S.L. de Haas, P. Hess, C. Qiu, S. Buchmann, M. Scherz, T. Weller, W. Fischli, M. Clozel, F. Jenck, (2007) Promotion of sleep by targeting the orexin system in rats, dogs and humans. Nat Med. 13(2): 150-5.

91. Peyron, C., D.K. Tighe, A.N. van den Pol, L. de Lecea, H.C. Heller, J.G. Sutcliffe, T.S. Kilduff, (1998) Neurons containing hypocretin (orexin) project to multiple neuronal systems. J Neurosci. 18(23): 9996-10015.

92. Rosenwasser, A.M., (2009) Functional neuroanatomy of sleep and circadian rhythms. Brain Res Rev. 61(2): 281-306.

93. Rosin, D.L., M.C. Weston, C.P. Sevigny, R.L. Stornetta, P.G. Guyenet, (2003) Hypothalamic orexin (hypocretin) neurons express vesicular glutamate transporters VGLUT1 or VGLUT2. J Comp Neurol. 465(4): 593-603.

94. Chou, T.C., C.E. Lee, J. Lu, J.K. Elmquist, J. Hara, J.T. Willie, C.T. Beuckmann, R.M. Chemelli, T. Sakurai, M. Yanagisawa, C.B. Saper, T.E. Scammell, (2001) Orexin (hypocretin) neurons contain dynorphin. J Neurosci. 21(19): RC168.

95. Saito, Y.,H. Nagasaki, (2008) The melanin-concentrating hormone system and its physiological functions. Results Probl Cell Differ. 46: 159-79.

96. Rondini, T.A., C. Rodrigues Bde, A.P. de Oliveira, J.C. Bittencourt, C.F. Elias, (2007) Melanin-concentrating hormone is expressed in the laterodorsal tegmental nucleus only in female rats. Brain Res Bull. 74(1-3): 21-8.

97. Rondini, T.A., J. Donato, Jr., C. Rodrigues Bde, J.C. Bittencourt, C.F. Elias, (2010) Chemical identity and connections of medial preoptic area neurons expressing melanin-concentrating hormone during lactation. J Chem Neuroanat. 39(1): 51-62.

98. Guan, J.L., K. Uehara, S. Lu, Q.P. Wang, H. Funahashi, T. Sakurai, M. Yanagizawa, S. Shioda, (2002) Reciprocal synaptic relationships between orexin- and melanin-concentrating hormone-containing neurons in the rat lateral hypothalamus: a novel circuit implicated in feeding regulation. Int J Obes Relat Metab Disord. 26(12): 1523-32.

99. Torterolo, P., S. Sampogna, F.R. Morales, M.H. Chase, (2006) MCH-containing neurons in the hypothalamus of the cat: searching for a role in the control of sleep and wakefulness. Brain Res. 1119(1): 101-14.

100. van den Pol, A.N., C. Acuna-Goycolea, K.R. Clark, P.K. Ghosh, (2004) Physiological properties of hypothalamic MCH neurons identified with selective expression of reporter gene after recombinant virus infection. Neuron. 42(4): 635-52.

101. Apergis-Schoute, J., P. Iordanidou, C. Faure, S. Jego, C. Schone, T. Aitta-Aho, A. Adamantidis, D. Burdakov, (2015) Optogenetic evidence for inhibitory signaling from orexin to MCH neurons via local microcircuits. J Neurosci. 35(14): 5435-41.

102. Rao, Y., M. Lu, F. Ge, D.J. Marsh, S. Qian, A.H. Wang, M.R. Picciotto, X.B. Gao, (2008) Regulation of synaptic efficacy in hypocretin/orexin-containing neurons by melanin concentrating hormone in the lateral hypothalamus. J Neurosci. 28(37): 9101-10.

103. Mori, M., M. Harada, Y. Terao, T. Sugo, T. Watanabe, Y. Shimomura, M. Abe, Y. Shintani, H. Onda, O. Nishimura, M. Fujino, (2001) Cloning of a novel G protein-coupled receptor, SLT, a subtype of the melanin-concentrating hormone receptor. Biochem Biophys Res Commun. 283(5): 1013-8.

104. Sailer, A.W., H. Sano, Z. Zeng, T.P. McDonald, J. Pan, S.S. Pong, S.D. Feighner, C.P. Tan, T. Fukami, H. Iwaasa, D.L. Hreniuk, N.R. Morin, S.J. Sadowski, M. Ito, A. Bansal, B. Ky, D.J. Figueroa, Q. Jiang, C.P. Austin, D.J. MacNeil, A. Ishihara, M. Ihara, A. Kanatani, L.H. Van der Ploeg, A.D. Howard,

Q. Liu, (2001) Identification and characterization of a second melanin-concentrating hormone receptor, MCH-2R. Proc Natl Acad Sci U S A. 98(13): 7564-9.

105. Hawes, B.E., E. Kil, B. Green, K. O'Neill, S. Fried, M.P. Graziano, (2000) The melanin-concentrating hormone receptor couples to multiple G proteins to activate diverse intracellular signaling pathways. Endocrinology. 141(12): 4524-32.

106. Qu, D., D.S. Ludwig, S. Gammeltoft, M. Piper, M.A. Pelleymounter, M.J. Cullen, W.F. Mathes, R. Przypek, R. Kanarek, E. Maratos-Flier, (1996) A role for melanin-concentrating hormone in the central regulation of feeding behaviour. Nature. 380(6571): 243-7.

107. Shimada, M., N.A. Tritos, B.B. Lowell, J.S. Flier, E. Maratos-Flier, (1998) Mice lacking melanin-concentrating hormone are hypophagic and lean. Nature. 396(6712): 670-4.

108. Ludwig, D.S., N.A. Tritos, J.W. Mastaitis, R. Kulkarni, E. Kokkotou, J. Elmquist, B. Lowell, J.S. Flier, E. Maratos-Flier, (2001) Melanin-concentrating hormone overexpression in transgenic mice leads to obesity and insulin resistance. J Clin Invest. 107(3): 379-86.

109. Borowsky, B., M.M. Durkin, K. Ogozalek, M.R. Marzabadi, J. DeLeon, B. Lagu, R. Heurich, H. Lichtblau, Z. Shaposhnik, I. Daniewska, T.P. Blackburn, T.A. Branchek, C. Gerald, P.J. Vaysse, C. Forray, (2002) Antidepressant, anxiolytic and anorectic effects of a melanin-concentrating hormone-1 receptor antagonist. Nat Med. 8(8): 825-30.

110. Peyron, C., E. Sapin, L. Leger, P.H. Luppi, P. Fort, (2009) Role of the melanin-concentrating hormone neuropeptide in sleep regulation. Peptides. 30(11): 2052-9.

111. Torterolo, P., P. Lagos, J.M. Monti, (2011) Melanin-concentrating hormone: a new sleep factor? Front Neurol. 2: 14.

112. Verret, L., R. Goutagny, P. Fort, L. Cagnon, D. Salvert, L. Leger, R. Boissard, P. Salin, C. Peyron, P.H. Luppi, (2003) A role of melanin-concentrating hormone producing neurons in the central regulation of paradoxical sleep. BMC Neurosci. 4: 19.

113. Ahnaou, A., W.H. Drinkenburg, J.A. Bouwknecht, J. Alcazar, T. Steckler, F.M. Dautzenberg, (2008) Blocking melanin-concentrating hormone MCH1 receptor affects rat sleep-wake architecture. Eur J Pharmacol. 579(1-3): 177-88.

114. Jego, S.,A. Adamantidis, (2013) MCH neurons: vigilant workers in the night. Sleep. 36(12): 1783-6.

115. Guyon, A., G. Conductier, C. Rovere, A. Enfissi, J.L. Nahon, (2009) Melanin-concentrating hormone producing neurons: Activities and modulations. Peptides. 30(11): 2031-9.

116. Huang, H., C. Acuna-Goycolea, Y. Li, H.M. Cheng, K. Obrietan, A.N. van den Pol, (2007) Cannabinoids excite hypothalamic melanin-concentrating hormone but inhibit hypocretin/orexin neurons: implications for cannabinoid actions on food intake and cognitive arousal. J Neurosci. 27(18): 4870-81.

117. Elias, C.F., C.E. Lee, J.F. Kelly, R.S. Ahima, M. Kuhar, C.B. Saper, J.K. Elmquist, (2001) Characterization of CART neurons in the rat and human hypothalamus. J Comp Neurol. 432(1): 1-19.

118. Hanriot, L., N. Camargo, A.C. Courau, L. Leger, P.H. Luppi, C. Peyron, (2007) Characterization of the melanin-concentrating hormone neurons activated during paradoxical sleep hypersomnia in rats. J Comp Neurol. 505(2): 147-57.

119. Heller, H.C.,N.F. Ruby, (2004) Sleep and circadian rhythms in mammalian torpor. Annu Rev Physiol. 66: 275-89.

120. Lincoln, D.W., K. Hentzen, T. Hin, P. van der Schoot, G. Clarke, A.J. Summerlee, (1980) Sleep: a prerequisite for reflex milk ejection in the rat. Exp Brain Res. 38(2): 151-62.

121. Blyton, D.M., C.E. Sullivan, N. Edwards, (2002) Lactation is associated with an increase in slow-wave sleep in women. J Sleep Res. 11(4): 297-303.

122. Wermter, A.K., K. Reichwald, T. Buch, F. Geller, C. Platzer, K. Huse, C. Hess, H. Remschmidt, T. Gudermann, G. Preibisch, W. Siegfried, H.P. Goldschmidt, W.D. Li, R.A. Price, H. Biebermann, H. Krude, C. Vollmert, H.E. Wichmann, T. Illig, T.I. Sorensen, A. Astrup, L.H. Larsen, O. Pedersen, D. Eberle, K. Clement, J. Blundell, M. Wabitsch, H. Schafer, M. Platzer, A. Hinney, J. Hebebrand, (2005) Mutation analysis of the MCHR1 gene in human obesity. Eur J Endocrinol. 152(6): 851-62.

123. Cirauqui, N., J. Ceras, S. Galiano, S. Perez-Silanes, L. Juanenea, G. Rivera, I. Aldana, A. Monge, (2008) New amide derivatives as melanin-concentrating hormone receptor 1 antagonists for the treatment of obesity. Arzneimittelforschung. 58(11): 585-91.

124. Kokkotou, E., A.C. Moss, D. Torres, I. Karagiannides, A. Cheifetz, S. Liu, M. O'Brien, E. Maratos-Flier, C. Pothoulakis, (2008) Melanin-concentrating hormone as a mediator of intestinal inflammation. Proc Natl Acad Sci U S A. 105(30): 10613-8.

125. Lagos, P., P. Torterolo, H. Jantos, J.M. Monti, (2011) Immunoneutralization of melanin-concentrating hormone (MCH) in the dorsal raphe nucleus: effects on sleep and wakefulness. Brain Res. 1369: 112-8.

126. Stengel, A., M. Goebel, L. Wang, Y. Tache, (2010) Ghrelin, des-acyl ghrelin and nesfatin-1 in gastric X/A-like cells: role as regulators of food intake and body weight. Peptides. 31(2): 357-69.

127. Brailoiu, G.C., S.L. Dun, E. Brailoiu, S. Inan, J. Yang, J.K. Chang, N.J. Dun, (2007) Nesfatin-1: distribution and interaction with a G protein-coupled receptor in the rat brain. Endocrinology. 148(10): 5088-94.

128. Fort, P., D. Salvert, L. Hanriot, S. Jego, H. Shimizu, K. Hashimoto, M. Mori, P.H. Luppi, (2008) The satiety molecule nesfatin-1 is co-expressed with melanin concentrating hormone in tuberal hypothalamic neurons of the rat. Neuroscience. 155(1): 174-81.

129. Foo, K.S., H. Brismar, C. Broberger, (2008) Distribution and neuropeptide coexistence of nucleobindin-2 mRNA/nesfatin-like immunoreactivity in the rat CNS. Neuroscience. 156(3): 563-79.

130. Shimizu, H., I.S. Oh, K. Hashimoto, M. Nakata, S. Yamamoto, N. Yoshida, H. Eguchi, I. Kato, K. Inoue, T. Satoh, S. Okada, M. Yamada, T. Yada, M. Mori, (2009) Peripheral administration of nesfatin-1 reduces food intake in mice: the leptin-independent mechanism. Endocrinology. 150(2): 662-71.

131. Goebel-Stengel, M.,L. Wang, (2013) Central and peripheral expression and distribution of NUCB2/nesfatin-1. Curr Pharm Des. 19(39): 6935-40.

132. Kohno, D., M. Nakata, Y. Maejima, H. Shimizu, U. Sedbazar, N. Yoshida, K. Dezaki, T. Onaka, M. Mori, T. Yada, (2008) Nesfatin-1 neurons in

paraventricular and supraoptic nuclei of the rat hypothalamus coexpress oxytocin and vasopressin and are activated by refeeding. Endocrinology. 149(3): 1295-301.

133. Palasz, A., E. Rojczyk, K. Bogus, J.J. Worthington, R. Wiaderkiewicz, (2015) The novel neuropeptide phoenixin is highly co-expressed with nesfatin-1 in the rat hypothalamus, an immunohistochemical study. Neurosci Lett. 592: 17-21.
134. Konczol, K., O. Pinter, S. Ferenczi, J. Varga, K. Kovacs, M. Palkovits, D. Zelena, Z.E. Toth, (2012) Nesfatin-1 exerts long-term effect on food intake and body temperature. Int J Obes (Lond). 36(12): 1514-21.
135. Aydin, S., (2013) Role of NUCB2/nesfatin-1 as a possible biomarker. Curr Pharm Des. 19(39): 6986-92.
136. Garcia-Galiano, D., V.M. Navarro, J. Roa, F. Ruiz-Pino, M.A. Sanchez-Garrido, R. Pineda, J.M. Castellano, M. Romero, E. Aguilar, F. Gaytan, C. Dieguez, L. Pinilla, M. Tena-Sempere, (2010) The anorexigenic neuropeptide, nesfatin-1, is indispensable for normal puberty onset in the female rat. J Neurosci. 30(23): 7783-92.
137. Su, Y., J. Zhang, Y. Tang, F. Bi, J.N. Liu, (2010) The novel function of nesfatin-1: anti-hyperglycemia. Biochem Biophys Res Commun. 391(1): 1039-42.
138. Merali, Z., C. Cayer, P. Kent, H. Anisman, (2008) Nesfatin-1 increases anxiety- and fear-related behaviors in the rat. Psychopharmacology (Berl). 201(1): 115-23.
139. Konczol, K., I. Bodnar, D. Zelena, O. Pinter, R.S. Papp, M. Palkovits, G.M. Nagy, Z.E. Toth, (2010) Nesfatin-1/NUCB2 may participate in the activation of the hypothalamic-pituitary-adrenal axis in rats. Neurochem Int. 57(3): 189-97.
140. Gunay, H., R. Tutuncu, S. Aydin, E. Dag, D. Abasli, (2012) Decreased plasma nesfatin-1 levels in patients with generalized anxiety disorder. Psychoneuroendocrinology. 37(12): 1949-53.
141. Emmerzaal, T.L.,T. Kozicz, (2013) Nesfatin-1; implication in stress and stress-associated anxiety and depression. Curr Pharm Des. 19(39): 6941-8.
142. Goebel, M., A. Stengel, L. Wang, Y. Tache, (2009) Restraint stress activates nesfatin-1-immunoreactive brain nuclei in rats. Brain Res. 1300: 114-24.

143. Yoshida, N., Y. Maejima, U. Sedbazar, A. Ando, H. Kurita, B. Damdindorj, E. Takano, D. Gantulga, Y. Iwasaki, T. Kurashina, T. Onaka, K. Dezaki, M. Nakata, M. Mori, T. Yada, (2010) Stressor-responsive central nesfatin-1 activates corticotropin-releasing hormone, noradrenaline and serotonin neurons and evokes hypothalamic-pituitary-adrenal axis. Aging (Albany NY). 2(11): 775-84.

144. Dallman, M.F., N.C. Pecoraro, S.E. La Fleur, J.P. Warne, A.B. Ginsberg, S.F. Akana, K.C. Laugero, H. Houshyar, A.M. Strack, S. Bhatnagar, M.E. Bell, (2006) Glucocorticoids, chronic stress, and obesity. Prog Brain Res. 153: 75-105.

145. Domschke, K., S. Stevens, B. Pfleiderer, A.L. Gerlach, (2010) Interoceptive sensitivity in anxiety and anxiety disorders: an overview and integration of neurobiological findings. Clin Psychol Rev. 30(1): 1-11.

146. Afifi, M., (2007) Gender differences in mental health. Singapore Med J. 48(5): 385-91.

147. Ari, M., O.H. Ozturk, Y. Bez, S. Oktar, D. Erduran, (2011) High plasma nesfatin-1 level in patients with major depressive disorder. Prog Neuropsychopharmacol Biol Psychiatry. 35(2): 497-500.

148. Bloem, B., L. Xu, E. Morava, G. Faludi, M. Palkovits, E.W. Roubos, T. Kozicz, (2012) Sex-specific differences in the dynamics of cocaine- and amphetamine-regulated transcript and nesfatin-1 expressions in the midbrain of depressed suicide victims vs. controls. Neuropharmacology. 62(1): 297-303.

149. Heymsfield, S.B., A.S. Greenberg, K. Fujioka, R.M. Dixon, R. Kushner, T. Hunt, J.A. Lubina, J. Patane, B. Self, P. Hunt, M. McCamish, (1999) Recombinant leptin for weight loss in obese and lean adults: a randomized, controlled, dose-escalation trial. JAMA. 282(16): 1568-75.

150. Aydin, S., E. Dag, Y. Ozkan, F. Erman, A.F. Dagli, N. Kilic, I. Sahin, F. Karatas, T. Yoldas, A.O. Barim, Y. Kendir, (2009) Nesfatin-1 and ghrelin levels in serum and saliva of epileptic patients: hormonal changes can have a major effect on seizure disorders. Mol Cell Biochem. 328(1-2): 49-56.

151. Cirelli, C.,G. Tononi, (2000) On the functional significance of c-fos induction during the sleep-waking cycle. Sleep. 23(4): 453-69.

152. Kovacs, K.J., (2008) Measurement of immediate-early gene activation- c-fos and beyond. J Neuroendocrinol. 20(6): 665-72.
153. Sheng, M.,M.E. Greenberg, (1990) The regulation and function of c-fos and other immediate early genes in the nervous system. Neuron. 4(4): 477-85.
154. Chaudhuri, A., (1997) Neural activity mapping with inducible transcription factors. Neuroreport. 8(16): v-ix.
155. Shiromani, P.J.,W.J. Schwartz, (1995) Towards a molecular biology of the circadian clock and sleep of mammals. Adv Neuroimmunol. 5(2): 217-30.
156. Mendelson, W.B., R.D. Guthrie, G. Frederick, R.J. Wyatt, (1974) The flower pot technique of rapid eye movement (REM) sleep deprivation. Pharmacol Biochem Behav. 2(4): 553-6.
157. Kitka, T., Z. Katai, D. Pap, E. Molnar, C. Adori, G. Bagdy, (2009) Small platform sleep deprivation selectively increases the average duration of rapid eye movement sleep episodes during sleep rebound. Behav Brain Res. 205(2): 482-7.
158. Toth, Z.E.,E. Mezey, (2007) Simultaneous visualization of multiple antigens with tyramide signal amplification using antibodies from the same species. J Histochem Cytochem. 55(6): 545-54.
159. Paxinos G, W.C., (2007) The Rat Brain in Stereotaxic Coordinates. 6th ed. San Diego: Academic Press. .
160. Kantor, S., R. Jakus, B. Balogh, A. Benko, G. Bagdy, (2004) Increased wakefulness, motor activity and decreased theta activity after blockade of the 5-HT2B receptor by the subtype-selective antagonist SB-215505. Br J Pharmacol. 142(8): 1332-42.
161. McKinley, M.J., A.M. Allen, C.N. May, R.M. McAllen, B.J. Oldfield, D. Sly, F.A. Mendelsohn, (2001) Neural pathways from the lamina terminalis influencing cardiovascular and body fluid homeostasis. Clin Exp Pharmacol Physiol. 28(12): 990-2.
162. Stoppa, G.R., M. Cesquini, E.A. Roman, P.O. Prada, A.S. Torsoni, T. Romanatto, M.J. Saad, L.A. Velloso, M.A. Torsoni, (2008) Intracerebroventricular injection of citrate inhibits hypothalamic AMPK and

modulates feeding behavior and peripheral insulin signaling. J Endocrinol. 198(1): 157-68.

163. Yosten, G.L.,W.K. Samson, (2009) Nesfatin-1 exerts cardiovascular actions in brain: possible interaction with the central melanocortin system. Am J Physiol Regul Integr Comp Physiol. 297(2): R330-6.
164. Graf, M., R. Jakus, S. Kantor, G. Levay, G. Bagdy, (2004) Selective 5-HT1A and 5-HT7 antagonists decrease epileptic activity in the WAG/Rij rat model of absence epilepsy. Neurosci Lett. 359(1-2): 45-8.
165. Kantor, S., R. Jakus, R. Bodizs, P. Halasz, G. Bagdy, (2002) Acute and long-term effects of the 5-HT2 receptor antagonist ritanserin on EEG power spectra, motor activity, and sleep: changes at the light-dark phase shift. Brain Res. 943(1): 105-11.
166. Diniz Behn, C.G., E.B. Klerman, T. Mochizuki, S.C. Lin, T.E. Scammell, (2010) Abnormal sleep/wake dynamics in orexin knockout mice. Sleep. 33(3): 297-306.
167. MA Seaman, J.L.a.R.S., (1991) New Developments in pairwise multiple comparisons: Some powerful and practicable procedures. Psychological Bulletin. 110: 577-586.
168. Jouvet, D., P. Vimont, F. Delorme, (1964) [Study of Selective Deprivation of the Paradoxal Phase of Sleep in the Cat]. J Physiol (Paris). 56: 381.
169. Cohen, H.B.,W.C. Dement, (1965) Sleep: changes in threshold to electroconvulsive shock in rats after deprivation of "paradoxical" phase. Science. 150(3701): 1318-9.
170. Suchecki, D., L.L. Lobo, D.C. Hipolide, S. Tufik, (1998) Increased ACTH and corticosterone secretion induced by different methods of paradoxical sleep deprivation. J Sleep Res. 7(4): 276-81.
171. Vas, S., C. Adori, K. Konczol, Z. Katai, D. Pap, R.S. Papp, G. Bagdy, M. Palkovits, Z.E. Toth, (2013) Nesfatin-1/NUCB2 as a potential new element of sleep regulation in rats. PLoS One. 8(4): e59809.
172. Machado, R.B., S. Tufik, D. Suchecki, (2008) Chronic stress during paradoxical sleep deprivation increases paradoxical sleep rebound: association with prolactin

plasma levels and brain serotonin content. Psychoneuroendocrinology. 33(9): 1211-24.

173. Alam, M.N., H. Gong, T. Alam, R. Jaganath, D. McGinty, R. Szymusiak, (2002) Sleep-waking discharge patterns of neurons recorded in the rat perifornical lateral hypothalamic area. J Physiol. 538(Pt 2): 619-31.
174. Mitrofanis, J., (2005) Some certainty for the "zone of uncertainty"? Exploring the function of the zona incerta. Neuroscience. 130(1): 1-15.
175. Jurkowlaniec, E., W. Trojniar, J. Tokarski, (1990) The EEG activity after lesions of the diencephalic part of the zona incerta in rats. Acta Physiol Pol. 41(7): 85-97.
176. Liu, M., C. Blanco-Centurion, R. Konadhode, S. Begum, D. Pelluru, D. Gerashchenko, T. Sakurai, M. Yanagisawa, A.N. van den Pol, P.J. Shiromani, (2011) Orexin gene transfer into zona incerta neurons suppresses muscle paralysis in narcoleptic mice. J Neurosci. 31(16): 6028-40.
177. Hahn, J.D., (2010) Comparison of melanin-concentrating hormone and hypocretin/orexin peptide expression patterns in a current parceling scheme of the lateral hypothalamic zone. Neurosci Lett. 468(1): 12-7.
178. Koyama, Y., K. Takahashi, T. Kodama, Y. Kayama, (2003) State-dependent activity of neurons in the perifornical hypothalamic area during sleep and waking. Neuroscience. 119(4): 1209-19.
179. Lader, M., H.F. Andersen, T. Baekdal, (2005) The effect of escitalopram on sleep problems in depressed patients. Hum Psychopharmacol. 20(5): 349-54.
180. Vas, S., Z. Katai, D. Kostyalik, D. Pap, E. Molnar, P. Petschner, L. Kalmar, G. Bagdy, (2013) Differential adaptation of REM sleep latency, intermediate stage and theta power effects of escitalopram after chronic treatment. J Neural Transm. 120(1): 169-76.
181. Kumar, S., R. Szymusiak, T. Bashir, S. Rai, D. McGinty, M.N. Alam, (2007) Effects of serotonin on perifornical-lateral hypothalamic area neurons in rat. Eur J Neurosci. 25(1): 201-12.
182. Gillin, J.C., W. Jernajczyk, D.C. Valladares-Neto, S. Golshan, M. Lardon, S.M. Stahl, (1994) Inhibition of REM sleep by ipsapirone, a 5HT1A agonist, in normal volunteers. Psychopharmacology (Berl). 116(4): 433-6.

183. Jego, S., D. Salvert, L. Renouard, M. Mori, R. Goutagny, P.H. Luppi, P. Fort, (2012) Tuberal hypothalamic neurons secreting the satiety molecule Nesfatin-1 are critically involved in paradoxical (REM) sleep homeostasis. PLoS One. 7(12): e52525.

184. Boissard, R., P. Fort, D. Gervasoni, B. Barbagli, P.H. Luppi, (2003) Localization of the GABAergic and non-GABAergic neurons projecting to the sublaterodorsal nucleus and potentially gating paradoxical sleep onset. Eur J Neurosci. 18(6): 1627-39.

185. Cheeta, S., G. Ruigt, J. van Proosdij, P. Willner, (1997) Changes in sleep architecture following chronic mild stress. Biol Psychiatry. 41(4): 419-27.

186. Romanowski, C.P., T. Fenzl, C. Flachskamm, W. Wurst, F. Holsboer, J.M. Deussing, M. Kimura, (2010) Central deficiency of corticotropin-releasing hormone receptor type 1 (CRH-R1) abolishes effects of CRH on NREM but not on REM sleep in mice. Sleep. 33(4): 427-36.

187. Rachalski, A., C. Alexandre, J.F. Bernard, F. Saurini, K.P. Lesch, M. Hamon, J. Adrien, V. Fabre, (2009) Altered sleep homeostasis after restraint stress in 5-HTT knock-out male mice: a role for hypocretins. J Neurosci. 29(49): 15575-85.

188. Jacobs, B.L.,C.A. Fornal, (1991) Activity of brain serotonergic neurons in the behaving animal. Pharmacol Rev. 43(4): 563-78.

189. Calabrese, E.J.,L.A. Baldwin, (2001) U-shaped dose-responses in biology, toxicology, and public health. Annu Rev Public Health. 22: 15-33.

190. Gomori, A., A. Ishihara, M. Ito, S. Mashiko, H. Matsushita, M. Yumoto, T. Tanaka, S. Tokita, M. Moriya, H. Iwaasa, A. Kanatani, (2003) Chronic intracerebroventricular infusion of MCH causes obesity in mice. Melanin-concentrating hormone. Am J Physiol Endocrinol Metab. 284(3): E583-8.

191. Yamawaki, H., M. Takahashi, M. Mukohda, T. Morita, M. Okada, Y. Hara, (2012) A novel adipocytokine, nesfatin-1 modulates peripheral arterial contractility and blood pressure in rats. Biochem Biophys Res Commun. 418(4): 676-81.

192. Gao, X.B.,A.N. van den Pol, (2001) Melanin concentrating hormone depresses synaptic activity of glutamate and GABA neurons from rat lateral hypothalamus. J Physiol. 533(Pt 1): 237-52.
193. Gao, X.B.,A.N. van den Pol, (2002) Melanin-concentrating hormone depresses L-, N-, and P/Q-type voltage-dependent calcium channels in rat lateral hypothalamic neurons. J Physiol. 542(Pt 1): 273-86.
194. Kleinlogel, H., (1990) Analysis of the vigilance stages in the rat by fast Fourier transformation. Neuropsychobiology. 23(4): 197-204.
195. Bjorvatn, B., S. Fagerland, R. Ursin, (1998) EEG power densities (0.5-20 Hz) in different sleep-wake stages in rats. Physiol Behav. 63(3): 413-7.
196. Vanderwolf, C.H., (1969) Hippocampal electrical activity and voluntary movement in the rat. Electroencephalogr Clin Neurophysiol. 26(4): 407-18.
197. Jouvet, M., (1969) Biogenic amines and the states of sleep. Science. 163(3862): 32-41.
198. Buzsaki, G.,A. Draguhn, (2004) Neuronal oscillations in cortical networks. Science. 304(5679): 1926-9.
199. Macrides, F., H.B. Eichenbaum, W.B. Forbes, (1982) Temporal relationship between sniffing and the limbic theta rhythm during odor discrimination reversal learning. J Neurosci. 2(12): 1705-17.
200. Semba, K.,B.R. Komisaruk, (1984) Neural substrates of two different rhythmical vibrissal movements in the rat. Neuroscience. 12(3): 761-74.
201. Oddie, S.D.,B.H. Bland, (1998) Hippocampal formation theta activity and movement selection. Neurosci Biobehav Rev. 22(2): 221-31.
202. Sainsbury, R.S., J.L. Harris, G.L. Rowland, (1987) Sensitization and hippocampal type 2 theta in the rat. Physiol Behav. 41(5): 489-93.
203. McNaughton, N., B. Kocsis, M. Hajos, (2007) Elicited hippocampal theta rhythm: a screen for anxiolytic and procognitive drugs through changes in hippocampal function? Behav Pharmacol. 18(5-6): 329-46.
204. Leranth, C.,R.P. Vertes, (1999) Median raphe serotonergic innervation of medial septum/diagonal band of broca (MSDB) parvalbumin-containing neurons: possible involvement of the MSDB in the desynchronization of the hippocampal EEG. J Comp Neurol. 410(4): 586-98.

205. Dos Santos, L., T.G. de Andrade, H. Zangrossi, Jr., (2005) Serotonergic neurons in the median raphe nucleus regulate inhibitory avoidance but not escape behavior in the rat elevated T-maze test of anxiety. Psychopharmacology (Berl). 179(4): 733-41.

206. Hsiao, Y.T., S.B. Jou, P.L. Yi, F.C. Chang, (2012) Activation of GABAergic pathway by hypocretin in the median raphe nucleus (MRN) mediates stress-induced theta rhythm in rats. Behav Brain Res. 233(1): 224-31.

207. Lima, F.F., L.V. Sita, A.R. Oliveira, H.C. Costa, J.M. da Silva, R.A. Mortara, C.A. Haemmerle, G.F. Xavier, N.S. Canteras, J.C. Bittencourt, (2013) Hypothalamic melanin-concentrating hormone projections to the septo-hippocampal complex in the rat. J Chem Neuroanat. 47: 1-14.

208. Thakkar, M.M., R.E. Strecker, R.W. McCarley, (1998) Behavioral state control through differential serotonergic inhibition in the mesopontine cholinergic nuclei: a simultaneous unit recording and microdialysis study. J Neurosci. 18(14): 5490-7.

209. Jackson, J., C.T. Dickson, B.H. Bland, (2008) Median raphe stimulation disrupts hippocampal theta via rapid inhibition and state-dependent phase reset of theta-related neural circuitry. J Neurophysiol. 99(6): 3009-26.

14. Bibliography of the candidate's publications

14.1. Publications related to the PhD thesis

1. Vas S, Adori C, Konczol K, Katai Z, Pap D, Papp RS, Bagdy G, Palkovits M, Toth ZE Nesfatin-1/NUCB2 as a Potential New Element of Sleep Regulation in Rats. PLOS ONE 8:(4) p. e59809. 10 p. (2013)

2. Katai Z, Adori C, Kitka T, Vas S, Kalmar L, Kostyalik D, Tothfalusi L, Palkovits M, Bagdy G Acute escitalopram treatment inhibits REM sleep rebound and activation of MCH-expressing neurons in the lateral hypothalamus after long term selective REM sleep deprivation. PSYCHOPHARMACOLOGY 228:(3) pp. 439-449. (2013)

3. Vas S, Katai Z, Kostyalik D, Pap D, Molnar E, Petschner P, Kalmar L, Bagdy Differential adaptation of REM sleep latency, intermediate stage and theta power effects of escitalopram after chronic treatment. JOURNAL OF NEURAL TRANSMISSION 120:(1) pp. 169-176. (2013)

14.2. Publications that not related to the PhD thesis

1. Bergman P, Adori C, Vas S, Kai-Larsen Y, Sarkanen T, Cederlund A, Agerberth B, Julkunen I, Horvath B, Kostyalik D, Kalmar L, Bagdy G, Huutoniemi A, Partinen M, Hokfelt T Narcolepsy patients have antibodies that stain distinct cell populations in rat brain and influence sleep patterns. PROCEEDINGS OF THE NATIONAL ACADEMY OF SCIENCES OF THE UNITED STATES OF AMERICA 111:(35) pp. E3735-E3744. (2014)

2. Kostyalik D, Katai Z, Vas S, Pap D, Petschner P, Molnar E, Gyertyan I, Kalmar L, Tothfalusi L, Bagdy G Chronic escitalopram treatment caused dissociative adaptation in serotonin (5-HT) 2C receptor antagonist-induced effects in REM sleep, wake and theta wave activity. EXPERIMENTAL BRAIN RESEARCH 232:(3) pp. 935-946. (2014)

3. Kostyalik D, Vas S, Katai Z, Kitka T, Gyertyan I, Bagdy G, Tothfalusi L Chronic escitalopram treatment attenuated the accelerated rapid eye movement sleep transitions after selective rapid eye movement sleep deprivation: a model-based analysis using Markov chains. BMC NEUROSCIENCE 15:(1) Paper 120. 16 p. (2014)

4. Adori C, Ando RD, Balazsa T, Soti C, Vas S, Palkovits M, Kovacs GG, Bagdy G Low ambient temperature reveals distinct mechanisms for MDMA-induced serotonergic toxicity and astroglial Hsp27 heat shock response in rat brain. NEUROCHEMISTRY INTERNATIONAL 59:(5) pp. 695-705. (2011)

5. Kitka T, Adori C, Katai Z, Vas S, Molnar E, Papp RS, Toth ZE, Bagdy G Association between the activation of MCH and orexin immunorective neurons and REM sleep architecture during REM rebound after a three day long REM deprivation. NEUROCHEMISTRY INTERNATIONAL 59:(5) pp. 686-694. (2011)

6. Adori C, Ando RD, Ferrington L, Szekeres M, Vas S, Kelly PAT, Hunyady L, Bagdy G Elevated BDNF protein level in cortex but not in hippocampus of MDMA-treated Dark Agouti rats: A potential link to the long-term recovery of serotonergic axons NEUROSCIENCE LETTERS 478:(2) pp. 56-60. (2010)

7. Volk B, Nagy BJ, Vas S, Kostyalik D, Simig G, Bagdy G Medicinal chemistry of 5-HT5A receptor ligands: a receptor subtype with unique therapeutical potential CURRENT TOPICS IN MEDICINAL CHEMISTRY 10:(5) pp. 554-578. (2010)

8. Kalmar L, Bors A, Farkas H, Vas S, Fandl B, Varga L, Fust G, Tordai A Mutation screening of the C1 inhibitor gene among Hungarian patients with hereditary angioedema HUMAN MUTATION 22:(6) Paper 673. 8 p. (2003)

DOI: 10.14753/SE.2016.1869

15. Acknowledgements

First of all I would like to thank to my PhD supervisors, Prof. Gyorgy Bagdy and Dr. Zsuzsanna Tóth PhD for all their support during this process, guidance and expert knowledge helped shape my thinking.

A special thanks to Prof. Miklós Palkovits, Dr. Csaba Adori, and members of the Department of Anatomy, Histology and Embryology for introducing me into neuromorphology and giving me a ground in the anatomy of the rat brain.

Also, a large thank for all members of the Bagdy EEG Lab and the Department of Pharmacodynamics at the Semmelweis University past and present, for their time in assisting with the experiments, and for the friendship to make difficulties easy to cope with.

I am also grateful for all my co-authors for their assistance and ideas in the publications: Prof. Gyorgy Bagdy, Prof. Miklós Palkovits, Dr. Zsuzsanna Tóth, Dr. Csaba Ádori, Dr. Lajos Kalmar, Dr. Katalin Könczöl, Dr. Dorottya Pap, Dr. Rege Sugárka Papp, Dr. Zita Kátai, Dr. Diána Kostyalik, Dr. Tamás Kitka, Dr. László Tóthfalusi, Dr. Péter Petschner and Dr. Eszter Molnár.

Last but not least I would like to thank to my husband Lali and my sweet daughters Bori and Luca for their encouragement, understanding, patience and love. Without you all effort would have been worthless.

This work was supported by the Hungarian Academy of Sciences (MTA-SE Neuropsychopharmacology and Neurochemistry Research Group) and the National Development Agency (KTIA_NAP_13-1-2013-0001), Hungarian Brain Research Program - Grant No. KTIA_13_NAP-A-II/14.